

REPORT ON THE DATING OF NATURAL TERRAIN LANDSLIDES IN HONG KONG

GEO REPORT No. 170

R.J. Sewell & S.D.G. Campbell

**GEOTECHNICAL ENGINEERING OFFICE
CIVIL ENGINEERING AND DEVELOPMENT DEPARTMENT
THE GOVERNMENT OF THE HONG KONG
SPECIAL ADMINISTRATIVE REGION**

REPORT ON THE DATING OF NATURAL TERRAIN LANDSLIDES IN HONG KONG

GEO REPORT No. 170

R.J. Sewell & S.D.G. Campbell

**GEOTECHNICAL ENGINEERING OFFICE
CIVIL ENGINEERING AND DEVELOPMENT DEPARTMENT
THE GOVERNMENT OF THE HONG KONG
SPECIAL ADMINISTRATIVE REGION**

© The Government of the Hong Kong Special Administrative Region

First published, September 2005

Prepared by:

Geotechnical Engineering Office,
Civil Engineering and Development Department,
Civil Engineering and Development Building,
101 Princess Margaret Road,
Homantin, Kowloon,
Hong Kong.

PREFACE

In keeping with our policy of releasing information which may be of general interest to the geotechnical profession and the public, we make available selected internal reports in a series of publications termed the GEO Report series. The GEO Reports can be downloaded from the website of the Civil Engineering and Development Department (<http://www.cedd.gov.hk>) on the Internet. Printed copies are also available for some GEO Reports. For printed copies, a charge is made to cover the cost of printing.

The Geotechnical Engineering Office also produces documents specifically for publication. These include guidance documents and results of comprehensive reviews. These publications and the printed GEO Reports may be obtained from the Government's Information Services Department. Information on how to purchase these documents is given on the last page of this report.



R.K.S. Chan

Head, Geotechnical Engineering Office
September 2005



Frontispiece: Aerial Photograph of Relict Natural Terrain Landslides at the Sunset Peak West Landslide Site Taken on 24.1.63. The Large Landslide in the Centre of the Photograph Has Yielded an Average Age of 7.4 ± 1.3 ka Based on a Combination of Surface Exposure (Cosmogenic Nuclide) and Optically Stimulated Luminescence Dating

FOREWORD

This report describes the results of a detailed dating study of natural terrain landslides in Hong Kong undertaken by the Planning Division as part of an overall objective to advance the understanding of the causes and mechanisms of natural terrain landslides. Specifically, the aims of the study were to accumulate sufficient knowledge on the precision and accuracy of various dating methods to be able to produce guidelines on dating of natural terrain landslides, and to obtain sufficient numerical and relative age data in order to categorise relict natural terrain landslides in broad ages.

Dr R.J. Sewell, the senior author of the report, conducted much of the fieldwork and managed the project, in which he was supported by Dr S.D.G. Campbell, who also assisted in compiling the report. Other colleagues in GEO contributed to the study, including Dr R. Shaw, Ms A.M.H. Law, Ms D.L.K. Tang and Mr T.H.H. Hui. Aerial photograph interpretation and ground investigation supervision were largely undertaken by Maunsell Geotechnical Services Ltd., and Mr A. Dias in particular. Analytical Services were provided by the University of Waikato, Victoria University of Wellington, and the Australia National University.



(H.N. Wong)

Chief Geotechnical Engineer/Planning

ABSTRACT

Knowledge of numerical (absolute) and relative ages of relict natural terrain landslides in the Hong Kong Special Administrative Region (HKSAR) is important in assessing natural terrain landslide hazards and the design of mitigation measures. Relative ages of relict landslide clusters can be suggested by Aerial Photograph Interpretation (API). Previous determinations of numerical ages of relict landslides have mostly relied on radiocarbon dating of large, readily visible, but rare, organic fragments/debris, and some optically stimulated luminescence (OSL) dating.

In November 2001, the Geotechnical Engineering Office commenced an integrated pilot study of relative and direct dating techniques to assess the accuracy and reliability of previously used techniques and the applicability of recently developed techniques. Recent developments include 1) Accelerated Mass Spectrometry (AMS), enabling radiocarbon dating of extremely small fragments of organic debris (5 mg), and extending radiocarbon dating back to c. 50,000 yrs BP, and 2) in-situ produced cosmogenic isotopes, apparently not previously used in the HKSAR, enabling the time rocks have been exposed to cosmic radiation, i.e. within c.3 m of the surface, to be established. Results from these new techniques can be compared with numerical results from OSL, and relative results from API.

Dating was undertaken at 19 sites around the HKSAR following detailed geomorphological observations based on API. Datable features included in situ materials from landslide sources, landslide debris, and fluvial/alluvial material associated with, or influenced by, landslides. The results have revealed that direct dating of carefully selected, relict natural terrain landslide scars in Hong Kong is viable. The new techniques provide several examples of confirmation of relative ages determined from API.

With respect to radiocarbon dating, it is possible to date natural terrain landslides using fragments of disseminated charcoal down to a minimum weight of 5 mg identified and separated with the aid of a binocular microscope.

With respect to in-situ cosmogenic nuclide analysis using ^{10}Be and ^{26}Al , the sensitivity of the AMS technique is sufficiently high to measure exposure ages of surfaces associated with landslides of a few thousand years, despite the unfavourable circumstances of low latitude and low altitude.

With respect to luminescence dating, it is possible to successfully date large natural terrain landslide deposits up to 17 m thick using both the finegrain and Single Aliquot Regenerative (SAR) techniques despite potentially unfavourable circumstances affecting bleaching of sediment grains.

The numerical ages indicate that relict natural terrain landslides classified as large in the NTLI and LLS appear to be generally thousands and tens of thousands, rather than hundreds of years old. Smaller relict landslide features (e.g. relict open hillslope features) appear to be generally hundreds rather than thousands of years old. However, there are insufficient chronometric data on relict natural terrain landslides with which to determine landslide frequency magnitudes on a territory-wide basis.

CONTENTS

	Page No.
Title Page	1
PREFACE	3
FRONTISPIECE	4
FOREWORD	5
ABSTRACT	6
CONTENTS	7
1. INTRODUCTION	11
1.1 Background	11
1.2 Description of the Project	11
1.3 Scope and Objectives	11
2. EXISTING LANDSLIDE AGE DATA	12
3. SITE SELECTION	13
3.1 Current Landslide Investigation Sites	13
3.2 Integrated Landslide Investigation Study Areas	13
3.3 Large Relict Landslide Sites	14
3.4 Additional Sites	14
4. LANDSLIDE DATING TECHNIQUES	14
4.1 Terminology	15
4.2 Radiocarbon Dating	15
4.3 Luminescence Dating	16
4.4 Surface Exposure Dating	17
4.5 Maximum and Minimum Ages	18
5. AERIAL PHOTOGRAPH INTERPRETATION	20
5.1 Current Landslide Investigation Sites	20
5.1.1 Lai Cho Road	20
5.1.2 Lo Lau Uk	20
5.1.3 Pat Heung	20

	Page No.
5.1.4 Lei Pui Street	21
5.2 Integrated Landslide Investigation Study Areas	21
5.2.1 Ap Lei Chau Study Area	21
5.2.2 Tsing Shan Foothills Study Area	21
5.2.3 Sham Wat Debris Lobe Study Area	22
5.2.4 Mid-Levels Study Area	22
5.2.5 Tung Chung East Study Area	23
5.3 Large Relict Landslide Sites	23
5.3.1 Sunset Peak West	23
5.3.2 Tai O	23
5.3.3 Sai Tso Wan	24
5.3.4 Wong Lung Hang	24
5.3.5 Sham Wat East	24
5.4 Additional Sites	25
5.4.1 South East Tsing Yi	25
5.4.2 Lion Rock	25
5.4.3 Fei Ngo Shan	26
5.4.4 Seymour Cliffs	26
6. GROUND INVESTIGATION	26
6.1 Trial Pits	26
6.2 Boreholes	26
6.3 Surface Sampling	27
7. DESCRIPTIONS OF DATABLE FEATURES AND MATERIALS	27
7.1 Exposed Rock Surfaces	27
7.2 Alluvium	28
7.3 Colluvium	28
7.4 Buried Soil Horizons	29
8. DATING RESULTS AND INTERPRETATION	29
8.1 Current Landslide Investigation Sites	29
8.1.1 Lai Cho Road	29
8.1.2 Lo Lau Uk	30

	Page No.
8.1.3 Pat Heung	31
8.1.4 Lei Pui Street	32
8.2 Integrated Landslide Investigation Study Areas	33
8.2.1 Ap Lei Chau Study Area	33
8.2.2 Tsing Shan Landslide Study Area	34
8.2.3 Sham Wat Debris Lobe	37
8.2.4 Mid Levels Study Area	38
8.2.5 Tung Chung East Study Area	39
8.3 Large Relict Landslide Sites	40
8.3.1 Sunset Peak West	40
8.3.2 Tai O	41
8.3.3 Sai Tso Wan	42
8.3.4 Wong Lung Hang	44
8.4 Additional Sites	46
8.4.1 South East Tsing Yi	46
8.4.2 Lion Rock	46
8.4.3 Fei Ngo Shan	47
8.4.4 Seymour Cliffs	48
9. INDEPENDENT AGE CONTROL AND COMPARISONS OF THE DATING TECHNIQUES	48
9.1 Comparison Between ‘Leading Edge’ SAR Luminescence Ages and Radiocarbon Determinations	48
9.2 Comparison Between ‘LogNormal’ SAR Luminescence Ages and Finegrain Luminescence Ages	49
9.3 Comparison Between Finegrain Luminescence Ages and Radiocarbon Determinations	49
9.4 Comparison Between Luminescence Ages and Cosmogenic ¹⁰ Be Exposure Ages	49
10. COMPARISONS OF RELATIVE VERSUS NUMERICAL AGES	49
10.1 Relative Ages of Landslides Determined from Aerial Photograph Interpretation	50
10.2 Relative Ages of Colluvial Units Determined from Stratigraphic Observations	50

	Page No.
11. APPLICATION OF DATING TECHNIQUES TO SPECIFIC LANDSLIDE HAZARD MODELS	51
11.1 Open Hillslope Landslides	51
11.2 Channelised Debris Flows	51
11.3 Deep-seated Landslides	52
11.4 Rock Fall and Boulder Fall	52
12. CONCLUSIONS AND RECOMMENDATIONS	52
12.1 Dating of Natural Terrain Landslides	52
12.2 Recommended Numerical Dating Techniques	53
12.3 Return Periods for Relict Natural Terrain Landslides	54
12.4 Chronological Classification of Relict Natural Terrain Landslides	54
12.5 Further Work	55
13. KEY FINDINGS	55
14. REFERENCES	56
LIST OF TABLES	58
LIST OF FIGURES	79
LIST OF PLATES	123
APPENDIX: PRINCIPLES, ANALYTICAL PROCEDURES, CALIBRATIONS AND CALCULATIONS OF THE DATING METHODS	127

1. INTRODUCTION

1.1 Background

One of the aims of improving Hong Kong's slope safety standards under the Government's Policy Objective is to advance the understanding of the causes and mechanisms of landslides, so as to improve the reliability of landslide preventive or remedial works. Recently, attention has focussed on studies of natural terrain landslides, enabling the development of procedures for evaluating natural terrain hazards (e.g. Ng et al., 2002).

Natural terrain, as referred to in this report, follows the definition given in Ng et al. (2002), namely, "terrain that has not been modified substantially by human activity but includes areas where grazing, hill fires and deforestation may have occurred". The term "relict", as used in this report, also follows the general definition given by Ng et al. (2002), except where used in relation to the Natural Terrain Landslide Inventory or Large Landslide Study features when it is defined "in relation to landslides first observed on the earliest photographs available and with vegetation class C or D (Grass or Trees)."

Assessment and mitigation of natural terrain hazards involve interpretation of historical landslide data and consideration of the possible return periods of natural terrain failures. The estimation of return periods, based on historical landslide data assumes some constancy in the environmental controls of the landslides. Given the extreme change in sea level, and known climatic fluctuations that have occurred during the last 10-15,000 years (Fyfe et al., 2000 and references therein), this assumption is potentially unreliable. Therefore, knowledge of relict natural terrain landslide chronologies is essential both for providing more reliable estimations of the return periods of landslides for assessing their risk, and for understanding the causes and mechanisms of landslides.

1.2 Description of Project

This project addresses recommendations for further work arising from an earlier, preliminary, landslide dating study (King, 2001), which focussed on luminescence dating of colluvial and landslide debris deposits. The project was undertaken between April 2001 and the end of 2002. Specifically, the project was intended:

- (a) To accumulate sufficient knowledge on the precision and accuracy of various dating methods to be able to produce guidelines on dating of natural terrain landslides, and
- (b) To obtain sufficient numerical and relative age data on relict natural terrain landslides in order to categorise relict natural terrain landslides in broad ages.

1.3 Scope and Objectives

The scope of the project was limited to investigating the application of three principal dating techniques, namely radiocarbon dating, luminescence dating, and surface exposure dating, to relict natural terrain landslides in Hong Kong selected on the basis of observable

API relict features, such as those typically observed during natural terrain hazard studies. The principal objectives of the dating project included:

- (a) Evaluating the accuracy and reliability of selected dating techniques in order to determine which are the most appropriate techniques, or combinations of techniques, to apply to different types of natural terrain landslides in Hong Kong;
- (b) Selecting and dating suitable relict natural terrain features at specific landslide sites, which are currently, or have recently been, the subject of investigation under the LIC;
- (c) Selecting and dating suitable relict natural terrain features within areas where integrated (e.g. dating, API to confirm relative chronologies, ground investigation, hazard modeling, etc) landslide studies have already been undertaken;
- (d) Determining, based on an interpretation of the available aerial photographs, a relative chronology in selected areas where clusters of relict landslides are known to occur, and targeting and dating suitable relict natural terrain features in order to test in numerical terms, the relative chronology established;
- (e) Selecting and dating suitable relict natural terrain features where mitigation measures for boulder fall have recently been instigated, or where large relict landslides have been found in close proximity to existing developments;
- (f) Interpreting the age data, in relation to other data from API, etc, with a view to improving knowledge on return periods of relict natural terrain landslides in Hong Kong.

2. EXISTING LANDSLIDE AGE DATA

Existing landslide age data from relict natural terrain landslides in Hong Kong are generally sparse and restricted to luminescence ages from colluvial deposits. The largest number of luminescence ages were obtained from a colluvial lobe at Sham Wat on Lantau Island (King, 2001). However, other luminescence ages have been obtained from colluvial deposits in the northeast New Territories and on Hong Kong Island (Lai, 1997, 1998; Duller & Wintle, 1997).

The luminescence ages from the colluvial lobe at Sham Wat were measured using the optically stimulated luminescence (OSL) single aliquot regenerative (SAR) method, whereas those obtained by Duller & Wintle (1997) were obtained using the OSL multialiquot method. The luminescence ages obtained by Lai (1997, 1998) were measured using thermoluminescence (TL) techniques.

Luminescence ages reported by King (2001) for the Sham Wat Debris Lobe range from 1.4 to 27 ka. The youngest age came from a smaller, southern portion of the lobe which, on the basis of API, was considered to post-date the main lobe. The best age estimate for the lobe was achieved by averaging the age of an interpretation of the last significant bleaching event. This interpretation returned an age of no more than 2.2 ka for the main lobe and 1.4 ka for the southern lobe.

The two samples of colluvium analysed by Duller & Wintle (1997) returned ages of 196 ka and 38 ka. The older age came from a sample of colluvium below Mid-Levels, whereas the younger age came from colluvium on the flanks of Fei Ngo Shan in Kowloon.

The ages reported by Lai (1997, 1998), came from three principles sites: thick colluvium in a steep valley below Tai Mo Shan, colluvial lobes and aprons below Mid-Levels, and a colluvial lobe at a formerly coastal landslide site at Shum Wan Road. The reported ages of colluvium range from 19 ka for the Tai Mo Shan site, from 10 to 61 ka for the Mid-Levels site, and from 35 to 48 ka for the slope at Shum Wan Road.

3 SITE SELECTION

3.1 Current Landslide Investigation Sites

The first group of sites for the landslide dating study comprised those currently, or recently, the focus of detailed investigation of recent instability under Agreement No. CE 72/2000 - Landslide Investigation Consultancy (LIC) For Landslides Reported within Kowloon and the New Territories (Figure 1). These sites showed evidence of relict natural terrain landslides, in addition to recent instability, and included:

- (i) Slope 11NW-A/C9 above Lai Cho Road, Kwai Chung;
- (ii) The natural hillside above No. 92 Tak Shek Wu Kiu Tau near Pat Heung;
- (iii) The natural hillside above Lo Lau Uk near Tai Po; and
- (iv) The natural hillside above Lei Pui Street, Kwai Chung.

3.2 Integrated Landslide Investigation Study Areas

The second group of sites for the landslide dating study were selected from areas where integrated landslide studies had been undertaken previously by the Geotechnical Engineering Office (Figure 1). These study areas were chosen to enable comparison with results from the first group of sites and included:

- (i) The Mount Johnston Study Area;
- (ii) The Tung Chung East Study Area;
- (iii) The Sham Wat Debris Lobe Study Area;

- (iv) The Tsing Shan Foothills Area; and
- (v) The Mid-Levels Study Area.

3.3 Large Relict Landslide Sites

The third group of sites chosen for landslide dating comprised large relict landslide sites selected from the Large Landslide Study (LLS) database (Figure 1). Areas containing clusters of LLS features were identified as a first step. Specific landslide sites were then selected for further study based on complex histories of landslide development, proximity to other sites investigated as part of this study, and ease of access. Most of the landslide sites belonging to the third group were located on Lantau Island. The large relict landslide sites included:

- (i) Sunset Peak West;
- (ii) Tai O;
- (iii) Sham Wat East;
- (iv) Sai Tso Wan; and
- (v) Wong Lung Hang.

3.4 Additional Sites

Additional sites were selected for surface exposure dating where large boulder falls and rock falls were identified from API in the urban area of Kowloon and on Tsing Yi. Other sites were also included on the advice of the expert laboratory supervisor. The additional sites included:

- (i) South-east Tsing Yi,
- (ii) Lion Rock,
- (iii) Fei Ngo Shan,
- (iv) Seymour Cliffs.

4. LANDSLIDE DATING TECHNIQUES

A key objective of the landslide dating study was to accumulate sufficient knowledge on the precision and accuracy of various dating methods to be able to provide technical guidance as to which are the most appropriate techniques, or combinations of techniques, to apply to different types of relict natural terrain landslide in Hong Kong. Various dating techniques have potential application to dating of landslides. These include lichenometric dating, dendrochronology, optically stimulated luminescence (OSL) dating, cosmogenic

nuclide (surface exposure) dating, uranium-series dating, radiocarbon dating, weathering rind dating, palynology and micropalaeontology. However, several of these techniques require favourable material conditions (e.g. preserved tree material for dendrochronology, preserved tephra for Ar-Ar dating and Alpha-Recoil-Track (ART) dating, preserved scarps and boulders for surface exposure dating), while other techniques (e.g. weathering rind dating, palynological and micropaleontological dating) require external calibration and stratigraphic controls. In order to establish a reliable baseline age control dataset, it was necessary to focus on direct dating methods. Accordingly, three main numerical dating techniques were investigated, following recommendations by King (2001), and Sewell and Campbell (1998, 2001), namely: radiocarbon dating, luminescence dating, and cosmogenic nuclide (surface exposure) dating. The full dating reports are held in the Civil Engineering Library, Civil Engineering Department, and are reproduced in part in Appendix 1.

4.1 Terminology

The terminology used for describing geochronological data throughout this report follows recommendations contained in Noller et al. (2000). The term “date”, when used as a noun, is avoided in favour of “age” because “date” carries with it a notion of calendar years and a specific point in time. On the other hand, the term “age” refers to an interval of time measured back from the present and is more appropriate for describing the chronometric data (e.g. either in terms of “age estimates” or simply “ages”) especially where uncertainties, expressed as errors, are involved. The SI-derived abbreviation “ka” for “thousand years ago” measured from present is used in describing the ages for surface exposure dating and luminescence dating.

Conventionally, radiocarbon ages are reported as years ‘before present’ (BP) (i.e. before 1950). However, owing to variations in the proportion of radiocarbon in the atmosphere over time, and the discovery that the true half life of radiocarbon is 5730 years (Stuiver & Polach, 1977) and not the original measured value of 5568 years (“Libby” half-life), radiocarbon determinations are now calibrated with tree rings to determine the calendar year associated with the radiocarbon age. Both the conventional radiocarbon ages (^{14}C yr BP) and the “calibrated” ages (CalBP) are enumerated in this study, although for comparison tables with other dating techniques, the “calibrated” age plus 50 years is used.

Finally, the word “absolute” is avoided when used in reference to age estimates because of inherent uncertainties in the dating methods. In its place, the term “numerical” is used, which implies quantitative estimates of age, but within limits of statistical uncertainty whose ratios can be compared. The expression “numerical age” is used synonymously with the term “chronometric”.

4.2 Radiocarbon Dating

The most widely applied and generally accepted technique for dating of superficial deposits, both onshore and offshore, is radiocarbon dating. This technique relies on the measured concentration of the Carbon-14 isotope in organic material (e.g. charcoal, peat, wood, bone, shell, etc) within a deposit to provide an estimate of the age of the deposit. Organic material is commonly found disseminated within the landslide deposit particularly as fragments of charcoal. In addition, soil horizons buried by landslide deposits (colluvium)

may also yield preserved organic material. Organic material relating to landslides can also occur in (i) translocated pond deposits, (ii) flank-ridge deposits, and (iii) landslide-dammed lake and stream deposits.

Radiocarbon dating has an age range of pre-1950 (present time for the technique) to approximately 50,000 years before present. In Hong Kong, the age range of this dating technique overlaps with the earliest available aerial photographic records, taken in 1924 (partial coverage) and 1945 (more extensive coverage).

Forty-five samples for radiocarbon dating were submitted for analysis. These comprised:

- (i) Twenty hand samples from horizons containing significant quantities of carbon clearly visible in the field (e.g. from distinctive colluvial and soil horizons exposed within trial pits),
- (ii) Twenty-three samples of disseminated charcoal within colluvium and alluvium collected by U100 tubes, mostly comprising multiple fragments of organic material, and
- (iii) Two samples of disseminated charcoal from drill core.

Seven samples submitted for analysis returned 'Modern' or '>Modern' values (after Stuiver & Polach, 1977), and five samples yielded insufficient material to be dated (i.e. <5 mg minimum requirement for analysis). Of the nineteen ages that were obtained from disseminated organic material, five ages were judged to have been from incorporated older material, and four ages from younger material washed in from the surface. The remaining ten ages lie within range of the corresponding luminescence dates, and therefore are considered to be the most reliable estimates of the depositional age.

Conventional radiocarbon ages were determined by Accelerated Mass Spectrometry at the Rafter Radiocarbon Laboratory, Institute of Geological & Nuclear Sciences, New Zealand, following preparation and pre-treatment at the Radiocarbon Dating Laboratory, University of Waikato, New Zealand. Details of the sample preparation and analytical procedures are described in Appendix 1.

4.3 Luminescence Dating

Luminescence dating is a technique used for establishing the length of time since a sediment was last exposed to sunlight. This technique has previously been applied in Hong Kong on a limited scale to the dating of colluvium. The principle of the technique is based on a radiation dose which is acquired in the lattice defects of minerals (such as quartz and feldspar) by exposure to ionizing radiation from radioactive decay of ^{238}U , ^{232}Th and isotopes of ^{40}K in the surrounding sediment. Exposure of the mineral to daylight causes release of the stored energy in a process known as "bleaching". Optically stimulated luminescence (OSL) dating involves the use of different wavelengths of light to stimulate release of the stored energy in the form of a luminescence signal. Measurement of the luminescence output allows calculation of the time since the mineral was last exposed to daylight.

Luminescence dating has an effective age range from approximately 1000 years to 100s of thousands of years.

Both multiple aliquot and single aliquot luminescence dating methods were used in the analysis of Hong Kong samples. The multiple aliquot method was initially applied to silt-size fractions whereas the single aliquot method was applied to sand-size fractions. As most samples contained a fine silt fraction, the multiple aliquot method was used more generally. Eighty-nine samples were submitted for analysis, including twenty-one duplicate samples measured using both multiple and single aliquot methods for control purposes.

Sample preparation and luminescence measurements were done in the Luminescence Dating Laboratory, School of Earth Sciences, Victoria University of Wellington, New Zealand, and gamma spectrometry was carried out by the National Radiation Laboratory (NRL), Christchurch, New Zealand. Details of the analytical procedures are described in Appendix 1.

4.4 Surface Exposure Dating

Surface exposure dating is a relatively new technique that measures the buildup of in-situ produced cosmogenic nuclides that has occurred in a rock since it has been exposed to cosmic radiation. The technique has generally been used to date glacial surfaces in regions of high latitude or high altitude, or both, where the cosmic radiation is strongest (e.g. Nishiizumi et al. 1989, Barrows et al. 2001, Barrows et al. 2002). Prior to this study, there had been relatively few reports on the applications of the technique to dating of landslides (e.g. Nichols et al. 2000), and especially those occurring at low latitudes and close to sea-level.

The principle behind cosmogenic isotope dating (Zreda & Phillips, 2000) relates to the build up of cosmic nuclides in an exposed rock surface as a result of bombardment by cosmic ray particles (high energy neutrons and muons). Cosmic ray particles may penetrate up to 3 m into an exposed rock surface causing nuclear reactions that lead to the formation of new, cosmogenic nuclides. The concentration of these new nuclides depends on the time the material has been exposed to cosmic radiation. The most commonly used isotopes for surface exposure dating are ^{10}Be , ^{26}Al , and ^{36}Cl . These long-lived radioisotopes can be used to measure the age of rock surfaces from approximately 1000 to one million years old.

Sixty-three ^{10}Be ages and six ^{26}Al ages were obtained from samples in this study. These included samples from 34 landslide scars and 27 boulders within landslide debris, with several samples used for control purposes. The ^{26}Al ages were obtained on duplicate samples for quality control. The analytical procedures and sampling methodology used are described in Appendix 1.

Sample pretreatment and analytical measurements were carried out in the Department of Nuclear Physics, Research School of Physical Sciences and Engineering, Australia National University.

4.5 Maximum and Minimum Ages

For a particular landslide site, the concepts of maximum and minimum ages, as they apply to each of the three dating techniques, are important for a meaningful interpretation of the age data. Establishing the maximum and minimum ages from the chronometric data requires detailed knowledge of the geomorphological setting of the landslide site. Once the maximum and minimum ages for each data set are known (Figure 2), they provide limitations on how freely the age data can be used in calibration or comparison with other data sets, and inferences made thereon.

(i) Radiocarbon Dating

Most of the charcoal and other organic fragments within landslide deposits probably originated from incorporation of organic material into the landslide during its emplacement. However, they could also include organic material: from deeper horizons than that at surface at the time of the landslide; from reworked older debris deposits; from roots that have invaded the deposit subsequently; and, transported from surface and carried by groundwater (e.g. in erosion pipes) eventually to be laid down within the deposit.

Radiocarbon determinations on organic material incorporated in the landslide deposit, and on organic remains of buried soil, generally provide maximum ages for the landslide event (i.e. the age of emplacement could not be any older than the age of incorporated or buried material). Conversely, radiocarbon determinations on younger organic material transported from the surface by groundwater into the deposit, or on younger roots which have invaded the deposit subsequent to deposition, provide minimum ages for the landslide event (i.e. the age of emplacement could not be any younger than the age of introduced material).

Owing to the extremely small concentrations of ^{14}C to be measured and errors involved, young organic material (0 - 200 yr BP) is difficult to date precisely using the radiocarbon technique. In theory, radiocarbon determinations on organic material up to the present day should be possible. In practice, however, calibrated ages can generally only be reliably obtained on material that is older than c.200 yr BP. Many practitioners consider c.600 yr BP to be a more realistic lower limit of analytical precision.

In this report, radiocarbon ages which can not be reliably calibrated less than 200 yr BP are omitted from the discussion, although they are enumerated in the radiocarbon dating reports.

(ii) Luminescence Dating

The OSL technique relies on the sediment grains being completely 'bleached' at the time of deposition to remove all trace of a previous luminescence signal (i.e. the electron traps in the crystal lattice have been completely emptied). Since the OSL dating technique is based on the time elapsed since buried sediment grains were last exposed to sunlight, the measured OSL signal should therefore record a maximum age (i.e. the age of the sediment could not be any older than the age of last exposure to sunlight). The finegrain method of measurement, after Aitken and Xie (1992) and a protocol as described by Lang and Wagner (1997), was generally used where the samples consisted mainly of silt.

However, studies of modern sediments have shown that ‘partial’ or ‘incomplete’ bleaching can occur in aeolian, fluvial and marine settings (Murray & Olley, 2002). Where this is suspected, the ‘5% Leading Edge’ SAR method (Olley et al. 1998) is generally recommended as the lowest values of the dose distribution curve can be taken as the best estimate of the true dose since the sample was bleached. In cases where the results of both finegrain and SAR measurements are reported for partially bleached samples, the finegrain results would provide a minimum ‘average’ age (i.e. at worst, assuming none of the sediment grains have received sufficient exposure during the depositional event to fully bleach the OSL signal), and the SAR results would provide a maximum age (i.e. at best, all of the sediment grains have been fully bleached during the depositional event and, therefore, the sediment could not be any older than the age of last exposure to sunlight).

In this report, the luminescence results of twenty-one duplicate samples measured using both multiple and single aliquot methods for control purposes show that, in general, incomplete bleaching does not appear to have been important in the deposition of thick (>1 m thick) colluvial deposits. However, incomplete bleaching does appear to have occurred in the deposition of thin (<1 m thick) colluvial deposits, and alluvial deposits.

(iii) Surface Exposure Dating

Surface exposure dating depends on the build up of cosmogenic nuclides that has occurred in a rock surface since it was last exposed to cosmic radiation. Since cosmic ray particles may penetrate up to 3 m into an exposed rock surface, the true age of last exposure can only be determined if the exposed rock surface had no previously accumulated (inherited) cosmogenic signal (i.e. the exposed rock surface must originally have been deeper than 3 m below ground surface), and that the rock surface has been stable since it was exposed.

Therefore, with regard to cosmogenic dating of relict natural terrain landslides, it is important to ensure that samples are collected from scarps that are deeper than 3 m from the original ground surface. Boulders from the associated debris also need to be carefully selected to avoid, as far as possible, any possible cosmogenic inheritance effects.

Ideally the minimum scarp and boulder surface exposure ages for a relict natural terrain landslide should correspond to the time at which the landslide detached from its source area. However, in practice, several environmental factors can contribute to an underestimate of the true age. For example, younger apparent ages may be generated from (i) an eroded source area, (ii) a disturbed source area, or (iii) boulders in the associated debris which have subsequently been exhumed.

Conversely, overestimates of the true age of relict natural terrain landslides may be generated by (i) a source area which is less than 3 m deep, or (ii) boulders in the associated debris which have been derived from a source less than 3 m deep. The maximum surface exposure age is the maximum age of the rock surface that is permitted by the analytical data. Usually, the maximum surface age at relict natural terrain landslide sites is considered to be the age of the original ground surface.

5. AERIAL PHOTOGRAPH INTERPRETATION

Detailed aerial photograph interpretation (API) was carried out for all the main study areas and landslide sites to identify landslide features and material suitable for dating, and to establish a relative chronology of relict natural terrain landslide features. For each site, all available aerial photographs were reviewed, but low level aerial photographs, and those taken in 1963 in particular, were found to be the most useful. Key findings of the API for the main study areas are summarized below, and relative chronologies, where established, are summarized in Table 1. Detailed API reports are held by the Chief Geotechnical Engineer/Planning, Geotechnical Engineering Office, Civil Engineering Department (in GCP 2/A1/10-1).

5.1 Current Landslide Investigation Sites

Prominent relict landslide main scarps were investigated at the Lai Cho Road and Lei Pui Street sites, whereas composite landslides, without clearly definable main scarps, were investigated at the Lo Lau Uk and Pat Heung sites. Although no rock surfaces suitable for surface exposure dating were identified at the latter two sites, trial pits were excavated in colluvial debris to obtain material for luminescence and radiocarbon dating.

5.1.1 Lai Cho Road

A large composite escarpment featuring six smaller scarps was identified (Plate 1). Three of the scarps (A3, A5 & A6) were highly degraded and considered unsuitable for dating. However, the remaining three scarps (A1, A2 & A4) were more clearly defined with steep backscarps and sharp lateral boundaries. Suitable locations for surface exposure dating were identified. A relative chronology for these three scarps, based on API, suggested the largest feature (A4) was the oldest, and the smallest feature (A2) the youngest. Colluvial debris suitable for either luminescence or radiocarbon dating was only identified downslope of the smallest feature.

5.1.2 Lo Lau Uk

Two large depressions (A & B) were interpreted to have been formed by landslide activity. API revealed evidence of recent landslide activity in the two depressions. However, hummocky colluvium in the lower sections of the depressions was considered likely to preserve material from relict landslides, so presenting a suitable target for dating.

5.1.3 Pat Heung

Several depressions containing numerous relict landslide scars and debris deposits were identified. However, owing to the highly degraded character of main scarp regions, and modification of the lower slopes by surface trimming, debris could not be readily linked with sources. Nevertheless, one depression (No. 5) contained relatively undisturbed colluvium which was sampled for luminescence and radiocarbon dating. Colluvium within two other

depressions was also sampled for dating, from trial pits (No. 2 & 4) excavated for a separate landslide study, reported elsewhere (OAP, 2003).

5.1.4 Lei Pui Street

Detailed API was not carried out as this site was included in the dating study at a late stage. However, the geomorphology and site history are described in the Landslide Study Report (MGSL, 2002) on the debris flow that occurred in the natural hillside above Lei Pui Street on 1 September, 2001. This divided the area around the landslide site into three main terrain units: an upper terrain unit within deeply weathered coarse-grained granite and comprising numerous inferred relict landslides, thought to have released a large volume of landslide debris over geological time; a middle terrain unit immediately below the upper terrain unit, consisting mainly of fine-grained granite rock outcrops, with ledges hosting thin (<1 m thick) accumulations of landslide debris from the upper terrain unit; and a lower terrain unit below the rock outcrops of the middle terrain unit, comprising mainly colluvial debris aprons, more than 1 m thick, derived from landslides in the middle and upper terrain units. Material for luminescence and radiocarbon dating was obtained from trial pits, excavated in the lower terrain unit for the landslide study. In addition, one sample was collected from a thin debris on a ledge in the middle terrain unit. The rock scarp in the middle terrain unit was also sampled for surface exposure dating to determine age variation due to spalling, and possible correlation with relict debris at the base of the slope.

5.2 Integrated Landslide Investigation Study Areas

Mainly large relict landslide features in the integrated natural terrain hazard study areas were chosen for dating. Relict landslides with clearly defined main scarps and associated debris lobes were identified in several areas (e.g. Ap Lei Chau, Tsing Shan C, Sham Wat Debris Lobe), whereas in others, either the landslide source area only, was well-defined (Mid-Levels), or the debris lobe only, was well-defined (Tung Chung East, Tsing Shan A, B).

5.2.1 Ap Lei Chau Study Area

Two relict landslide features (RLS1 & RLS2) with clearly defined main scarps and debris lobes were identified (Plate 2). Although geographically separated, RLS 2 was considered older than RLS 1 based on its generally more degraded appearance. However, owing to difficulties in obtaining suitable material, only the most prominent relict landslide (RLS 1) was selected for dating. Both the debris lobe (boulders) and main scarp were targeted for surface exposure dating, whereas luminescence and radiocarbon-dating techniques were used to date the colluvial deposits.

5.2.2 Tsing Shan Foothills Study Area

Three relict landslide (TSA, TSB, TSC) sites were selected for the dating study in the Tsing Shan foothills study area. These relict landslide sites typically comprised a well-defined main debris lobe, with variously degraded source areas. Only one of the sites

(TSC) possessed rock faces and associated boulders suitable for surface exposure dating. Trial pits were excavated at the other sites to identify relict colluvial layers and obtain material for luminescence and radiocarbon dating.

At the TSA site, two relict landslide (RLS 1 & RLS 2) source areas were identified from API as feeding a single main debris lobe. The RLS 1 feature was considered to be younger than RLS 2. Three trial pits were sited in the single main debris lobe to identify suitable materials for dating which could have been derived from either source areas.

The API for the relict landslide at the TSB site identified a poorly defined, highly degraded, source area, linked with a prominent main debris lobe. Three trial pits were located in the central part of the main debris lobe to identify suitable materials for dating.

Initial API at the TSC landslide site interpreted the large landslide feature as comprising a well-defined source escarpment, and an adjacent debris lobe containing sporadic large boulders and a narrow tongue of colluvium. The scarp area and several large boulders protruding from the surface of the colluvium were selected for surface exposure dating. Four trial pits, two trial trenches and two boreholes were also sited in the colluvium to provide material for luminescence and radiocarbon dating. During the ground investigation, recent surface deformation, consistent with an active slow-moving translational slide was observed.

5.2.3 Sham Wat Debris Lobe Study Area

The Sham Wat Debris Lobe was previously the subject of a detailed investigation (King, 1998), including a preliminary dating study (King, 2001). The dating study concluded that the apparent age of the deposit was about 35 ka on the basis of standard luminescence dating methods. However, this age was considered to be a gross overestimate because subsequent analysis using dose distributions, based on the assumption of incomplete bleaching, returned ages as young as 1.4 ± 0.2 ka, with a likely age range between 1,000 years and 23 ka.

The Lobe comprises a single large northern debris lobe, the main lobe, and a subordinate southern lobe. The main lobe has a well-defined source area marked by a prominent rock escarpment. Numerous large boulders protrude from the surface of the debris lobe and these, together with the main scarp region, provided suitable rocks for surface exposure dating. The main lobe has been mapped, on the basis of API, as extending across the main river valley draining into Sham Wat Wan and it almost certainly blocked the river at one time. Accordingly, a trial pit was excavated in alluvial materials immediately upstream of the main debris lobe to extract datable material that might reveal when the main river was last blocked, and potentially establish the minimum age of the last major landslide event. Undisturbed samples from previous ground investigation studies, including U100 and drill core samples, were also submitted for luminescence dating.

5.2.4 Mid-Levels Study Area

The most clearly defined and accessible possible relict landslide in the Mid-Levels study area is located immediately NW of Victoria Peak. Although the landslide comprises a

single well-defined apparent head scarp, an associated debris lobe is not obvious, in part due to the extensive development at this location. Therefore, surface exposure dating of the head scarp region was the only viable dating option considered.

5.2.5 Tung Chung East Study Area

Three large depressions (A, B, & C) characterise the Tung Chung East Study area on the northwest slopes of Por Kai Shan, North Lantau. The depressions contain no clearly definable large relict landslide features and appear to have formed from numerous small recurrent landslide events. Although no scarps suitable for surface exposure dating were identified, large debris fan deposits at the base of the depressions were considered likely to preserve a record of past landslide events. Therefore, two trial pits were excavated in the debris fan deposits to obtain material for luminescence and radiocarbon-dating.

5.3 Large Relict Landslide Sites

Clusters of features were selected from features contained in the LLS database. The relative chronology of relict landslides was established by API at each site for comparison with numerical dating results. Except for the Sunset Peak West site, where material from both source area and debris were dated, most of the material for dating was obtained from depositional lobes rather than source areas. In general, this reflected the relative degradation of the source areas.

5.3.1 Sunset Peak West

Six large relict landslide features (Nos. 1-6) were identified, several of which are thought to have formed from multiple landslide events (Frontispiece). They consist of large debris lobes formed from the build up of numerous smaller-scale debris flows originating from the middle and upper slope areas. In one relict landslide (No. 5), the debris deposits could be confidently matched with the source area. Therefore, this landslide was selected for surface exposure dating using rock surfaces in the source area and large boulders protruding from the debris lobe, in addition to luminescence dating of material in the debris lobe. The other debris lobes were dated only using luminescence techniques, since no suitable organic material for radiocarbon dating was recovered. Four trial pits and two boreholes were excavated and drilled respectively in the main debris lobes to obtain material for dating. Based on API, the relative order of landslide age, from youngest to oldest, is interpreted as Nos. 2, 3, 5, 6, 1 and 4.

5.3.2 Tai O

Six drainage depressions (Dep. Nos. A-F) were identified, each containing large colluvial deposits (debris fans). However, none of the colluvial deposits overlap and none could be linked with certainty to an individual large landslide event. The debris fans formed at the base of each drainage depression are considered to be the products of multiple smaller debris flows and debris slides. These debris fan deposits appear to overlie large debris aprons that extend from the mid-slope to the toe of natural terrain between the major

depressions. Three of the largest debris fans (Debris Fans A-C) were chosen for luminescence and radiocarbon-dating and three trial pits and three boreholes were excavated and drilled respectively to obtain samples. As the site is adjacent to the shoreline, boreholes were used to sample colluvial deposits interbedded with estuarine deposits, potentially containing organic material, at the toe of the debris fans. Trial pits in the debris fans were excavated to sample colluvial layers derived from multiple landslide events.

5.3.3 Sai Tso Wan

Six large depressions (Nos. 1-6) were identified. Depressions Nos. 1-3 comprise source areas containing numerous relict landslide scars with debris trails that amalgamate downslope into a complex series of overlapping debris lobes. Depressions Nos. 1 and 2 are interpreted to have originated possibly as single large landslide events, but were later modified by persistent recurrent landsliding. However, none of the existing debris lobes at the base of the three depressions was matched with certainty to a source. Depressions Nos. 4-6 feature separate well-defined colluvial lobes downslope from their source areas. They are each thought to have formed by single large landslide events. Owing to the complex character of the source areas and evidence of multiple landslide events, surface exposure dating was not considered viable for any of the main depressions. However, six trial pits and one borehole were excavated and drilled respectively in colluvial debris from the six depressions to sample colluvial layers for luminescence and radiocarbon-dating. Based on API, the relative ages of the major depressions and related debris lobes are interpreted from oldest to youngest as: Nos. 4-6, No. 1, No. 2 and Nos. 3.

5.3.4 Wong Lung Hang

Three principal catchments (Catchments A, B, & C) were identified as containing numerous relict landslide scars within the upper and mid-slope areas. Three large colluvial lobes (Debris Lobe Nos. 1, 2, & 3) were identified in the lower portions of Catchments A, B, & C. Whereas Debris Lobe A was considered to have formed by accumulation from several debris flows, Debris Lobes Nos. 2 and 3 were considered to represent single large landslide events emanating from Catchments B and C respectively. However, it was not possible to identify the sources of the landslides due to the complex character of the source areas for Catchments B and C, and modification by subsequent landslides. Four trial pits were excavated at the Wong Lung Hang site to obtain material suitable for dating. One trial pit was located in Debris Lobe No. 1 to determine whether individual layers within the debris flow deposits could be identified and dated. Based on API, Debris Lobe No. 2 was considered to have been deflected by, and therefore was younger than, Debris Lobe No. 3. Consequently, a trial pit was excavated in Debris Lobe No. 2 to obtain samples for luminescence and radiocarbon-dating to confirm the relative age interpretation. Attempts to date Debris Lobe No. 3 centred on the premise that this large colluvial deposit may have blocked the river for a period of time, leading to the build up of a pond, lake, or alluvial flat behind the colluvial deposit. A slight deflection of the river channel, a slight change in elevation of the river bed, and the presence of several very large (>5 m diameter) boulders provided evidence for possible damming of the river. In addition to a trial pit located in the centre of the main debris, one trial pit was positioned immediately upstream of Debris Lobe No. 3 to obtain material (possible organic-rich pond, lake, or alluvial deposits) for

luminescence and radiocarbon dating. Three large colluvial boulders within Debris Lobe No. 3 were also selected for surface exposure dating.

5.3.5 Sham Wat East

Two large relict landslides were identified, the API of which, and of the adjacent terrain, revealed five main bodies of colluvial debris (Debris Lobes Nos. 1-5). However, owing to the complex character of the scarps in the source areas, and the poorly defined form of the debris lobes, none of the debris lobes could be related with certainty to single large landslide events. The varied form of the debris deposits, both rounded and planar, suggests that they accumulated from a series of pulses rather than as a large single landslide event. It was not possible to determine with confidence from API, the relative age of the debris lobes. Accordingly, owing to the uncertainties of the relationships between the debris lobes and possible source areas, no sampling for dating was carried out at this site.

5.4 Additional Sites

Four additional relict landslide sites were included in Task C at a late stage in the sampling phase. These sites were chosen specifically for surface exposure dating where API indicated extremely large boulders had fallen, around the urban areas of Kowloon and Tsing Yi, and to provide age control on spalling of granitic rock surfaces.

5.4.1 South East Tsing Yi

Two large relict landslides with indistinct source areas on the southeast side of Tsing Yi were selected for study. The relict landslide features comprise two steep cliff areas, each characterised by distinctive sheeting joints (Sheeting Joint No. 1 and Sheeting Joint No. 2), and below each of which lie large accumulations of boulder-bearing colluvial debris. The relict landslide features were considered particularly suitable for surface exposure dating because of their distinctive source areas and associated debris lobes. The presence of very large (>5 m diameter) boulders within the colluvial lobes also provided strong evidence that the colluvial deposits were the products of single large landslide events. Three boulders and three rock surfaces were selected for surface exposure dating. Based on API, Sheeting Joint No. 2 and associated debris were considered to be younger than Sheeting Joint No. 1.

5.4.2 Lion Rock

Three extremely large (20 m diameter) boulders within debris fan deposits below Lion Rock were selected for surface exposure dating (Plate 3). Two of the boulders lie within the same colluvial deposit (Colluvium No. 5), whereas the third boulder lies in an adjacent colluvial deposit (Colluvium No. 2). The source areas of the boulders from the upper flanks of Lion Rock, and the relative ages of the colluvial deposits containing the boulders, could not be confidently determined from the API.

5.4.3 Fei Ngo Shan

Three extremely large (5-10 m diameter) boulders within a single large colluvial unit (Unit No. 1) below the southwest flanks of Fei Ngo Shan were targeted for surface exposure dating. The boulders are considered to have been derived from collapse of emergent corestones near the summit of Fei Ngo Shan but their precise source location cannot be determined from API.

5.4.4 Seymour Cliffs

Sheeting joints at Seymour Cliffs, Mid-Levels, were sampled for surface exposure dating principally to determine the age variation on rock surfaces with a history of spalling. Three samples for exposure dating were collected from the granite sheeting joints, and adjacent cliffs of fine ash vitric tuff.

6. GROUND INVESTIGATION (GI)

A total of 41 trial pits (max. 3 m deep) and nine boreholes were commissioned as part of the dating study. These were spread over 11 landslide locations where landslide debris had clearly been identified. The locations of trial pits and boreholes for these sites were selected on the basis of API (Section 5), with a view to determining the chronologies of multiple event landslide sites, confirming the results of surface exposure dating where appropriate, and verifying the relative chronologies proposed on the basis of API. Additional GI data and samples were obtained at two landslide sites that were the subject of separate natural terrain hazard studies by consultants (MGSL 2002, OAP 2003).

6.1 Trial Pits

Eighty-five 500x100 mm steel tube (U100) samples of landslide deposits were collected for luminescence and radiocarbon-dating during the GI. Samples were collected from the walls of trial pits in all except one case, where a steel tube was driven vertically into surface colluvium. Where possible, all major stratigraphic horizons in trial pits were sampled. Some bulk grab samples were also taken for control purposes.

6.2 Boreholes

For the boreholes, triple-tube core barrels with foam flush were used to achieve maximum core recovery. Samples were selected for luminescence and radiocarbon dating from seven boreholes, while a further 11 samples were obtained from core samples from previous GIs at three sites: Sham Wat Debris Lobe, Lamma Island coastal landslide site, and Sai Tso Wan coastal landslide site.

6.3 Surface Sampling

Rock sampling for surface exposure dating of the landslide source areas and boulder field areas was undertaken by in-house staff with the cooperation of an expert laboratory supervisor. A total of sixty-three samples were collected, mainly from sites identified from API. Rock surface field measurements are held by the Chief Geotechnical Engineer/Planning, Geotechnical Engineering Office, Civil Engineering Department (in GCP 2/A1/10-1).

7. DESCRIPTIONS OF DATABLE FEATURES AND MATERIALS

7.1 Exposed Rock Surfaces

Well-defined landslide main and minor scarps with a minimum depth of 3 m and featuring well-exposed rock surfaces, or very large (>10 m diameter) boulders protruding from colluvium, provided the most suitable targets for surface exposure dating. Careful and precise selection of the sampling site was carried out to minimise the effects of shielding and spalling, etc, which could bias the results towards minimum ages. In theory, the best constrained landslide ages are likely to be obtained by surface exposure dating of both the main scarp and the associated debris. However, in this study a direct link between the scarp and debris was not often established, and in several cases sampling was either restricted to the scarp area alone, or the debris. For the latter, the most promising results came from sampling of very large boulders. These boulders were commonly joint bounded slabs, of the order of 25-30 m across, as was the case at the Lion Rock and Fei Ngo Shan sites.

The most appropriate sampling locations on the scarp surfaces were those where the horizon was least shielded from cosmic radiation by the effects of topography and vegetation. Careful measurements of bearings and angles, subtended by key points on the horizon, were recorded. Where possible, a minimum of four to five samples from a scarp surface were collected. Anomalously highly weathered surfaces were avoided to minimise the possibility of the exposure ages being greater than the age of the landslide. Occasional duplicate samples from a face at different heights were obtained to calibrate the variation of cosmic ray penetration with depth. Some control samples were also collected from areas adjacent to the landslide main scarps to establish the age of the original land surface.

Large, stable boulders protruding from the landslide debris were chosen for surface exposure dating. Ideally, the boulders were joint-bounded with joints facing upwards. The least weathered surfaces were chosen as sites for sampling, and structures such as joints and cleavage, were measured to assist with determining the original orientations of the boulders in the source area. Samples were selected near the middle of the boulders, to minimise the possibility of exposure ages being substantially greater than the age of the landslide. This situation could arise where the boulder retained an in situ cosmogenic isotope component from its previous history of exposure to cosmic radiation, e.g. where the source area of the boulder was within 3 m of the original land surface prior to detachment. In such a case, the cosmogenic isotope content of the boulder (from which the exposure age is calculated) would comprise two components: one acquired after detachment and deposition of the boulder, and the other acquired while still in situ (i.e. prior to its detachment). Under these circumstances, the assumptions used to calculate the exposure age would be invalid, and the calculated age would overestimate the age of exposure of the boulder to cosmogenic radiation at its present location.

Rock samples for exposure dating were generally no more than 50 mm thick (Plate 4). They were collected using a hammer and chisel, taking care to avoid damage to the surfaces. A minimum of 500 g of rock sample was collected. In rare cases, multiple pieces of a rock surface were collected, but only where it was not possible to split off larger samples. Where more than one piece of rock was collected, they were collected from the same depth on a scarp or boulder surface. All observations at the site which could affect the genesis of cosmogenic isotopes (and so the exposure age), including measurements of horizon, site conditions, elevation, etc, were recorded.

7.2 Alluvium

Alluvium was sampled for luminescence and radiocarbon-dating at several sites, where pond or alluvial deposits were suspected to have resulted from damming of a river or stream by landslide debris. Samples were collected either as bulk grab samples, or within U100 steel tubes, from within trial pits. The alluvium generally comprised weakly bedded coarse to fine sand and silt, with local accumulations of charcoal fragments.

In most cases, alluvial layers exposed in the trial pits were within 1 m of the surface. Samples for analysis were collected from each distinctive alluvial layer, and especially where organic material was observed, with care taken to avoid material disturbed by anthropogenic reworking close to the surface. Most areas where pond deposits were suspected, had previously been sites of cultivation.

Samples for luminescence and radiocarbon dating were obtained using U100 steel tubes driven into the sidewalls of trial pits. Splits of samples for luminescence dating were kept sealed to avoid any risk of exposure to light. Samples for radiocarbon dating were examined under a binocular microscope to identify and separate obvious fragments of charcoal. A portion of each U100 sample was retained for reference.

7.3 Colluvium

Colluvium, composed of a heterogeneous, structureless mass of soil and rock materials, was sampled for luminescence and radiocarbon dating at most of the major landslide sites. In some cases the landslide debris lobes could not be directly linked with landslide scarps and appeared to be the product of cumulative landslide events.

Sample sites for the dating of debris lobes were selected on the basis of relative landslide chronologies established from API. In general, the trial pit locations were selected to yield maximum stratigraphic information. For example, areas of overlap between debris lobes were investigated to confirm relative landslide chronologies. In most cases, however, the colluvium exposed in the trial pit comprised a single, structureless layer, in which case only one U100 sample was recovered. In many cases, the trial pits in colluvium could not be excavated to the specified depth of 3 m due to the bouldery character of the debris. However, multiple U100 samples were taken where layers of colluvium could be identified.

Boreholes were used to sample colluvium from particularly thick debris lobe deposits. Triple tube core barrels with foam flush were used for maximum core recovery, and to obtain, where possible, undisturbed material at the base of the debris lobe.

After splitting the U100 tubes to obtain a sample for luminescence dating, the remaining portion of the sample was examined under a binocular microscope to identify and separate fragments of charcoal. In several cases, tiny fragments of charcoal disseminated within the colluvium sample were extracted (Plate 5).

7.4 Buried Soil Horizons

In rare cases, buried soil horizons were exposed in trial pits (Plate 6). These horizons generally comprised a thin (*c.* 10 mm) layer of organic matter covered by colluvial debris, and commonly were rich in charcoal. Most of the identified buried soil horizons were less than 1 m deep. Grab samples of the organic material were obtained for radiocarbon dating.

8. DATING RESULTS AND INTERPRETATION

The following account summarizes the results from, and interpretation of, each of the nineteen landslide sites selected for dating. For each landslide site, the results are presented as: a site map showing sample locations; a data table summarizing all age data; and an error bar chart. Chemical data and age calculations are contained in the dating reports. These are separated into phases which reflect the different batches of samples submitted for analysis during the study.

8.1 Current Landslide Investigation Sites

8.1.1 Lai Cho Road

(i) Sampling and Dating

The relict landslide scarps were sufficiently distinct as to enable the application of all three dating techniques. Samples for surface exposure dating were collected from the well-preserved A1 escarpment (Figure 3). Three samples (LCR-01, LCR-03 and LCR-04) were collected from the A2 landslide, from both sides of the U-shaped scarp immediately above the larger A1 landslide scarp. A further sample (LCR-02), from the A1 landslide scarp, was collected 10 m southeast of LCR-01. In addition, one borehole (BH1) and one trial pit (TP1) were located in colluvium immediately below the A1 and A2 scarps to provide material for luminescence and radiocarbon dating. A second trial pit (TP2) was located in colluvium below the larger and more degraded A4 escarpment. One main colluvial unit was identified in each of the two trial pits.

A total of seven samples were dated (Table 2 and Figure 4), comprising three surface exposure ages from the A2 landslide scarp, one surface exposure age from the A1 landslide scarp, one finegrain OSL age from colluvium in each of the two trial pits, and one radiocarbon determination from disseminated carbon within the colluvium.

(ii) Results and Interpretation

The ^{10}Be exposure ages from the A2 landslide scarp range from 6.5 ± 0.9 ka to 5.0 ± 0.9 ka. A normalised χ^2 test on these ages ($\chi^2/\nu = 0.82$) suggests they are a single population

with a mean age of 6.0 ± 0.8 ka. The ^{10}Be exposure age from the A1 landslide scarp is 7.5 ± 0.9 ka, suggesting the A1 scarp is slightly older than the A2 scarp.

The colluvial unit in TP2 downslope of the A4 feature yielded a finegrain OSL age of 26.4 ± 2.4 ka, whereas the colluvial unit in TP1 downslope of the A1 and A2 scarps yielded a finegrain OSL age of 3.48 ± 0.32 ka. Both OSL measurements provide minimum ages for the respective colluvial units. However, these data are generally consistent with the relative landslide chronology based on API (Section 5.1(i)) suggesting that the A4 landslide scarp is the oldest, and the A2 landslide scarp the youngest.

Disseminated carbon within the colluvium below the A1 and A2 scarps returned an age of 611 ± 47 ^{14}C yr BP (660 - 530 CalBP). This radiocarbon age is significantly younger than the finegrain OSL age from the same sample (TP1) and is likely to reflect infiltration of transported material.

Overall, three main landslide events at c.26 ka (A4), c.7.5 ka (A1) and c.6.0 ka (A2) are indicated. The finegrain luminescence age for colluvium from TP1 suggests a minimum age of c.3.5 ka for the last major landslide (exposure) event.

8.1.2 Lo Lau Uk

(i) Sampling and Dating

In addition to the recent landslide activity, the API report indicated the strong likelihood of relict landslide events. Accordingly, these relict events were the focus of the dating investigations. The lack of exposed rock surfaces in the scarp area and the lack of suitable boulders in the associated debris meant that only luminescence and radiocarbon dating techniques could be applied.

Three samples for luminescence and radiocarbon dating were recovered (Figure 5): two U100 samples from colluvium at depths of 1.0 m and 0.9 m respectively, from trial pits TP1 and TP2, sited in the lower regions of the two large depressions, and one hand sample. In TP2, the sample for luminescence dating was collected just above a buried soil horizon. A radiocarbon determination was also made on a single fragment of charcoal (0.05 g) from the same sample.

Five ages were obtained (Table 3 and Figure 6), comprising two finegrain OSL ages and two SAR-OSL ages from colluvium, and one radiocarbon determination from disseminated charcoal within colluvium (TP2).

(ii) Results and Interpretation

The buried soil horizon in TP2 within Depression A is likely to be <200 years old, since two organic samples from this horizon yielded “modern” ages. A fragment of charcoal in the overlying colluvium, with a calibrated radiocarbon age of between 290 and 60 CalBP (conventional radiocarbon age 156 ± 40 ^{14}C yr BP), was probably derived from the buried soil horizon and incorporated during emplacement.

Colluvium immediately above the buried soil horizon in TP2 yielded a finegrain OSL age of 11.2 ± 2.9 ka and a 'Log Normal' SAR-OSL age (for quality control) of 11.0 ± 1.3 ka. These ages overlap, within 1σ error, to yield an average age of 11.1 ± 1.4 ka.

Compared with TP2, colluvium in TP1 at a similar depth (c.1 m), within Depression B, returned a finegrain OSL age of 21.8 ± 3.2 ka and a 'Log Normal' SAR-OSL age of 18.5 ± 2.3 ka. The finegrain and 'Log Normal' SAR luminescence ages are within 1σ error and yield an average age of 20.2 ± 2.3 ka.

In summary, the luminescence ages from Depressions A and B indicate a long history of instability with at least three events suggested: c.20 ka (Depression A), c.11 ka (Depression B), and <200 years (Depression B). The excellent agreement between 'Log Normal' SAR-OSL and finegrain OSL results suggests that incomplete bleaching during deposition of the sediment grains was not significant.

8.1.3 Pat Heung

(i) Sampling and Dating

As at the Lo Lau Uk site, the API revealed evidence for both relict and recent landslide activity, with the relict events being the focus of dating investigations. However, owing to the complexity of recent instability, a relative chronology of relict features could not be established. The lack of exposed rock surfaces in the scarp area and suitable boulders in the associated debris also meant that only luminescence and radiocarbon dating techniques could be applied.

Six samples of colluvium were collected for luminescence and radiocarbon dating (Figure 7). Two U100 samples were recovered from each of three trial pits (TP2, TP14 and TP17) located within Depressions Nos. 2, 4 and 5, respectively to provide the greatest information on relict landslide history.

A total of seven samples were dated (Table 4 and Figure 8), comprising six finegrain OSL ages from each of the U100 samples, and one radiocarbon age determination from a single charcoal fragment (0.01 g) from one of the U100 samples.

(ii) Results and Interpretation

Colluvium in TP2, sampled at depths of 0.7 m and 1.4 m, yielded finegrain OSL ages of 4.35 ± 0.53 ka and 27.1 ± 6.5 ka respectively. Similarly, in TP14, finegrain OSL ages of 2.85 ± 0.24 ka and 12.2 ± 2.1 ka were obtained for colluvium from depths of 1.3 m and 2.1 m respectively. Although these finegrain OSL ages should be regarded as minimum ages, a radiocarbon determination from the same sample taken at 1.3 m depth in TP 14 returned an age of $2,581 \pm 42$ ^{14}C yr BP (2780 - 2700 CalBP), in close agreement with OSL age. Overall, the age data from TP2 and TP14 suggest the presence of two chronologically distinct colluvial units in each of the trial pits.

Finegrain OSL ages of 15.7 ± 1.9 ka and 17.2 ± 2.2 ka, from depths of 2.5 m and 1.5 m respectively in TP17, lie within 1σ error. These data suggest a single unit of colluvium with average age of 16.5 ± 1.1 ka, despite the dated samples being stratigraphically inverted.

In summary, the age data indicate a long history of slope instability, with three major periods of ancient landslide activity at: c.27 ka (Depression No. 2), c.10.1 - 16.5 ka (Depressions Nos. 4 and 5); and c.2.7 - 4.4 ka (Depressions Nos. 2 and 4).

8.1.4 Lei Pui Street

(i) Sampling and Dating

Five rock surfaces in the middle terrain unit at the landslide site above Lei Pui Street were sampled for surface exposure dating to investigate both age variation due to the effects of spalling, and possible correlation with relict debris at the base of the slope (Figure 9). Five U100 samples for radiocarbon and luminescence dating were also collected from three trial pits in the lower terrain unit at the base of the slope (TP6 and TP7), and within adjacent debris (TP9), to investigate the age of overlapping colluvial layers.

A total of 14 ages were obtained, comprising five ^{10}Be surface exposure ages, one ^{26}Al surface exposure age, six finegrain OSL ages, one SAR-OSL age, and one radiocarbon age determination (Table 5 and Figure 10).

(ii) Results and Interpretation

The surface exposure ages for the six samples vary from 4.9 to 96 ka indicating that the ages of the rock surfaces are highly variable. The ^{26}Al age (100 ± 13 ka) obtained for quality control from a duplicate sample, is in good agreement with the ^{10}Be age (96.3 ± 7.9 ka).

A single sample from an SPT tube driven into unconsolidated colluvium on a ledge within the middle terrain unit, yielded a finegrain OSL age of 1.92 ± 0.14 ka. A 'Log Normal' SAR-OSL age for the same sample of 2.03 ± 0.18 ka is in good agreement (within 1σ error) with the finegrain OSL age, suggesting that incomplete bleaching during deposition of the sediment was not significant.

Samples of colluvium in TP6 and TP7, at depths of 1.3 and 1.1 m respectively, have overlapping finegrain OSL ages (within 1σ error) of 6.01 ± 0.4 ka and 6.62 ± 0.49 ka (average age 6.3 ± 0.4 ka). A single fragment of charcoal (0.02 g) from the same depth (1.1 m) in TP7 yielded a considerably older radiocarbon age of $20,127 \pm 119$ ^{14}C yr BP (23512 - 23108 CalBP), and is most likely explained by the presence of reworked organic material. In general, the OSL data suggest the shallowest samples from TP6 and TP7 belong to the same colluvial unit.

Samples of colluvium from depths of 0.69 m and 1.22 m in TP9 yielded overlapping ages (within 1σ error), although stratigraphically inverted, of 9.19 ± 0.81 ka and 8.25 ± 0.67 ka (average age 8.7 ± 0.7 ka). A slightly older age of 11.5 ± 0.1 ka was obtained from colluvium in TP7 at a depth of 1.7 m.

Overall, the luminescence data from the lower terrain unit suggest two units of colluvium (Unit 1, c.11.5 - 8.7 ka and Unit 2, c.6.3 ka), while unconsolidated colluvium from a surface ledge within the middle terrain unit is distinctly younger (Unit 3, c.2.0 ka).

The surface exposure age data cannot be directly correlated with the luminescence or radiocarbon age data. However, with one exception (c.96 ka), the range of cosmogenic ages is of the same order as the luminescence and radiocarbon ages for the relict colluvium. This suggests that spalling and detachment of blocks, and generation of associated debris, have occurred sporadically over tens of thousands of years.

8.2 Integrated Landslide Investigation Study Areas

8.2.1 Ap Lei Chau Study Area

(i) Sampling and Dating

Despite the presence of two clearly defined relict landslide features (RLS1 & RLS2) (see Section 5.2 (i)), only one feature (RLS1) provided suitable material for dating. Therefore, the relative chronology established on the basis of API could not be confirmed.

For surface exposure dating, two samples were collected from the RLS1 landslide (Figure 11), and two more were collected for control purposes from adjacent, degraded escarpments outside the landslide scar. Although three trial pits were excavated in the debris lobe downslope of the RLS1 scarp, only one (TP4) revealed colluvium suitable for luminescence and radiocarbon dating.

A total of eight samples were dated, comprising five surface exposure ages, two finegrain OSL ages, and one radiocarbon determination (Table 6 and Figure 12). Two ^{10}Be exposure ages were obtained from the RLS1 landslide, one from the scarp and one from a boulder, whereas three cosmogenic isotope ages (two ^{10}Be and one ^{26}Al) were determined on the adjacent rock scarps. The ^{26}Al age was obtained on a duplicate sample as a quality control measure. OSL and radiocarbon ages were determined from samples of colluvium at depths of 0.8 m, 1.1 m, and 0.9 m, respectively, in TP4. The radiocarbon age was obtained from a single fragment (0.02 g) of charcoal disseminated in the colluvium.

(ii) Results and Interpretation

The cosmogenic isotope measurements for the RLS1 landslide returned overlapping ^{10}Be exposure ages (within 1σ error) for the scarp and a boulder of 11.1 ± 1.6 ka and 10.8 ± 2.3 ka, respectively (average age 11.0 ± 0.2 ka). The two ^{10}Be exposure ages for the adjacent, more degraded features returned values of 72.5 ± 3.9 ka and 77.4 ± 5.6 ka, whereas the ^{26}Al exposure age on the latter sample yielded a value of 66.3 ± 39 ka. Finegrain OSL measurements on samples of colluvium at depths of 0.8 and 1.1 m in TP4 returned overlapping ages (within 1σ error) of 13.3 ± 2.2 ka and 12.2 ± 1.4 ka, respectively (average age 12.8 ± 0.8 ka).

The surface exposure and luminescence ages for the RLS1 landslide are therefore in generally good agreement, and combining these ages, the normalised χ^2 test for the four samples ($\chi^2/\nu = 0.31$) suggests they are part of a single population with an average age of 11.9 ± 1.1 ka, which can be considered as a maximum age for the RLS1 landslide. However, the surface exposure ages for adjacent rock scarps are considerably older, albeit overlapping ages (within 1σ error), of 75.2 ± 3.5 ka. This age is generally confirmed by the ^{26}Al age determination, measured on the same material.

The charcoal in (TP4) returned a radiocarbon age of $1,734 \pm 42$ ^{14}C yr BP (1,740 - 1,530 CalBP). This age is considerably younger than the luminescence ages established for the colluvium and suggests infiltration of organic material. Therefore, some degree of reworking within the soil profile cannot be ruled out.

8.2.2 Tsing Shan Landslide Study Area

(A) Tsing Shan A Landslide Site

(i) Sampling and Dating

Owing to the lack of exposed rock surfaces in the scarp area and the lack of suitable boulders in the associated debris, only luminescence and radiocarbon dating techniques could be applied. Trial pits were sited at the intersection of the two main relict debris lobes (RLS1 & RLS 2) to investigate the age of overlapping colluvial layers. The most suitable material for luminescence and radiocarbon dating (Figure 13) was collected in trial pit TPA3 from three layers of colluvium, although the effects of anthropogenic disturbance associated with grave excavation could not be ruled out.

A total of five ages were obtained, comprising three finegrain OSL ages from three samples, and one SAR-OSL age and one radiocarbon age from a duplicate sample (Table 7a and Figure 14).

(ii) Results and Interpretation

The samples for finegrain luminescence analysis in trial pit TPA3 were collected from depths of 0.3 m, 0.5 m, and 1.7 m and yielded ages of 0.908 ± 0.097 ka, 9.83 ± 1.0 ka, and 0.675 ± 0.71 ka, respectively. The SAR-OSL age on a duplicate sample from the 0.3 m horizon yielded a 'Log Normal' value of 0.63 ± 0.05 ka, whereas the 'Leading Edge' interpretation returned a value of 0.51 ± 0.05 ka. A radiocarbon determination on the same duplicate sample yielded a conventional radiocarbon age of 124 ± 45 yr BP (280 - 170 CalBP).

The poor agreement between the finegrain and SAR luminescence ages from trial pit TPA3 indicates that the colluvial sequence may have been partly disturbed. This is also suggested by the order of magnitude difference in age between colluvium collected from 0.5 m and 1.7 m, by the apparent inversion of the colluvial sequence, and by the proximity of the trial pits to local graves. The relatively young radiocarbon age obtained on organic material in the shallowest sample from TPA3, compared with the luminescence ages, also suggests disturbance. If this interpretation is correct, then the radiocarbon age and the 'Leading Edge' SAR-OSL age would reflect the disturbance date (maximum age).

However, several alternative explanations relating to landslide emplacement processes may also be valid. For example, the finegrain sediments in the middle colluvial layer may have been subject to incomplete bleaching during transport. Another possibility is that the middle colluvium layer in TPA3 may represent the basal portion of an older, colluvial deposit thrust into position over younger material. Thirdly, anomalous fading may have affected the luminescence age of the deepest colluvial layer to return an underestimate of true age.

Despite the limitations described above, the luminescence ages suggest that an early landslide event may have occurred approximately 10,000 years ago, whereas the most recent landslide events may have occurred between 250 and 1,000 years ago.

(B) Tsing Shan B Landslide Site

(i) Sampling and Dating

In common with the Tsing Shan A site, dating of the Tsing Shan B landslide site could only be approached using luminescence and radiocarbon techniques owing to the lack of suitable rock surfaces for surface exposure dating. The most complete stratigraphic sequence was revealed in trial pit TPB3 within the Main Debris Lobe (Figure 15), although none of the five colluvial layers identified yielded organic material suitable for radiocarbon dating.

A total of five luminescence ages were obtained, comprising the five colluvial units sampled from depths of 0.5 m, 1.4 m, 1.7 m, 2.4 m, and 3.1 m (Table 7b and Figure 16). The sample from 2.4 m consisted of a thin (30 mm) interbed of fine colluvium within a thicker unit.

(ii) Results and Interpretation

The colluvial units in trial pit TPB3, from shallowest to deepest, returned ages of 15.1 ± 1.3 ka (0.5 m), 3.05 ± 0.29 ka (1.4 m), 62.0 ± 1.7 ka (1.7 m), 63.3 ± 8.7 ka (2.4 m), and 9.44 ± 0.7 ka (3.1 m), respectively.

The luminescence ages indicate that the colluvial units are in stratigraphic order, except for the deepest unit. However, the observed stratigraphy could be explained if the upper colluvial units were thrust over the younger colluvium as a translational mass. This would then suggest a maximum age of c.9.5 ka for the landslide. The colluvial layers sampled at 1.7 m and 2.4 m have identical ages, within 1σ error, suggesting that they were deposited at approximately the same time.

Overall, three main colluvial units can be recognised: Unit A, 62.7 ± 0.9 ka (1.5-3 m), Unit B, 28.8 ± 4.4 ka (1.4 m), and Unit C, c.15 ka (<1 m). A fourth colluvial unit, (Unit D) identified at approximately 3.1 m depth, may represent the age of the last major landslide event at c.9,500 years ago.

(C) Tsing Shan C Landslide Site

(i) Sampling and Dating

The Tsing Shan C large landslide (Figure 17) was found to be suitable for the application of all three dating techniques. Samples for surface exposure dating were collected across a large main scarp area, and also from several large boulders protruding from the colluvium immediately downslope of the main scarp. Four trial pits were excavated on the margins of the landslide to obtain material, interpreted as levee deposits from API, for luminescence and radiocarbon dating. Samples were taken mainly from trial pit TPC3, on the southern flank, which exposed the most complete stratigraphy. Two boreholes (BHC1,

BHC2) and two trial trenches, excavated within the lower parts of the main landslide, revealed the feature to be an active, slow-moving, deep-seated (4-5 m) landslide.

A total of 18 samples were dated, comprising seven surface exposure ages, nine luminescence ages, and two radiocarbon determinations (Table 7c and Figure 18).

(ii) Results and Interpretation

Four ^{10}Be exposure ages obtained from the main scarp region returned widely ranging values of 2.8 ± 1.2 ka, 10.2 ± 0.75 ka, 5.5 ± 1.9 ka and 43.2 ± 2.1 ka, respectively. Similarly, three large boulders immediately downslope of the main scarp face yielded variable ^{10}Be exposure ages of 11.0 ± 1.3 ka, 8.3 ± 1.6 ka, and 19.4 ± 1.1 ka.

The range of surface exposure ages (2.7 - 43.3 ka), especially in source area, suggests that there has been long-lived instability. Although this broad distribution of ages could be explained by a single large failure exposing rock surfaces with varying degrees of cosmogenic inheritance, most of the samples for cosmogenic dating were collected near the base of the main scarp, well below (i.e. > 3 m) the assumed original land surface, suggesting that a single event is unlikely. Furthermore, none of the luminescence, radiocarbon, or cosmogenic ages within the colluvium is easily correlated with the ages in the scarp area.

Four colluvial units, sampled from depths of 0.7 m, 1.0 m, 1.7 m and 2.4 m in trial pit TPC3, returned finegrain OSL ages of 2.15 ± 0.19 ka, 16.8 ± 1.2 ka, 18.3 ± 2.5 ka, and 6.84 ± 0.51 ka, respectively. Two samples (HK12397 and HK12396) at 1.0 m and 1.7 m have almost identical ages, within 1σ error, and the 'Log Normal' SAR-OSL ages (14.1 ± 1.5 ka, 16.4 ± 1.9 ka) obtained on duplicate samples are similarly in close agreement (Table 7c). Although conventional radiocarbon ages obtained on these samples (HK12396) are considerably younger ($1,376 \pm 51$ ^{14}C yr BP) and older ($23,107 \pm 129$ ^{14}C yr BP) respectively, it is likely this age variation is due to the inclusion of reworked organic material. Overall, the luminescence results suggest that the colluvial units at 1.0 m and 1.7 m were emplaced during the same landslide event.

Poor agreement exists between the finegrain and SAR luminescence ages (Table 7c) performed on the shallowest sample (0.7 m) from TPC3. However, this could be explained if the uppermost material in TPC3 has undergone incomplete bleaching. Accordingly, if the 'Leading Edge' SAR-OSL age (1.03 ± 0.08 ka) is considered to reflect the last exposure event, then the calibrated radiocarbon age (1,390 - 1,220 CalBP) obtained on the same sample provides general confirmation of this age.

Two finegrain OSL ages from a borehole sample (BHC2, 2.4 m) and a trial trench sample (4.5 m) from the middle portion of the main landslide, returned values of 44.6 ± 4.9 ka and 6.48 ± 0.7 ka, respectively. The OSL age from the trial trench is within 1σ error of the finegrain OSL age obtained from the lowermost colluvial unit in TPC3 (6.84 ± 0.51 ka).

The oldest age (44.6 ± 4.9 ka) colluvium identified in BHC2 (2.4 m) provides a minimum age for the onset of instability at the site, suggesting that landslide activity has continued periodically over the past 44,600 years. It is noteworthy that the oldest surface exposure age (^{10}Be 43.2 ± 2.1 ka) obtained from the landslide site is within 1σ error of the oldest age colluvium (Table 7).

Considering the limitations on the chronometric data and potential correlations, it is possible to identify four distinctive landslide events at the Tsing Shan C landslide site. The average ages of these landslide events are: Event 1 $c.44$ ka, Event 2 $c.16.4$ ka, Event 3 $c.6.7$ ka, and Event 4 $c.1.2$ ka.

8.2.3 Sham Wat Debris Lobe

(i) Sampling and Dating

The most comprehensive set of age data for the current study has come from the Sham Wat Debris Lobe as the site was found particularly suitable for the application of surface exposure dating and luminescence dating. Unlike the previous dating study (King, 2001), the data set in this study includes independent age controls.

Samples for surface exposure dating were collected from the prominent rock escarpment forming the source area for the main lobe (SWD-01 to SWD-05), as well as large boulders (SWD-06 to SWD-10) within the associated debris (Figure 19). In addition, samples of colluvium from drill core obtained during a previous study (King, 1998) were used for luminescence dating. These samples were collected from boreholes within the main (BH1, BH9A, BH9B, and BH11A) and southern (BH3, BH7) debris lobes. Except for two samples (BH1, 17.2 m, and BH9B, 8.1 m), most borehole samples were collected from depths of between 4.2 and 7.5 m. Only one colluvial layer was identified in the boreholes suggesting that the main, and southern debris lobes, were both emplaced as single units in single events. Trial pit (TP4) was excavated in alluvium upstream of the main debris lobe to provide material for luminescence and radiocarbon dating.

A total of 27 samples were dated, comprising 11 surface exposure ages, 13 luminescence ages, and three radiocarbon determinations (Table 8 and Figure 20).

(ii) Results and Interpretation

The five scarp ^{10}Be exposure ages from the main lobe range from 19.7 ± 2.2 ka to 38.0 ± 5.2 ka. The youngest age is an obvious outlier (SWD-04), and may reflect a spalled surface after the main event. If this age is excluded, the mean age of the remaining four scarp samples is 32.1 ± 6.2 ka.

The five boulder ^{10}Be exposure ages from the debris are much more variable, ranging from 33.1 ± 3.0 ka to 285 ± 23 ka. A single ^{26}Al exposure age (283 ± 36 ka) measured on a duplicate sample (SWD-07) is in good agreement with the ^{10}Be age (285 ± 23 ka). Combining the youngest boulder age with the four main scarp ages described above yields an average age of 32.3 ± 5.4 ka. The normalised χ^2 test on these five samples ($\chi^2/\nu = 1.72$) suggests they are part of a single population.

Five finegrain OSL ages from colluvial debris of the main lobe range from 27.9 ± 3.6 ka to 54.2 ± 5.2 ka, whereas two samples (HK17958 and HK12359) collected from the southern lobe (BH3, BH7) yielded finegrain OSL ages of 34.2 ± 3.8 ka and 23.9 ± 3.6 ka, respectively. Three 'Log Normal' SAR-OSL ages measured on duplicate samples (HK17956, HK17957 and HK12359) as an independent check on the accuracy and reliability of the luminescence results yielded values within 2σ error of the finegrain ages. In contrast

to earlier 'Leading Edge' SAR-OSL dose distribution results reported by King (2001), the luminescence results suggest that 'incomplete bleaching' of sediment grains during deposition of the Sham Wat Debris Lobe was not significant.

The oldest dated sample (HK17960) from the main debris lobe was collected from alluvial sand near the base of the lobe in drillhole BH9B, and is likely to be an outlier. If this age is excluded, the remaining luminescence ages lie between 27.9 ± 4.6 ka and 35.2 ± 3.8 ka, with an average age of 31.6 ± 3.3 ka. The two finegrain OSL ages from the southern lobe are identical, within 1σ error, to the luminescence ages of the main lobe suggesting that the two lobes were emplaced at a similar time.

A normalised χ^2 test on the ten best cosmogenic and luminescence ages for the Sham Wat Debris Lobe ($\chi^2/\nu = 1.12$) suggest they are part of a single population with an average age of 31.9 ± 0.9 ka. This value is considered to provide the most reliable age estimate of the Sham Wat Debris Lobe. Furthermore, the absence of any obvious stratigraphy, and the apparent uniformity in age with thickness of the deposit (4.3 - 17.3 m), suggest that the debris lobe was emplaced, more or less completely, in a single event. The apparent absence of incomplete bleaching of the sediment grains also suggests that the grains were fully exposed to sunlight during the depositional process.

Two samples of alluvium collected from depths of 0.1 m and 0.7 m in TP4, have yielded finegrain OSL ages of 6.22 ± 0.69 ka and 13.9 ± 1.9 ka, respectively. A 'Leading Edge' SAR-OSL age on a duplicate of one of these samples (HK12473) returned a value of 1.6 ± 0.16 ka, in strong discordance with the finegrain age. Three samples of alluvium collected from depths of 0.1 m, 0.3 m, and 0.4 m have also yielded radiocarbon ages of $1,489 \pm 40$ ^{14}C yr BP (1,520 - 1,290 CalBP), $3,167 \pm 43$ ^{14}C yr BP (3,480 - 3,320 CalBP), and $1,285 \pm 39$ ^{14}C yr BP (1,300 - 1,120 CalBP), respectively.

Although the finegrain OSL ages from TP4 are distinctly older than the three radiocarbon determinations on charcoal fragments from similar alluvial horizons, the 'Leading Edge' SAR-OSL age for HK12473 is in broad agreement with at least two of the radiocarbon measurements. In view of this agreement, and evidence from elsewhere concerning the application of the 'Leading Edge' SAR-OSL technique to dating of alluvium (e.g. Murray & Olley, 2002), it is likely that the alluvium between 0.1 and 0.7 m in TP4 contains incompletely bleached grains and has an age range of approximately 1.1 - 1.8 ka.

The radiocarbon and luminescence ages for sediments from TP4 are substantially younger than the luminescence and cosmogenic ages determined for the main debris lobe. Although the data from TP4 provide minimum ages on blockage of the valley by the landslide debris, the sediments are unlikely to have been ponded as an immediate response to emplacement of the main debris lobe. Younger landslide events that led to blockage of the main valley, spanning 30,000 years of environmental change, can not be ruled out.

8.2.4 Mid Levels Study Area

(i) Sampling and Dating

Five samples were collected for surface exposure dating from the main scarp area of a relict landslide feature NW of Victoria Peak (Figure 21). The samples included one (ML-04) considered only marginally suitable for dating because of unusual alteration characteristics.

Therefore, a duplicate sample (ML-05) was collected from the same location. No associated landslide debris was identified downslope from the relict feature.

(ii) Results and Interpretation

A total of five ^{10}Be surface exposure ages, ranging in value from <39 ka (ML-04) to 6.0 ± 1.6 ka (ML-01), were returned for the well-defined relict landslide main scarp (Table 9 and Figure 22). All of the samples were collected from relatively steep faces, more than 3 m below the inferred original land surface. Excluding the altered sample (ML-04), the normalised χ^2 test on the remaining four samples ($\chi^2/\nu = 0.54$) suggest they are part of a single population with a mean age of 7.2 ± 0.9 ka. This is considered the best age estimate for the landslide.

8.2.5 Tung Chung East Study Area

(i) Sampling and Dating

Material from two trial pits (TP17 and TP19), excavated near the head of Depression B (Figure 23) as part of a previous study (HAPL, 1999), was used for radiocarbon dating. In addition, material for luminescence dating was collected during this study from one trial pit (TP1) at the toe of the catchment draining Depression C.

A total of six ages were obtained (Table 10 and Figure 24), comprising four radiocarbon ages from charcoal fragments within two horizons (0.9 and 1.2 m) in TP17, one radiocarbon age from charcoal in TP19 (1.0 m deep), and one finegrain OSL age from colluvium in TP1 (2.2 m deep).

(ii) Results and Interpretation

Two samples of charcoal from the lower (1.2 m) horizon in TP17 returned identical radiocarbon ages, within 1σ error, of 337 ± 58 ^{14}C yr BP (510 - 290 CalBP) and 378 ± 58 ^{14}C yr BP (520 - 310 CalBP). Charcoal from the upper horizon (0.9 m) in TP17 yielded a radiocarbon age of 223 ± 49 ^{14}C yr BP (230 - 130 CalBP), whereas charcoal from a similar depth (1.0 m) in TP19 yielded an age of 200 ± 48 ^{14}C yr BP (320 - 60 CalBP). Colluvium recovered from TP1 at the toe of the catchment draining Depression C returned a finegrain OSL age of 13.5 ± 1.8 ka.

Unlike most other landslide sites within the present study, the radiocarbon ages at the Tung Chung East landslide site are associated mainly with shallow buried soil profiles ($<c.1.2$ m deep) in colluvial deposits, derived from relatively shallow open hillslope failures. However, the luminescence age from colluvium at the toe of the catchment draining Depression C records the age of a larger (>2.2 m thick), possibly a channelised debris flow, event.

Overall, three main landslide events are indicated by the age data. The oldest event (Event 1, c.13.5 ka) is recorded by the finegrain OSL age from TP1. Two younger landslide events (Event 2, 520 - 290 CalBP, and Event 3, 320 - 60 CalBP), are indicated by calibrated radiocarbon ages from TP17 and TP19, which are in stratigraphic order. However, the

overlapping ages serve to highlight a limitation of radiocarbon dating when applied to relatively young (<600 yr BP) deposits.

8.3 Large Relict Landslide Sites

8.3.1 Sunset Peak West

(i) Sampling and Dating

The sampling and dating programme largely focussed on features related to landslide No. 5 (Figure 25), owing to its well-defined source area and associated debris lobe. However, debris lobes of two other landslides (Nos. 3 and 6) were also dated for comparison with the relative chronology established by API. Several control samples were included (i) to calibrate ^{10}Be measurements, (ii) to provide data on the ages of rock surfaces adjacent to the main scarp, and (iii) to establish the approximate ages of the intervening debris lobes.

Samples for surface exposure dating were principally collected from the scarp and debris lobe regions of landslide No. 5 (Figure 25). One trial pit (TP2) and one borehole (BH1) in the debris lobe of landslide No. 5, and three trial pits (TP1, TP3 & TP4) in the debris lobes of landslide Nos. 3 and 6, were excavated to obtain material for radiocarbon and luminescence dating. One further borehole (BH2) was drilled in ancient colluvium between the debris lobes of landslide Nos. 5 and 6, to provide control samples.

A total of eighteen samples were dated (Table 11 and Figure 26), comprising 12 surface exposure ages from relict landslide No. 5, including two ages for control purposes, and six luminescence ages from landslide Nos. 3, 5, and 6. No material suitable for radiocarbon dating was identified.

(ii) Results and Interpretation

Three ^{10}Be exposure ages from the scarp/source area of landslide No. 5 age vary from 9.1 ± 1.1 ka to 7.4 ± 2.2 ka, with a mean age of 8.1 ± 0.9 ka. The youngest sample (TCR-01) came from the lower part of the scarp, whereas the oldest sample (TCR-02) came from the upper part of the scarp. A fourth sample (TCR-03), collected for control purposes from a rock surface adjacent to the main scarp, returned an age of 70.5 ± 6.1 ka.

The range of surface exposure ages from the scarp source area (9.1 - 7.4 ka) of landslide No. 5 can be explained in terms of variations in the degree of cosmogenic isotope inheritance. The youngest sample (7.4 ± 2.2 ka) was collected from the base of the main scarp, well below (>3 m) the presumed original surface and is unlikely to preserve an inherited cosmogenic signature from prior to the landslide. This sample indicates the minimum age of the landslide scarp. However, other samples collected at slightly higher levels and shallower depths in the main scarp are slightly older (7.7 ± 2.9 ka and 9.1 ± 1.1 ka), and may preserve partly inherited cosmogenic isotope signatures. The age of the rock surface adjacent to the main scarp (70.7 ± 6.0 ka) provides a minimum age of the original land surface prior to slope failure.

Four large boulders, protruding from the debris lobe of landslide No. 5, and analysed for surface exposure dating, yielded ^{10}Be exposure ages of 15.1 ± 2.5 ka (TCR-09), 27.2 ± 1.4

ka (TCR-08), 41.1 ± 3.9 ka (TCR-07), 52.0 ± 5.2 ka (TCR-10), 226.0 ± 7.8 ka (TCR-05) and 283.1 ± 9.8 ka (TCR-06). The two oldest samples (TCR-05 and TCR-06) from the same boulder were also dated using ^{26}Al . The independent ^{26}Al exposure ages (227.0 ± 18 ka and 284 ± 22.0 ka) are in very good agreement with the ^{10}Be exposure ages.

The oldest surface exposure age (284 ± 22 ka) among boulders protruding from the debris lobe of landslide No. 5 provides a maximum age for material from the source area. The ^{26}Al ages for two of these boulders provide general confirmation of the ^{10}Be ages. The range of surface exposure ages (c.15 - 52 ka) among the remaining boulders suggests that they all contain a measure of cosmogenic isotope inheritance (i.e. they were probably derived from source area depths of <3 m from the original land surface).

Finegrain OSL ages from landslide No. 5, for material from TP2 (1.5 m) and BH1 (1.2 m), returned ages of 5.57 ± 0.4 ka and 7.04 ± 0.53 ka, respectively. These ages are in broad agreement with the minimum surface exposure ages determined for the source area. The combined luminescence data for the debris lobe and cosmogenic isotope age data for the source area of landslide No. 5, give an average age of 7.4 ± 1.3 ka. This is the best estimate of the age of the landslide.

A finegrain OSL age of 8.95 ± 1.05 ka was obtained from a levee of colluvial debris from landslide No. 3 (TP1, 1.2 m). Finegrain OSL ages from TP3 (0.9 m) and TP4 (1.8 m) within debris of landslide No. 6, returned values of 16.5 ± 2.8 ka and 7.3 ± 0.63 ka, respectively. With the exception of TP3, the luminescence ages for colluvium from landslide No. 3 and landslide No. 6 lie within the range of ages for colluvium from Landslide No. 5. This suggests a period of general instability in the area between c.9.1 and c.5.6 ka. Overall, the luminescence age data are generally consistent with the relative landslide chronology determined from API.

A finegrain OSL age from colluvial debris (in BH2 at 2.5 depth) between the lobes of landslide No. 5 and landslide No. 6, returned a value of 24.3 ± 2.5 ka. This OSL age confirms the API that this material is likely to be composed of relatively ancient colluvium.

8.3.2 Tai O

(i) Sampling and Dating

The main purpose of the dating at Tai O was to establish the chronology of the colluvium in the three main debris fans (Figure 27). Samples for luminescence and radiocarbon dating were collected from trial pits (TP1-TP3) within these debris fans, and from boreholes (BH1-BH3) drilled at their base. Owing to the complexity of source areas of the main debris fans, no suitable sites for surface exposure dating were identified. Trial pits in the middle portions of the debris fans sampled shallow horizons, whereas boreholes in the toe areas of the fans sampled deeper material, and interbedded estuarine deposits.

A total of 12 ages were obtained from eight samples (Table 12 and Figure 28), comprising six finegrain OSL ages, two SAR-OSL ages on duplicate samples, and four radiocarbon determinations.

(ii) Results and Interpretation

Shallow (0.8 m) colluvium from TP1 in Debris Fan A returned a finegrain OSL age of 0.821 ± 0.147 ka, whereas colluvium at 2.5 m depth in an adjacent borehole (BH1) yielded a finegrain OSL age of 4.38 ± 0.53 ka.

Charcoal from a buried soil horizon within Debris Fan B (TP2 at a depth of 1.1 m) yielded two radiocarbon ages of $1,195 \pm 44$ ^{14}C yr BP (1,260 - 970 CalBP) and $1,122 \pm 43$ ^{14}C yr BP (1,170 - 930 CalBP). The enclosing colluvium of the soil horizon yielded both finegrain OSL and 'Log Normal' SAR-OSL ages of 1.11 ± 0.16 ka and 1.02 ± 0.07 ka, respectively. Colluvium at the toe of Debris Fan B, at a depth of 4.0 m in BH2, yielded a finegrain OSL age of 20.3 ± 3.2 ka.

Colluvium in Debris Fan C, from a depth of 1.0 m in TP3, yielded both finegrain OSL and 'Log Normal' SAR-OSL ages of 4.26 ± 0.37 ka and 1.54 ± 0.20 ka, respectively, whereas a radiocarbon determination on charcoal from the same horizon, returned a value of $11,758 \pm 72$ ^{14}C yr BP (14,150 - 13,350 CalBP). Colluvium, from 6.3 m deep at the toe of Debris Fan C, returned a finegrain OSL age of 20.6 ± 2.1 ka.

Although it was not possible to confirm the relative chronology for the three debris fans from API, the OSL and radiocarbon age data for shallow (<1.1 m) colluvium from Debris Fan A and Debris Fan B reveal overlapping ages of c.1,000 yr BP. In particular, there is good agreement between the radiocarbon ages and the finegrain OSL and 'Lognormal' SAR-OSL ages for colluvium in trial pit TP2.

Colluvium at deeper levels (4-6 m) within Debris Fan B and Debris Fan C (BH2 and BH3) also yield overlapping OSL ages of c.20,000 yr BP, although the radiocarbon age from BH3 is spurious. The finegrain OSL age from BH1 (2.5 m) suggests an event c.4,400 years ago. This is supported by a finegrain OSL age of similar magnitude for colluvium from TP3. However, the unusually wide variation in OSL and radiocarbon ages from shallow colluvium in Debris Fan C could be explained by anthropogenic activity associated with grave excavation. Accordingly, the stratigraphy from TP3 may be partly disturbed and the age data difficult to relate to landslide events.

Overall, a comparison of the luminescence and radiocarbon age data for the three debris fans suggest that major landslide events occurred c.20,000, c.10,000, c.4,400 and c.1,000 yr BP.

8.3.3 Sai Tso Wan

(i) Sampling and Dating

The main purpose at this composite site was to establish numerical ages for selected large landslides, and to compare these with the relative landslide chronology from API. Samples for luminescence and radiocarbon dating were collected from six trial pits (TP5 - TP11) and one borehole (BH4) sited within four of the six main drainage depressions (Depressions. Nos. 1, 2, 5 and 6, Figure 29). Three trial pits (TP7, TP8 and TP9) were sited within the largest depression (Dep. No. 2) to date colluvium related to three specific relict landslide features. Borehole BH4 was sited at the toe of a debris fan derived mainly from drainage depression No. 2.

A total of 19 ages were obtained from 12 samples (Table 13 and Figure 30), comprising nine finegrain OSL ages, three SAR-OSL ages from duplicate samples, and seven radiocarbon determinations, three from hand samples, three from U100 steel tubes, and one from drill core.

(ii) Results and Interpretation

Single event landslides were considered from API to have formed the debris lobes of Depressions Nos. 5 and 6. Colluvium from 0.8 m depth within debris of these Depressions (TP10 and TP11) yielded finegrain OSL ages of 14.8 ± 1.8 ka and 11.8 ± 2.0 ka, respectively, with an average age of 13.3 ± 2.1 ka.

Finegrain OSL ages of 1.65 ± 0.18 ka and 14.4 ± 1.7 ka were also returned from the main lobe of Depression No. 2 (TP8), and from debris of Relict Landslide No. 1 (TP9), respectively. However, an SAR-OSL age on a duplicate sample from TP8 returned a 'Log Normal' value of 3.93 ± 1.08 ka, and a 'Leading Edge' value of 11.5 ± 0.9 ka, both of which are inconsistent with the finegrain OSL age.

According to the API, the debris lobes for Depressions Nos. 1 and 2 formed from cumulative landslide events. With respect to Depression No. 2., the finegrain OSL age for TP9 (14.4 ± 1.7 ka) and the 'Leading Edge' SAR-OSL age for TP8 (11.5 ± 0.9 ka) are within error of the luminescence ages returned for the debris lobes of Depressions Nos. 5 (14.8 ± 1.8 ka) and 6 (11.8 ± 2.0 ka). These ages suggest that several of the large landslide features at the Sai Tso Wan site might have similar ages. Combining the luminescence age data from the four trial pits gives an average age of 13.1 ± 1.7 ka.

Samples from TP6 near the confluence of Depressions Nos. 1 and 2 comprised mostly shallow alluvium. Finegrain OSL ages of 2.82 ± 0.62 ka and 1.34 ± 0.11 ka were obtained on alluvial samples from depths of 0.1 m and 0.6 m, respectively. However, an SAR-OSL age on the same material from 0.1 m yielded a 'Log Normal' value of 0.79 ± 0.10 ka and a 'Leading Edge' value of 0.36 ± 0.03 ka, in marked contrast to the finegrain OSL age. Moreover, fragments of charcoal within the alluvium collected from depths between 0.2 and 0.6 m in TP6 have yielded radiocarbon ages ranging from 170 ± 46 ^{14}C yr BP (300 - 60 CalBP) to 703 ± 47 ^{14}C yr BP (730 - 620 CalBP). Together, the 'Leading Edge' SAR-OSL age interpretation and radiocarbon determinations suggest that the shallow (0.1 - 0.6 m) alluvium in TP6 is probably less than 700 years old.

Colluvium from 1.0 m depth in Relict Landslide No. 2 (TP7) yielded a finegrain OSL age of 3.57 ± 0.32 ka, a 'Log Normal' SAR-OSL age of 2.66 ± 0.30 ka, a 'Leading Edge' SAR-OSL age of 1.52 ± 0.15 ka, and a radiocarbon age of $2,416 \pm 45$ ^{14}C yr BP (2,550 - 2,340 CalBP). Since the 'Log Normal' SAR-OSL age is comparable with the calibrated radiocarbon age (2,550 - 2,340 CalBP) for the same sample, this is the best estimate of the age of the colluvium.

A finegrain OSL age of 7.93 ± 0.68 ka was obtained from the colluvial lobe at the base of Depression No. 1 (TP5). This age is unlike any other nearby. Either a separate event occurred c.8.0 ka for which no other record has so far been observed, or the sample has been incompletely bleached, in which case, a 'Leading Edge' SAR-OSL dating approach would be

more applicable. It is noteworthy that the sample in TP5 came from 0.8 m deep, well within the depth range of incompletely bleached alluvial samples in nearby TP6.

Colluvium from 2.6 m deep in BH4 at the toe of Depression No. 2, yielded a finegrain OSL age of 10.5 ± 1.2 ka, and a radiocarbon age of $10,658 \pm 116$ ^{14}C yr BP (13,000 - 12,300 CalBP). These ages are generally consistent with the ages of colluvium from trial pits nos. 8 and 9 in the middle portions of Depression No. 2, and with the ages of debris in Depressions Nos. 5 and 6 (see above).

Overall, the luminescence and radiocarbon age data for debris lobes suggest that large landslide events at Sai Tso Wan occurred mainly between approximately 15,000 and 8,000 years ago. Smaller landslide events may have occurred between approximately 3,000 and 1,000 years ago. However, alluvium that has accumulated near the toe of the two main drainage depressions is probably <700 years old, although the ages obtained from TP6 are close to the lower limit of analytical precision for luminescence and radiocarbon dating. Overall, the age data confirm the relative chronology established from API.

8.3.4 Wong Lung Hang

(i) Sampling and Dating

Despite the numerous clusters of relict landslide scarps, dating principally focussed on colluvial materials in three main debris lobes draining Catchments A, B, and C (Figure 31). Debris Lobe Nos. 2 and 3 were considered, on the basis of API, to represent the deposits of two large landslides (debris flows) which partly blocked the main northwest flowing stream. Debris Lobe No. 1 was considered to be an accumulation of debris from Catchment A.

Samples of colluvium from Debris Lobes Nos. 1, 2, and 3 (Figure 31), were collected for luminescence and radiocarbon dating from three trial pits (TP5, TP6, and TP7). In addition, one further trial pit (TP8) within alluvium immediately upstream of Debris Lobe No. 3, provided material for luminescence and radiocarbon dating. Three large boulders (WLH-01, WLH-02, and WLH-03) in the main river channel within Debris Lobe No. 3 were sampled for surface exposure dating.

A total of twenty-one ages were obtained (Table 14 and Figure 32), comprising three surface exposure ages, six finegrain OSL ages, five SAR-OSL ages, and seven radiocarbon determinations. Most of the radiocarbon determinations were obtained from samples of charcoal within stream alluvium (TP8), whereas most of the OSL ages were from colluvium.

(ii) Results and Interpretation

The three large boulders exposed in the main river channel returned widely ranging ^{10}Be exposure ages of 39.2 ± 2.7 ka, 64.6 ± 5.1 ka and 29.6 ± 1.7 ka. They provide a maximum age for Debris Lobe No. 3 of 64.8 ± 6.8 ka.

Colluvium from Debris Lobe No. 3 (TP7, 0.5 m) yielded a finegrain OSL age of 5.18 ± 0.61 ka. A 'Log Normal' SAR-OSL age for the same sample from TP7 returned a value of 5.74 ± 0.35 ka, indicating that it lies within 1σ error of the finegrain OSL age. A radiocarbon determination on a small fragment (0.02 g) of charcoal from TP7 (0.5 m)

returned a value of $13,800 \pm 67$ ^{14}C yr BP (17,100 - 16,050 CalBP), which is considerably older than the OSL ages. This is almost certainly the result of incorporated older organic material. Overall, the finegrain OSL and SAR-OSL ages from TP7 provide the best estimate of the age for Debris Lobe No. 3, with an average value of 5.46 ± 0.40 ka.

A finegrain OSL age of 4.58 ± 0.60 ka was obtained for colluvium from Debris Lobe No. 2 (TP6, 1.0 m). This age is slightly younger than, but overlaps with, the estimated age for Debris Lobe No. 3 (see above). According to the API, colluvium from Debris Lobe 2 was considered to have been partly deflected by material from Debris Lobe No. 3, and thereby, to be slightly younger in age. This interpretation is generally confirmed by the luminescence age from TP6, although there is no independent confirmation of this age.

Colluvium from TP5 (1.7 m) in Debris Lobe No. 1 yielded a finegrain OSL age of 18.0 ± 2.4 ka, whereas a 'Log Normal' SAR-OSL age for the same sample returned a similar value, within 1σ error, of 15.9 ± 1.6 ka. A radiocarbon determination on a single (0.02 g) fragment of charcoal within the colluvium returned a value of 230 ± 42 ^{14}C yr BP (310 - 60 CalBP).

The luminescence data from TP5 indicate that colluvium within Debris Lobe No. 1 was most likely deposited between 20.4 and 14.3 ka. The considerably younger age obtained from disseminated charcoal (230 ± 42 ^{14}C yr BP (310 - 60 CalBP)) within the same sample is almost certainly the result of infiltration of transported material.

TP8 was excavated in alluvium immediately upstream of the Debris Lobe No. 3 to date possible ponding caused by Debris Lobe No. 3 blocking the main stream channel (Figure 31). Five radiocarbon determinations and six OSL ages were obtained from several alluvial horizons in the trial pit. These comprised three hand samples containing charcoal, one from a depth of 0.8 m and two from 0.9 m, which yielded radiocarbon ages of 377 ± 49 ^{14}C yr BP (510 - 310 CalBP), 535 ± 39 ^{14}C yr BP (570 - 500 CalBP) and 194 ± 47 ^{14}C yr BP (310 - 60 CalBP), respectively. Three U100 samples were also collected for luminescence and radiocarbon dating, at depths 0.3 m, 0.5 m, and 0.8 m. The sample from 0.3 m yielded a finegrain OSL age of 5.17 ± 0.38 ka, while a 'Leading Edge' SAR-OSL age for same sample returned a value of 0.51 ± 0.07 ka. The sample from 0.5 m yielded a finegrain OSL age of 3.39 ± 0.35 ka and a 'Leading Edge' SAR-OSL age of 0.77 ± 0.06 ka, whereas fragments of charcoal from the same sample returned a radiocarbon age of 349 ± 58 ^{14}C yr BP (510 - 300 CalBP). The sample from 0.8 m yielded a finegrain OSL age of 1.35 ± 0.09 ka, and a 'Leading Edge' SAR-OSL age of 0.27 ± 0.02 ka, whereas charcoal from the same sample yielded a radiocarbon age of $2,482 \pm 43$ ^{14}C yr BP (2740 - 2430 CalBP).

The 'Leading Edge' SAR-OSL values (Table 14, Figure 32) are generally in close agreement with the associated radiocarbon data. This independent confirmation of age using the 'Leading Edge' SAR-OSL approach suggests that the alluvial samples have been incompletely bleached, similar to the alluvial samples from the Sai Tso Wan and Sham Wat Debris Lobe landslide sites (see Sections 9.2(iii) and 9.3(iii)). Overall, the 'Leading Edge' SAR-OSL ages and radiocarbon determinations suggest that the alluvium in TP8 was deposited between 200 and 500 years ago. Therefore, the alluvium is unlikely to be directly associated with ponding related to the emplacement of Debris Lobe No. 3.

In summary, the age data for the Wong Lung Hang site are generally consistent with the relative landslide chronology determined from API, and suggest that large-scale landslide events forming Debris Lobe No. 1, and Debris Lobe Nos. 2 and 3 occurred at c.20 - 14 ka,

and c.5.5 - 4.8 ka, respectively. Debris Lobe No. 2 is only slightly younger than Debris Lobe No. 3. Younger events may have occurred between 3,000 and 1,000 years ago. The alluvium immediately upstream of Debris Lobe No. 3 appears to be less than 1,000 years old.

8.4 Additional Sites

8.4.1 South East Tsing Yi

(i) Sampling and Dating

Samples for surface exposure dating were collected from various locations within two large colluvial lobes (Debris Lobe No. 4 and Colluvium No. 1), and their source escarpments (Sheeting Joint Nos. 1 and 2), at the Tsing Yi landslide site (Figure 33).

A total of seven samples (TY-01 to TY-07) were collected, although one sample (TY-06) was not analysed. The analysed samples comprised three large boulders (TY-01 to TY-03) from colluvial debris, and three rock surfaces (TY-04, TY-05 and TY-07) from adjacent escarpments (Table 15 and Figure 34).

(ii) Results and Interpretation

The two analysed boulders (TY-01 and TY-02) within Debris Lobe No. 4 returned almost identical ^{10}Be surface exposure ages of 47.7 ± 4.1 ka and 47.3 ± 4.0 ka, respectively. The third boulder, within the adjacent Colluvium No. 1, yielded a ^{10}Be surface exposure age of 35.3 ± 3.1 ka. The two analysed samples (TY-04 and TY-07) from Sheeting Joint No. 1 returned ^{10}Be surface exposure ages of 44.8 ± 3.7 ka and 48.5 ± 4.0 ka, respectively. A duplicate of sample TY-04, also returned a ^{26}Al exposure age of 40.5 ± 12 ka, in broad agreement with ^{10}Be exposure age. Sheeting Joint No. 5 returned a ^{10}Be surface exposure age of 11.0 ± 1.6 ka.

The surface exposure ages for the South East Tsing Yi landslide site are remarkably consistent and indicate that most of the debris in the colluvial lobes were derived from the Sheeting Joint No. 1 escarpment. A normalised χ^2 test on the five cosmogenic samples ($\chi^2/\nu = 0.23$) from Sheeting Joint No. 1 and Debris Lobe No. 4 suggest they are part of a single population with a mean age of 45.8 ± 3.2 ka. A single outlier, represented by a boulder age of 35.3 ± 3.1 ka (TY-03), could be explained if this boulder was originally buried during the original landslide event, but was subsequently exhumed. The younger surface exposure age for Sheeting Joint No. 5 (11.0 ± 1.6 ka) is consistent with the relative chronology established from API (see Section 5.4).

8.4.2 Lion Rock

(i) Sampling and Dating

Samples for surface exposure dating were collected from three very large (20 m diameter) isolated boulders within debris fan deposits forming parts of three colluvial lobes on the southern side of Lion Rock, to the north of Chui Chuk Garden (Figure 35).

Three ^{10}Be exposure ages were obtained from samples from the upper surfaces of boulders (Table 16 and Figure 36).

(ii) Results and Interpretation

Sample LR-01, located on the boundary between Colluvium No. 2 and Colluvium No. 3, returned an age of 3.7 ± 0.4 ka. Samples LR-02 and LR-03, within Colluvium No 5, returned ages of 3.8 ± 0.5 ka and 2.3 ± 0.4 ka, respectively.

The surface exposure ages for the boulders are in general agreement, with at least two boulders having identical ages, within 1σ error. The age data suggest that the boulders were all detached from their source areas between c.1.9 - 4.3 ka, with LR-01 and LR-02 being emplaced in an older event (c.3.8 ka), and LR-03 (c.2.3 ka) being emplaced in a younger event (Figure 36).

With respect to the API (Figure 35), the data suggest that the boulders LR-02 and LR-03 are younger than their surrounding colluvium (Colluvium No. 5). They may have been emplaced as single rock fall events onto, and, or bulldozing into, the older colluvium, rather than as boulders within a debris slide or debris flow. Compared with the API, the age for LR-01 also suggests that Colluvium No. 3 is younger than c.3.3 ka.

8.4.3 Fei Ngo Shan

(i) Sampling and Dating

Samples were collected for surface exposure dating from the upper surfaces of three large boulders within a relatively tight cluster in a single colluvial unit (Unit No. 1) on the southern flanks of Fei Ngo Shan, immediately above the road (Jat's Incline) (Figure 37).

Three samples were analysed (Table 17 and Figure 38). Sample FNS-01 was collected nearest the road, whereas samples FNS-02 and FNS-03 were collected approximately 40m to the southeast of sample FNS-01.

(ii) Results and Interpretation

All three boulders yielded identical ^{10}Be exposure ages, within 1σ error. Sample FNS-01 returned an age of 58.8 ± 5.3 ka, whereas samples FNS-02 and FNS-03 returned ages of 60.4 ± 5.5 ka and 54.7 ± 4.8 ka, respectively.

The surface exposure ages are in close agreement. A normalised χ^2 test on the three surface exposure ages ($\chi^2/\nu = 0.34$) suggest they are part of a single population with a mean age of 58.0 ± 2.9 ka. Due to the complexity and general degradation of the upper flanks of Fei Ngo Shan, the source of the boulders is uncertain. However, the API and absolute age data suggest that the host colluvium and large boulders were emplaced at approximately the same time.

8.4.4 Seymour Cliffs

(i) Sampling and Dating

Samples were collected for surface exposure dating from rock surfaces forming sheeting joints, and a prominent cliff, at the site, informally known as Seymour Cliffs, above Seymour Road, Mid-Levels (Figure 39).

Three samples (SC-01, SC-02 and SC-03) were analysed (Table 18 and Figure 40). SC-01 and SC-03 were taken from two locations on a prominent granite sheeting joint in the lower cliff, whereas SC-02 was from an upper prominent cliff formed of vitric tuff, above the granite sheeting joints.

(ii) Results and Interpretation

The ^{10}Be surface exposure ages for the three samples are rather variable. SC-02 and SC-03 returned ages of 17.1 ± 2.4 ka and 21.4 ± 2.0 ka respectively, which overlap marginally, within 1σ error. SC-01, derived approximately 30 m above SC-03, yielded a surface exposure age of 31.5 ± 3.3 ka.

The age data suggest that the granite sheeting joint surface has been subject to periodic spalling, and is variable in age. The orientation of relict landslide scars on the sheeting joint surface (Figure 39), coupled with the overlapping ages for SC-02 and SC-03, further suggests that detachment of jointed granite blocks may have been assisted by entrainment within rock falls derived from the cliffs above.

9. INDEPENDENT AGE CONTROL AND COMPARISONS OF THE DATING TECHNIQUES

Except for the additional sites where surface exposure dating only was carried out, independent age control was established at all of the landslide sites using at least two, and sometimes three, of the dating techniques available. In addition, the SAR luminescence ages and ^{26}Al ages provided independent tests of the accuracy and reliability of the finegrain luminescence and ^{10}Be cosmogenic dating techniques, respectively. General duplicates were also periodically taken at random, particularly for radiocarbon analysis. With the exception of site measurements required for cosmogenic sampling, no contextual or relative age information on samples was provided to the analytical laboratories. Neither was there any communication between the laboratories, nor was there special ordering of the samples submitted to the laboratories for processing and measurement (i.e. the laboratories carried out essentially blind tests). In light of these measures, the following discussion compares the results for the various dating techniques.

9.1 Comparison between 'Leading Edge' SAR Luminescence Ages and Radiocarbon Determinations

Good agreement between 'Leading Edge' SAR luminescence ages and radiocarbon determinations was achieved for six samples from Tsing Shan, Sham Wat, Wong Lung Hang and Sai Tso Wan sites (Table 19a). The samples all came from relatively shallow depths

(<1.0 m), and mostly from material considered to be alluvium. In one case (HK12376), material may have been disturbed by anthropogenic activity. In general, the luminescence ages are slightly older than the range of calibrated radiocarbon ages (95% confidence level), although this difference is narrowed slightly if 50 years is added to account for the 1950 age datum.

9.2 Comparison between ‘Log Normal’ SAR Luminescence Ages and Finegrain Luminescence Ages

Excellent independent age control was achieved for nine samples from the Sai Tso Wan, Tsing Shan, Wong Lung Hang, Lo Lau Uk and Lei Pui Street landslide sites using ‘Log Normal’ SAR luminescence ages compared with finegrain luminescence ages (Table 19b). All of the samples were of colluvium, and most from depths of c.1m or greater. In most cases, the ‘Log Normal’ SAR ages are slightly younger than the finegrain ages, although almost all of the ages are within 1σ error.

9.3 Comparison between Finegrain Luminescence Ages and Radiocarbon Determinations

Good agreement between finegrain luminescence ages and radiocarbon determinations was obtained for four samples from the Pat Heung, Tai O and Sai Tso Wan landslide sites (Table 19c). All samples were of colluvium and recovered from depths of c.1 m or greater. A duplicate radiocarbon age (HK12419) at the Tai O site provided further confirmation of the age determination, whereas a duplicate ‘Log Normal’ SAR luminescence age from the Tai O site also provided an excellent match. At one of the Sai Tso Wan sites (TP7, HK12480), good agreement was obtained between the ‘Log Normal’ SAR age and the radiocarbon age, although the finegrain luminescence age is within 2σ error.

9.4 Comparison between Luminescence Ages and Cosmogenic ^{10}Be Exposure Ages

Four landslides sites have exhibited good agreement between luminescence ages and cosmogenic ^{10}Be exposure ages (Table 19d). The most comprehensive set of control samples has come from the Sham Wat Debris Lobe where six samples have yielded independent finegrain ages which are within 1σ error of the average ^{10}Be exposure age determined from four scar samples and one boulder sample. In addition, ‘Log Normal’ SAR ages on three samples from the Sham Wat Debris Lobe have provided further confirmation of the cosmogenic ages.

10. COMPARISONS OF RELATIVE VERSUS NUMERICAL AGES

One objective of the dating study was to evaluate the chronometric data in relation to other age data, such as the relative ages of landslides determined from API, and the relative ages of colluvial units determined from stratigraphic observations in trial pits. The purpose of this evaluation was two fold: i) to see whether the API was sufficiently accurate and precise to be used to determine the relative ages of landslides where no chronometric data were available, and ii) to see whether the chronometric data were compatible with the stratigraphy.

10.1 Relative Ages of Landslide Determined from API

Determining the relative ages of landslides from API was generally only possible at those sites where clusters of landslides displayed overlapping relationships. Accordingly, out of the nineteen landslide sites investigated, only eight sites enabled a relative chronology to be established. These included the Lai Cho Road landslide site, the Ap Lei Chau landslide site, the Tsing Shan A landslide site, the Sham Wat Debris Lobe, the Sunset Peak West landslide site, the Sai Tso Wan landslide site, the Wong Lung Hang landslide site and the South East Tsing Yi landslide site. However, owing to various sampling difficulties (see Chapter 4) not all landslides from these sites were datable. In two cases (Ap Lei Chau and Tsing Shan A), only one landslide could be dated so that the relative chronology established from API could not be confirmed. Of the remaining six landslide sites, the relative ages determined from API are generally comparable to the numerical ages, except for the Sham Wat Debris Lobe. The API suggested that the Sham Wat Debris Lobe comprised a main lobe, and a younger southern lobe. However, the chronometric data strongly suggest that the debris lobe was emplaced as a single large event.

In summary, of the six landslide sites that were suited to analysis, five showed broad agreement between the relative landslide chronology determined from API and the landslide chronology determined from chronometric data.

10.2 Relative Ages of Colluvial Units Determined From Stratigraphic Observations

Stratigraphic observations within trial pits may permit the relative ages of colluvial units to be determined where each debris layer is assumed to have been deposited in systematic order. However, in some landslides (e.g. translational slides) it is possible for an older basal debris layer to directly overlie younger debris leading to apparent reversals in the stratigraphy. Nevertheless, in most cases the multiple layered debris deposits can be expected to display a normal stratigraphy, especially where alluvium is preserved.

Trial pits at several open hillslope landslide sites yielded well-preserved colluvial and alluvial layers that permitted a test of the accuracy and reliability of both radiocarbon and luminescence dating techniques.

In trial pit TP19 at the Tung Chung East landslide site, two buried soil horizons containing organic material, separated by distinctive colluvial units, were sampled for radiocarbon dating. The radiocarbon dating results were found to be consistent with the observed stratigraphy. These results were subsequently confirmed by dates obtained on organic material at similar depths in an adjacent trial pit (TP17).

Similarly, in trial pit TP6 at the Sai Tso Wan landslide site, three layers of alluvium were dated, but this time using luminescence techniques. The results were found to be entirely consistent with the observed stratigraphy. Thus, the relative ages of colluvial and alluvial units in these shallow open hillslope landslides, determined from the observed stratigraphy, appear to be reliable. The results also provide a measure of confidence in the radiocarbon and luminescence dating techniques, particularly their application to dating relatively shallow deposits.

11. APPLICATIONS OF DATING TECHNIQUES TO SPECIFIC LANDSLIDE HAZARD MODELS

The results of this dating study enable interim guidelines to be drawn on which dating technique, or combination of dating techniques, is suitable for the main landslide hazard models (Open Hillslope Landslide, Channelised Debris Flow, Deep Seated Landslide, Rock Fall and Boulder Fall) found in Hong Kong. The potential applications of dating techniques to these five hazard models are now considered sequentially.

11.1 Open Hillslope Landslides

Open hillslope landslides in Hong Kong, including debris slides and debris avalanches, are generally characterised by shallow detachment of partially or fully saturated debris on steep slopes (Ng et al. 2002). The resulting debris units are relatively thin and may preserve buried soil profiles at their base. Rock scarps are generally not formed, and the debris usually do not contain large (>1 m) boulders. Such deposits, therefore, are best suited to radiocarbon and/or OSL dating techniques. If organic-rich buried soil profiles are not preserved, material suitable for radiocarbon analysis may be present as finely disseminated charcoal fragments within the debris. However, in such cases, care should be exercised to avoid any possibility of including reworked material, or material introduced by infiltration or root penetration. For debris less than 1 m thick, the 'Leading Edge' SAR OSL method is recommended since the sediment is likely to have been transported a short distance, possibly under turbulent and/or turbid conditions, and may have been incompletely bleached. For debris greater than 1 m thick, including debris slides and debris avalanches, which may have traveled greater distances, the finegrain OSL or 'Log Normal' SAR OSL method is recommended. An example of this type of hazard model which has been successfully dated using a combination of luminescence dating and radiocarbon dating methods is the Lo Lau Uk landslide site (Dep. B, see Section 8.1.2).

11.2 Channelised Debris Flows

Channelised debris flows result from saturated debris, derived from one or more open hillslope landslides, entering a stream channel, and mixing with stream water to produce a slurry flow or hyper-concentrated flow (Ng et al. 2002). Channelised debris flows have much greater mobility than open hillslope landslides and generally produce thicker colluvial units. The methods best suited to dating of debris derived from channelised debris flow are radiocarbon and/or OSL. Material suitable for radiocarbon dating may be present as finely disseminated fragments of charcoal. For OSL dating, the finegrain or 'Log Normal' SAR methods are recommended, although where alluvium is present immediately overlying the debris deposit, the 'Leading Edge' SAR method may be applicable. Rock scarps may be exposed in the upper stream channels as a result of the erosional processes during entrainment of debris, and along with their derivative boulders, may provide suitable sites for surface exposure dating. However, in order to obtain meaningful results, these scarps and related boulders must originally have been deeper than 3 m from surface. Examples of this type of hazard model which have been successfully dated using a combination of surface exposure dating and luminescence dating methods include the Sunset Peak West (Landslide No. 5, see Section 8.3.1) and the Ap Lei Chau (RLS1 Landslide, see Section 8.2.1) landslide sites.

11.3 Deep-seated Landslides

Displacement of large, intact masses by sliding or avalanching along a basal rupture surface will often expose deep rock scarps (i.e. > 3 m deep from the original land surface) and produce thick debris deposits containing numerous boulders. These deep-seated landslides are therefore best suited to combinations of dating techniques. Rock scarps in the detachment area may provide suitable sites for surface exposure dating, along with derivative boulders in the landslide debris. Finegrain and 'Leading Edge' SAR OSL methods may also be applied to the landslide debris, along with radiocarbon dating methods if suitable organic material (see above) is present. Examples of this type of model which have been successfully dated using a combination of surface exposure dating, luminescence dating, and radiocarbon dating methods include the Sham Wat Debris Lobe (see Section 8.2.3), Tai O (Debris Fan B, see Section 8.3.2), and South East Tsing Yi (Sheeting Joint No. 1 and Debris Lobe No. 4, see Section 8.4.1) landslide sites.

11.4 Rock Fall and Boulder Fall

Large (> 3 m), isolated, angular and rounded rock fragments, which may have been transported by rolling, bouncing, and sliding from their detachment areas, are best dated using surface exposure dating. Commonly, the detachment locations of these rocks and boulders are not known and care must be exercised to avoid any possibility that these large rock fragments have been exhumed. If accessible, debris beneath the rocks and boulders may be suitable for OSL dating. Examples of successfully dated rock falls and boulder falls using cosmogenic isotopes include the Lion Rock (see Section 8.4.2) and Fei Ngo Shan (see Section 8.4.3) sites.

12. CONCLUSIONS AND RECOMMENDATIONS

12.1 Dating of Natural Terrain Landslides

The following general conclusions are made with respect to dating of natural terrain landslides:

- (a) This study has shown that direct dating of carefully selected, relict natural terrain landslide scars in Hong Kong is viable.
- (b) The correct interpretation of the chronometric data depends on detailed geomorphological observations taken prior to and during sampling.
- (c) The chronometric data may yield maximum and minimum ages of the landslides and their deposits, rather than their actual emplacement age.
- (d) With respect to cosmogenic nuclide analysis using ^{10}Be and ^{26}Al , the sensitivity of the AMS technique is sufficiently high to measure exposure ages of surfaces associated with landslides of a few thousand years, despite the unfavourable circumstances of low latitude and low altitude.

- (e) With respect to luminescence dating, it is possible to successfully date large natural terrain landslide deposits up to 17 m thick using both the finegrain and SAR techniques despite the unfavourable circumstances affecting bleaching of sediment grains.
- (f) With respect to radiocarbon dating, it is possible, with care to avoid reworked material, to date natural terrain landslides using fragments of disseminated charcoal down to a minimum weight of 5 mg identified and separated with the aid of a binocular microscope.

12.2 Recommended Numerical Dating Techniques

The following techniques are recommended for direct dating of relict natural terrain landslides in Hong Kong:

- (a) For large landslides with well-defined main scarps and associated debris lobes, in situ surface exposure dating (cosmogenic nuclides ^{10}Be , ^{26}Al) is recommended. Minimum numbers of five samples from the main scarp area, and five samples of boulders from the debris lobe, are recommended.
- (b) For large landslides with a poorly defined main scarp, but a well-defined debris lobe, a combination of luminescence dating and radiocarbon dating is recommended. Finegrain luminescence dating or 'LogNormal' SAR luminescence dating is recommended for colluvial deposits. For best results, samples should be collected from trial pits in U100 tubes below a depth of at least 1 m. Organic material suitable for radiocarbon dating should be recovered from the U100 sample tube. If necessary, the sample should be examined under a binocular microscope to recover suitable organic material. In particularly thick (>3 m) colluvial deposits, samples for luminescence dating should be obtained by triple tube core barrel drilling using foam as the flushing medium.
- (c) For dating of alluvial deposits, 'Leading Edge' SAR luminescence dating and radiocarbon dating is recommended. Samples of alluvium should be collected within 1 m or less of the ground surface. Organic material suitable for radiocarbon dating should also be collected. If necessary, the alluvium should be examined under a binocular microscope to recover suitable organic material.
- (d) For dating of relict shallow open hillslope failures, either luminescence dating (finegrain or SAR), or radiocarbon

dating of buried soil profiles with care to avoid reworked material, is recommended.

12.3 Return Periods for Relict Natural Terrain Landslides

The following general conclusions can be made with respect to return periods of relict natural terrain landslides in Hong Kong:

- (a) Relict natural terrain landslides classified as large in the NTLI (i.e. scar >20 m wide) and LLS (i.e. scarp >20 m wide) appear to be generally thousands and tens of thousands, rather than hundreds of years old.
- (b) Smaller relict landslide features (e.g. relict open hillslope failures) that can be identified from API are generally hundreds rather than thousands of years old, although further detailed investigation of the numerical (absolute) ages of these smaller events is required. Older events of this magnitude may be more degraded, and as a result, very difficult to identify on the basis of API.
- (c) There are insufficient chronometric data on relict natural terrain landslides with which to establish landslide frequency magnitudes on a territory-wide basis.

12.4 Chronological Classification of Relict Natural Terrain Landslides

The following general conclusions are made with respect to landslide chronologies determined from API:

- (a) The Tsing Yi site is the oldest large landslide feature (main scarp and associated debris) dated in this study. Accordingly, 50,000 years may be close to the upper limit for recognition of such features by API.
- (b) The relative chronologies for clusters of natural terrain landslides identified from API generally compare favourably with the numerical ages. However, there is insufficient evidence as yet to conclude that API alone can provide a consistently reliable means of determining relative chronologies in such circumstances.
- (c) The chronometric data indicate that relict natural terrain landslides identified by API, which preserve well-defined main scarps and associated debris lobes, may be thousands rather than hundreds of years old.

- (d) There is potential evidence of ancient landscape surfaces in Hong Kong up to 280,000 years old.

12.5 Further Work

It is useful to conduct further work in the following areas:

- (a) Consideration should be given to extending the API relative chronology by examining the relative degradation of relict natural terrain landslides, both large and small, to give a better indication of the upper limit for recognition of such features.
- (b) The potential application of other in-situ produced cosmogenic nuclides, such as ^{36}Cl in K-feldspar, to date rock surfaces formed as recently as 500 years old, should be investigated.
- (c) Consideration should be given to investigating other techniques for dating of relict natural terrain landslides, such as lichenometry and the thickness of weathering rinds of boulders/exposures, using the numerical age data presented in this report as a basis for calibration.
- (d) Further dating tests should be carried out on selected natural terrain landslides and geomorphological features to gain further experience in applying the dating techniques and to categorise different types of relict landslides into broad age groups.

13. KEY FINDINGS

Direct dating of carefully selected, relict natural terrain landslide scars in Hong Kong is viable with the following provisos:

- (a) Correct sampling and handling procedures are essential to obtaining a reliable age data set.
- (b) Accurate interpretation of the numerical age data depends on detailed geomorphological observations made prior to and during sampling.
- (c) The numerical age data may yield maximum and minimum ages of the landslides and their deposits, rather than the age of the landslide event itself.

Relict natural terrain landslides in Hong Kong can be categorised in broad ages with the following general considerations:

- (d) Well-defined relict landslide features, identified from API and with scars greater than 20 m wide, appear to be generally thousands rather than hundreds of years old.
- (e) Relict landslide features identified from API with scars less than 20 m wide appear to be generally hundreds rather than thousands of years old.
- (f) The upper limit of recognition by API of relict natural terrain landslides in Hong Kong may be about 50,000 years.

14. REFERENCES

- Aitken, M. & Xie, J. (1992). Optical dating using infra-red diodes: young samples. Quaternary Science Reviews Vol. 11, pp. 147-152.
- Barrows, T.T., Stone, J.O., Fifield, L.K. & Cresswell, R.G. (2001). Late Pleistocene Glaciation of the Kosciuszko Massif, Snowy Mountains, Australia. Quaternary Research, Vol. 55, pp. 179-189.
- Barrows, T.T., Stone, J.O. Fifield, L.K. & Cresswell, R.G. (2002). The timing of the Last Glacial Maximum in Australia. Quaternary Science Review, Vol. 21, pp. 159-173.
- Duller, G.A.T. & Wintle, A.G. (1996). Luminescence dating of alluvial and colluvial deposits in Hong Kong. Institute of Earth Studies, University of Wales. Report for the Geotechnical Engineering Office, Civil Engineering Department, Hong Kong, 30 p.
- Fyfe, J.A., Shaw, R., Campbell, S.D.G., Lai, K.W. & Kirk, P.A. (2000). The Quaternary Geology of Hong Kong. Geotechnical Engineering Office, Civil Engineering Department, Hong Kong SAR Government, 208 p. plus 6 maps.
- King, J.P. (1998). Natural Terrain Landslide Study: The Sham Wat Debris Lobe; Interim Report. Technical Note TN 6/98, Geotechnical Engineering Office, Hong Kong SAR Government, 37 p. plus 1 drawing.
- King, J.P. (2001). Luminescence Dating of Colluvium and Landslide Deposits in Hong Kong. GEO Technical Note No. TN 1/2001. Geotechnical Engineering Office, Civil Engineering Department, Hong Kong, 65 p.
- Lai, K.W. (1997). Quaternary evolution of on-shore superficial deposits of Hong Kong. Proceedings of the Fourth International Conference on the Evolution of the East Asian Environment, Hong Kong, pp. 178-188.
- Lai, K.W. (1998). The Pleistocene alluvium and deluvium-proluvium in Hong Kong. Guangdong Geology, Vol. 13, pp 71-78.
- Lang, A. & Wagner, G.A. (1997). Infrared stimulated luminescence dating of Holocene colluvial sediments using the 410nm emission. Quaternary Geochronology (Quaternary Science Reviews) Vol. 16, pp. 393-396.

- MGSL (2002). Detailed study of the 1 September 2001 debris flow on the natural hillside above Lei Pui Street. Landslide Study Report LSR 8/2002, Landslip Investigation Division, Geotechnical Engineering Office, Civil Engineering Department, Hong Kong, 127 p.
- Murray, A.S. & Olley, J.M. (2002). Precision and Accuracy in the Optically Stimulated Luminescence Dating of Sedimentary Quartz: A Status Review. Geochronometria, Vol. 21, pp. 1-16.
- Ng, K.C., Parry, S., King, J.P., Franks, C.A.M. & Shaw, R. (2001). Guidelines for Natural Terrain Hazard Studies. Special Project Report SPR 1/2002, Geotechnical Engineering Office, Hong Kong, 136 p.
- Nichols, K.K., P.R. Bierman, and M. Caffee. (2000). The Blackhawk keeps its secrets: Landslide dating using in-situ 10-Be. Geological Society of America Abstracts with Programs, Vol. 32(7), A-400.
- Nishiizumi, K., Finkel, R.C., Kohl, C.P. (1989). Cosmic ray production rates of ¹⁰Be and ²⁶Al in quartz from glacially polished rocks. Journal of Geophysical Research, Vol. 94, pp. 17907-17915.
- Noller, J.S., Sowers, J.M., Colman, S.M. & Pierce, K.L. (2000). Introduction to Quaternary Geochronology. In J.S. Noller, J.M. Sowers, & W.R. Lettis (editors) Quaternary Geochronology: Methods and Applications, American Geophysical Union, pp 1-10.
- Ove Arup & Partners (OAP) (2003). Natural Terrain Hazard Study at Pat Heung, Yuen Long. Advisory Division Report 1/2003, Advisory Division, Geotechnical Engineering Office, Civil Engineering Department, Hong Kong, 266 p.
- Olley, J.M., Caitcheon, G.C. & Murray, A.S. (1998). The Distribution of Apparent Dose as Determined by Optically Stimulated Luminescence in Small Aliquots of Fluvial Quartz: Implications for Dating Young Sediments. Quaternary Science Reviews (Quaternary Geochronology), Vol. 17, pp. 1033-1040.
- Sewell, R.J. & Campbell, S.D.G. (1998). Absolute Age-dating of Hong Kong Volcanic and Plutonic Rocks, Superficial Deposits, and Faults. Geological Report 2/1998, Planning Division, Geotechnical Engineering Office, Civil Engineering Department, Hong Kong, 163 p.
- Sewell, R.J. & Campbell, S.D.G. (2001). Absolute Age-dating of Hong Kong Volcanic and Plutonic Rocks, Superficial Deposits, and Faults. GEO Report No. 118. Geotechnical Engineering Office, Civil Engineering Department, Hong Kong, 153 p.
- Stuiver, M. & Polach H.A. (1977). Discussion: Reporting of ¹⁴C Data. Radiocarbon, Vol. 19, No. 3, pp. 355-363.
- Zreda, M.G. & Phillips, F.M. (2000). Cosmogenic Nuclide Buildup in Surficial Materials. In: J.S. Noller, J.M. Sowers, & R. Lettis (editors) Quaternary Geochronology: Methods and Applications, American Geophysical Union, pp 61-76.

LIST OF TABLES

Table No.		Page No.
1	Summary of Geomorphological Characteristics, Stratigraphy and Age Data for Each of the Landslide Sites	60
2	Luminescence Ages, Radiocarbon Determinations and Cosmogenic Exposure Ages for the Lai Cho Road Landslide Site	61
3	Luminescence Ages and Radiocarbon Determinations for the Lo Lau Uk Landslide Site	62
4	Luminescence Ages and Radiocarbon Determinations for the Pat Heung Landslide Site	63
5	Luminescence Ages, Radiocarbon Determinations and Cosmogenic Exposure Ages for the Lei Pui Street Landslide Site	64
6	Luminescence Ages, Radiocarbon Determinations and Cosmogenic Exposure Ages for the Ap Lei Chau Landslide Site	65
7a	Luminescence Ages and Radiocarbon Determinations for the Tsing Shan A Landslide Site	66
7b	Luminescence Ages for the Tsing Shan B Landslide Site	66
7c	Luminescence Ages and Radiocarbon Determinations for the Tsing Shan C Landslide Site	66
7d	Cosmogenic Exposure Ages for the Tsing Shan C Landslide Site	66
8	Luminescence Ages, Radiocarbon Determinations and Cosmogenic Exposure Ages for the Sham Wat Debris Lobe	67
9	Cosmogenic Exposure Ages for the Mid-Levels Landslide Site	68
10	Luminescence Ages and Radiocarbon Determinations for the Tung Chung East Landslide Site	69
11	Luminescence Ages and Cosmogenic Exposure Ages for the Sunset Peak West Landslide Site	70

Table No.		Page No.
12	Luminescence Ages and Radiocarbon Determinations for the Tai O Landslide Site	71
13	Luminescence Ages and Radiocarbon Determinations for the Sai Tso Wan Landslide Site	72
14	Luminescence Ages, Radiocarbon Determinations and Cosmogenic Exposure Ages for the Wong Lung Hang Landslide Site	73
15	Cosmogenic Exposure Ages for the Southeast Tsing Yi Landslide Site	74
16	Cosmogenic Exposure Ages for the Lion Rock Boulders Site	75
17	Cosmogenic Exposure Ages for the Fei Ngo Shan Boulders Site	76
18	Cosmogenic Exposure Ages for the Seymour Cliffs Site	77
19	Age Comparisons Among the Different Dating Techniques	78

Table 1 - Summary of Geomorphological Characteristics, Stratigraphy and Age Data for Each of the Landslide Sites (*1=youngest)

Study Area	Landslide Type	Features/Lobes	Landslide Vol. (Est.)	Age Result	Strata	API * Order
Sham Wat DL	Deep Seated	Main Lobe RF Main Lobe Deb. Southern Lobe Pond	850,000 m ³ 150,000 m ³	19.7 - 37.9 ka 27.9 - 284 ka 32 ka 1285 Yr	Massive Massive 3 Layers	2 2 1
Lai Cho Road	Deep Seated	Lobe A1 Lobe A2 Lobe A4	40,000 m ³ 10,000 m ³ 100,000 m ³	7.5 ka 5.0 - 6.6 ka 26.4 ka	Massive	2 1 3
Wong Lung Hang	Deep Seated	Lobe No. 1 Lobe No. 2 Lobe No. 3 Pond No. 3	70,000 m ³	18 ka 4.58 ka 5.18 ka .194 - 3.39 ka	2 Layers 3 Layers Massive 3 Layers	1 2
Sunset Peak West	Deep Seated	Levee South 2 Rock Scar No. 5 Lobe No. 5 Levee South 5 Lobe No. 6 Ancient Debris	4,000 m ³ 60,000 m ³	8.95 ka 7.5-9.1 ka 5.57 - 283 ka 7.04 ka 7.3, 16.5 ka 24.3 ka	3 Layers Massive 5 Layers 3 Layers 5 Layers	1 2 2 3 4
Tsing Yi	Deep Seated	Lobe No. 4 Coll. No. 1 Sheeting Joint 1 Sheeting Joint 2	50,000 m ³	47.6, 47.2 ka 35.2 ka 44.7, 48.4 ka 11.0 ka		1 2 2 1
Tsing Shan C	Deep Seated	Levee North Levee South Main Lobe Rock Scar	40,000 m ³	19.4 ka 8 - 11 ka 2.8 - 43 ka	2 Layers 5 Layers 3 Layers	1 1 2 1
Tsing Shan A	Deep Seated	Main Lobe 1	15,000 m ³	6.06 ka	3 Layers	
North Lamma	Deep Seated	Rock Scar	13,000 m ³	665 - 7756 Yr		
Ap Lei Chau	Deep Seated	RLS 1 RLS 2 Rock Face	12,500 m ³	10.8 - 11.1 ka 72.5, 77.4 ka	2 Layers 3 Layers	1 2 3
Tsing Shan B	Deep Seated	Main Lobe	5,000 m ³	3.05 ka	6 Layers	
Mid Levels	Deep Seated	Rock Scar	4,000 m ³	6.9 ka		
Tai O	Open Hillside	Debris Fan A Debris Fan B Debris Fan C	2,000 m ³	825 Yr 1.2 ka 4.3 ka	2 Layers 3 Layers Massive	2 1 1
Lei Pui Street	Rock Faces	Sheeting Joints		4.8 - 96 ka		
Sai Tso Wan	Open Hillside	Dep. No. 1 Dep. No. 2 Dep. No. 5 Dep. No. 6 RL No. 1 RL No. 2	700 m ³	7.9 ka 672 - 703 Yr 14.8 ka 11.8 ka 1.6 ka 3.5 ka	2 Layers 5 Layers 2 Layers Massive Massive 2 Layers	2 1 3 3 1 1
Pat Heung	Open Hillside	Dep. No. 2 Dep. No. 4 Dep. No. 5	35 m ³ 415 m ³ 385 m ³	4.3 ka 2.5 ka 15.7 ka	2 Layers 3 Layers 3 Layers	2 1 3
Fei Ngo Shan	Rock Fall	Lobe Unit No. 1	150 m ³	57.7 ka		
Lion Rock	Rock Fall	Lobe No. 5 Lobe No. 3	150 m ³ 150 m ³	2.3 - 5.2 ka 3.7 ka		1 1
Tung Chung E.	Open Hillside	Dep. No. B Dep. C Fan	50 m ³	200 - 378 Yr 13.5 ka	3 Layers 2 Layers	1 2
Lo Lau Uk	Deep Seated	Dep. A Dep. B	20 m ³	156 Yr	3 layers Massive	1 2
Seymour Cliffs	Rock Faces	Sheeting Joints Tuff Cliff	5 m ³	21 - 31 ka 17 ka		

Table 2a - Luminescence Ages and Radiocarbon Determinations for the Lai Cho Road Landslide Site

Depth (m)	Sample	WLL Lab No.	Wk Lab No.	Trial Pit	Finegrain (ka)	¹⁴ C yr BP	CalBP*
0.6	HK12363	199	11879	TP1	3.48±0.32	611±47	660 - 530
0.7	HK12364	200		TP2	26.4±2.4		

Table 2b - Cosmogenic Exposure Ages for the Lai Cho Road Landslide Site

Sample	Lab No.	Rock	Type	Cosmogenic ¹⁰ Be (ka)
HK12274	LCR-01	Granite	Scar	6.4±1.1
HK12275	LCR-02	Granite	Scar	7.5±1.0
HK12276	LCR-03	Granite	Scar	6.5±0.9
HK12277	LCR-04	Granite	Scar	5.0±0.9

*The 'probability method' has been used for calibrating the radiocarbon ages using the 'Oxcal' programme and the InCal98 calibration curve. The age range shown is for the 95% confidence level.

Table 3 - Luminescence Ages and Radiocarbon Determinations for the Lo Lau Uk Landslide Site

Depth (m)	Sample	WLL Lab No.	Wk Lab No.	Trial Pit	'Log Normal' SAR (ka)	Finegrain (ka)	'Leading Edge' SAR (ka)	¹⁴ C yr BP	CalBP*
1.0	HK12361	197		TP1	18.5±2.3	21.8±3.2	5.1±1.7		
0.9	HK12362	198		TP2	11.0±1.3	11.2±2.9	2.52±1.24		
1.0	HK17967		11570	TP2				156±40	290 - 60

*The 'probability method' has been used for calibrating the radiocarbon ages using the 'Oxcal' programme and the InCal98 calibration curve. The age range shown is for the 95% confidence level.

Table 4 - Luminescence Ages and Radiocarbon Determinations for the Pat Heung Landslide Site

Depth (m)	Sample	WLL Lab No.	Wk Lab No.	Trial Pit	Finegrain (ka)	¹⁴ C yr BP	CalBP*
1.4	HK12401	233		TP2	27.1±6.5		
0.7	HK12402	234		TP2	4.35±0.53		
2.1	HK12403	235		TP14	12.2±2.1		
1.3	HK12404	236	11886	TP14	2.85±0.24	2,581±42	2,780 - 2,700
2.5	HK12405	237		TP17	15.7±1.9		
1.5	HK12406	238		TP17	17.2±2.2		

*The 'probability method' has been used for calibrating the radiocarbon ages using the 'Oxcal' programme and the InCal98 calibration curve. The age range shown is for the 95% confidence level.

Table 5a - Luminescence Ages and Radiocarbon Determinations for the Lei Pui Street Landslide Site

Depth (m)	Sample	WLL Lab No.	Wk Lab No.	Trial Pit	'Log Normal' SAR (ka)	Finegrain (ka)	'Leading Edge' SAR (ka)	¹⁴ C yr BP	CalBP*
<0.2	HK12360	196		SPT	2.03±0.18	1.92±0.14	0.78±0.11		
1.3	HK12367	203		TP6		6.01±0.40			
1.1	HK12368	204	11881	TP7		6.62±0.49		20,127±119	23,512 - 23,108
1.7	HK12369	205		TP7		11.5±0.1			
0.7	HK12370	206		TP9		9.19±0.81			
1.2	HK12371	207		TP9		8.25±0.67			

Table 5b - Cosmogenic Exposure Ages for the Lei Pui Street Landslide Site

Sample	Lab No.	Rock	Type	Cosmogenic ¹⁰ Be (ka)	Cosmogenic ²⁶ Al (ka)
HK12310	LPS-01	Granite	Scar	4.9±0.7	
HK12311	LPS-02	Granite	Scar	28.5±2.5	
HK12312	LPS-03	Granite	Scar	96.3±7.9	100±13
HK12313	LPS-04	Granite	Scar	16.3±1.7	
HK12314	LPS-05	Granite	Scar	21.4±1.9	

*The 'probability method' has been used for calibrating the radiocarbon ages using the 'Oxcal' programme and the InCal98 calibration curve. The age range shown is for the 95% confidence level.

Table 6a - Luminescence Ages and Radiocarbon Determinations for the Ap Lei Chau Landslide Site

Depth (m)	Sample	WLL Lab No.	Wk Lab No	Trial Pit	Finegrain (ka)	^{14}C yr BP	CalBP*
1.1	HK12366	202	11880	TP4	12.2±1.4	1,734±42	1,740 - 1,530
0.8	HK12365	201		TP4	13.3±2.2		

Table 6b - Cosmogenic Exposure Ages for the Ap Lei Chau Landslide Site

Sample	Lab No.	Rock	Type	Cosmogenic ^{10}Be (ka)	Cosmogenic ^{26}Al (ka)
HK12315	ALC-01	Volcanic	Control	72.7±6.4	
HK12316	ALC-02	Volcanic	Scar	11.1±1.6	
HK12317	ALC-03	Volcanic	Control	77.6±7.8	66.3±39
HK12318	ALC-04	Volcanic	Boulder	10.8±2.2	

*The 'probability method' has been used for calibrating the radiocarbon ages using the 'Oxcal' programme and the InCal98 calibration curve. The age range shown is for the 95% confidence level.

Table 7a - Luminescence Ages and Radiocarbon Determinations for the Tsing Shan A Landslide Site

Depth (m)	Sample	WLL Lab No.	Wk Lab No.	Trial Pit	'Log Normal' SAR (ka)	Finegrain (ka)	'Leading Edge' SAR (ka)	¹⁴ C yr BP	CalBP*
*0.3	HK12376	221	11882	TPA3	0.63±0.05	0.91±0.1	0.51±0.05	124±45	280 - 170
0.5	HK12377	222		TPA3		9.8±1			
1.7	HK12378	223		TPA3		0.68±0.07			

Table 7b - Luminescence Ages for the Tsing Shan B Landslide Site

Depth (m)	Sample	WLL Lab No.	Wk Lab No.	Trial Pit	Finegrain (ka)
1.4	HK12384	224		TPB3	28.8±4.4
1.7	HK12385	225		TPB3	62.0±7.7
2.4	HK12386	226		TPB3	63.3±8.7
0.5	HK12387	227		TPB3	13.9±1.3
3.1	HK12388	228		TPB3	9.44±0.70

Table 7c - Luminescence Ages and Radiocarbon Determinations for the Tsing Shan C Landslide Site

Depth (m)	Sample	WLL Lab No.	Wk Lab No.	Trial Pit	'Log Normal' SAR (ka)	Finegrain (ka)	'Leading Edge' SAR (ka)	¹⁴ C yr BP	CalBP*
0.7	HK12398	232	11885	TPC3	1.73±0.14	2.15±0.19	1.03±0.08	1,376±51	1,390 - 1,220
2.4	HK12395	229		TPC3		6.84±0.51			
1.7	HK12397	231		TPC3	14.1±1.5	18.3±2.5	8.77±0.98		
1.0	HK12396	230	11883	TPC3	16.4±1.9	16.8±1.2	8.89±1.57	23,107±129	23,400 - 22,850
4.5	HK12410	239		TTC		6.48±0.7			
2.5	HK12411	240		BHC2		44.6±4.9			

Table 7d - Cosmogenic Exposures Ages for the Tsing Shan C Landslide Site

Sample	Lab No.	Rock	Type	Cosmogenic ¹⁰ Be (ka)
HK12303	TSC-01	Granite	Scar	2.7±1
HK12304	TSC-02	Granite	Scar	10.3±1.0
HK12305	TSC-03	Granite	Scar	5.3±1.7
HK12306	TSC-04	Granite	Scar	43.3±3.7
HK12307	TSC-05	Granite	Boulder	11.0±1.2
HK12308	TSC-06	Granite	Boulder	8.3±1.7
HK12309	TSC-07	Granite	Boulder	19.4±1.7

*The 'probability method' has been used for calibrating the radiocarbon ages using the 'Oxcal' programme and the InCal98 calibration curve. The age range shown is for the 95% confidence level.

Table 8a - Luminescence Ages and Radiocarbon Determinations for the Sham Wat Debris Lobe

Depth (m)	Sample	WLL Lab No	Wk Lab No	Trial Pit	'Log Normal' SAR (ka)	Finegrain (ka)	'Leading Edge' SAR (ka)	¹⁴ C yr BP	CalBP*
7.6	HK17956	152		BH1	32.9±2.4	28.6±3.1	20.0±3.9		
17.3	HK17957	153		BH1	32.5±2.1	32.0±2.1	21.5±2.3		
4.3	HK17958	154		BH3		34.2±3.8			
6.5	HK12359	195		BH7	27.5±3.4	23.9±3.6	11.4±1.4		
6.0	HK17959	155		BH9A		27.9±4.6			
8.0	HK17960	156		BH9B		54.2±5.2			
6.6	HK17961	157		BH11A		35.2±3.8			
0.1	HK12473	250	11896	TP4	2.74±0.28	6.22±0.69	1.6±0.16	1,489±40	1,520 - 1,290
0.7	HK12471	269		TP4		13.9±1.9			
0.3	HK12425		11887	TP4				3,167±43	3,480 - 3,320
0.4	HK12423		11652	TP4				1,285±39	1,300 - 1,120

Table 8b - Cosmogenic Exposure Ages for the Sham Wat Debris Lobe

Sample	Lab No.	Rock	Type	Cosmogenic ¹⁰ Be (ka)	Cosmogenic ²⁶ Al (ka)
HK12293	SWD-01	Volcanic	Scar	37.1±4.5	
HK12294	SWD-02	Volcanic	Scar	38.0±5.2	
HK12295	SWD-03	Volcanic	Scar	26.3±4.6	
HK12296	SWD-04	Volcanic	Scar	19.7±2.2	
HK12297	SWD-05	Volcanic	Scar	27.3±4.5	
HK12298	SWD-06	Volcanic	Boulder	33.1±3.0	
HK12299	SWD-07	Volcanic	Boulder	285±23	283±36
HK12300	SWD-08	Volcanic	Boulder	281±23	
HK12301	SWD-09	Volcanic	Boulder	227±19	
HK12302	SWD-10	Volcanic	Boulder	103±8.9	

*The 'probability method' has been used for calibrating the radiocarbon ages using the 'Oxcal' programme and the InCal98 calibration curve. The age range shown is for the 95% confidence level.

Table 9 - Cosmogenic Exposure Ages for the Mid-Levels Landslide Site

Sample	Lab No.	Rock	Type	Cosmogenic ^{10}Be (ka)
HK12278	ML-01	Volcanic	Scar	6.0 ± 1.6
HK12279	ML-02	Volcanic	Scar	7.0 ± 1.2
HK12280	ML-03	Volcanic	Scar	7.7 ± 1.3
HK12281	ML-04	Volcanic	Scar	< 39
HK12282	ML-05	Volcanic	Scar	8.2 ± 1.2

Table 10 - Luminescence Ages and Radiocarbon Determinations for the Tung Chung East Landslide Site

Depth (m)	Sample	WLL Lab No.	Wk Lab No.	Trial Pit	Finegrain (ka)	¹⁴ C yr BP	CalBP*
2.2	HK12433	242		TP1	13.5±1.8		
1.2	HK12268		10481	TP17		337±58	510 - 290
0.9	HK12270		10483	TP17		223±49	230 - 130
0.9	HK12271		10484	TP17		378±58	520 - 310
0.5	HK12273		10486	TP19		200±48	320 - 60

*The 'probability method' has been used for calibrating the radiocarbon ages using the 'Oxcal' programme and the InCal98 calibration curve. The age range shown is for the 95% confidence level.

Table 11a - Luminescence Ages for the Sunset Peak West Landslide Site

Depth (m)	Sample	WLL Lab No.	Trial Pit	Finegrain (ka)
1.2	HK12434	266	TP1	9.0±1.05
1.5	HK12437	276	TP2	5.57±0.4
0.9	HK12438	246	TP3	16.5±2.8
1.8	HK12440	265	TP4	7.3±0.62
1.1	HK12442	253	BH1	7.04±0.53
2.5	HK12443	259	BH2	24.3±2.5

Table 11b - Cosmogenic Exposure Ages for the Sunset Peak West Landslide Site

Sample	Lab No.	Rock	Type	Cosmogenic ¹⁰ Be (ka)	Cosmogenic ²⁶ Al (ka)
HK12283	TCR-01		Scar	7.4±1.1	
HK12284	TCR-02		Scar	9.1±1.1	
HK12285	TCR-03		Scar	70.7±6	
HK12286	TCR-04	Volcanic	Scar	7.7±2.9	
HK12287	TCR-05	Volcanic	Boulder	227±18	246±34
HK12288	TCR-06	Volcanic	Boulder	284±22	255±38
HK12289	TCR-07	Volcanic	Boulder	40.9±3.7	
HK12290	TCR-08	Volcanic	Boulder	27.3±2.4	
HK12291	TCR-09	Volcanic	Boulder	15.1±1.6	
HK12292	TCR-10	Volcanic	Boulder	52.0±6.4	

Table 12 - Luminescence Ages and Radiocarbon Determinations for the Tai O Landslide Site

Depth (m)	Sample	WLL Lab No.	Wk Lab No.	Trial Pit	'Log Normal' SAR (ka)	Finegrain (ka)	'Leading Edge' SAR (ka)	¹⁴ C yr BP	CalBP*
0.8	HK12455	260		TP1		0.82±0.15			
1.1	HK12419		11648	TP2				1,195±44	1,260 - 970
1.1	HK12458	271	11893	TP2	1.02±0.07	1.11±0.16	0.84±0.06	1,122±43	1,170 - 930
1.5	HK12432		11888	TP3				7300±49	8,190 - 7,970
1.0	HK12461	273	11894	TP3	1.54±0.20	4.26±0.37	0.60±0.08	11,758±72	14,150 - 3,350
1.0	HK12463	249		BH1		4.38±0.53			
3.9	HK12466	245		BH2		20.3±3.2			
6.2	HK12468	272		BH3		20.6±2.1			

*The 'probability method' has been used for calibrating the radiocarbon ages using the 'Oxcal' programme and the InCal98 calibration curve. The age range shown is for the 95% confidence level.

Table 13 - Luminescence Ages and Radiocarbon Determinations for the Sai Tso Wan Landslide Site

Depth (m)	Sample	WLL Lab No.	Wk Lab No.	Trial Pit	'Log Normal' SAR (ka)	Finegrain (ka)	'Leading Edge' SAR (ka)	¹⁴ C yr BP	CalBP*
0.8	HK12474	274		TP5		7.93±0.68			
0.1	HK12479	254		TP6	0.79±0.10	2.82±0.62	0.36±0.03		
0.2	HK12420		11649	TP6				170±46	300 - 60
0.3	HK12421		11650	TP6				672±47	690 - 540
0.4	HK12422		11651	TP6				703±47	730 - 620
0.6	HK12477	248	11897	TP6		1.34±0.11		530±42	650 - 580
1.0	HK12480	257	11898	TP7	2.66±0.30	3.57±0.32	1.52±0.15	2,416±45	2,550 - 2,340
0.3	HK12483	275	11899	TP8	3.93±1.08	1.65±0.18	11.5±0.9	222±40	230 - 130
0.8	HK12485	243		TP9		14.4±1.7			
0.8	HK12487	244		TP10		14.8±1.8			
0.8	HK12489	255		TP11		11.8±2.0			
2.6	HK12490	266	11900	BH4		10.5±1.2		10,658±116	13,000 - 12,300

*The 'probability method' has been used for calibrating the radiocarbon ages using the 'Oxcal' programme and the InCal98 calibration curve. The age range shown is for the 95% confidence level.

Table 14a - Luminescence Ages and Radiocarbon Determinations for the Wong Lung Hang Landslide Site

Depth (m)	Sample	WLL Lab No.	Wk Lab No.	Trial Pit	'Log Normal' SAR (ka)	Finegrain (ka)	'Leading Edge' SAR (ka)	¹⁴ C yr BP	CalBP*
1.7	HK12445	242	11889	TP5	15.9±1.6	18.0±2.4	5.87±0.82	230±42	230 - 130
1.0	HK12447	274		TP6		4.58±0.6			
0.5	HK12449	247	11890	TP7	5.74±0.35	5.18±0.61	3.13±0.35	13,800±67	17,100 - 16,050
0.8	HK12413		11565	TP8				535±39	570 - 500
0.9	HK12414		11566	TP8				377±49	510 - 310
0.9	HK12417		11569	TP8				194±47	310 - 60
0.5	HK12452	251	11892	TP8	1.17±0.09	3.39±0.35	0.77±0.06	349±58	510 - 300
0.3	HK12453	252		TP8	1.14±0.13	5.17±0.38	0.51±0.07		
0.8	HK12451	256	11891	TP8	0.35±0.03	1.35±0.09	0.27±0.02	2,482±43	2,740 - 2,430

Table 14b - Cosmogenic Exposure Ages for the Wong Lung Hang Landslide Site

Sample	Lab No.	Rock	Type	Cosmogenic ¹⁰ Be (ka)
HK12355	WLH-01	Volcanic	Boulder	39.3±3.8
HK12356	WLH-02	Volcanic	Boulder	64.8±6.8
HK12357	WLH-03	Volcanic	Boulder	29.7±2.7

*The 'probability method' has been used for calibrating the radiocarbon ages using the 'Oxcal' programme and the InCal98 calibration curve. The age range shown is for the 95% confidence level.

Table 15 - Cosmogenic Exposures Ages for the Southeast Tsing Yi Landslide Site

Sample	Lab No.	Rock	Type	Cosmogenic ^{10}Be (ka)	Cosmogenic ^{26}Al (ka)
HK12319	TY-01	Granite	Scar	47.7±4.1	
HK12320	TY-02	Granite	Scar	47.3±4.0	
HK12321	TY-03	Granite	Scar	35.3±3.1	
HK12322	TY-04	Granite	Scar	44.8±3.7	40.5±12
HK12323	TY-05	Granite	Scar	11.0±1.6	
HK12324	TY-07	Granite	Scar	48.5±4.0	

Table 16 - Cosmogenic Exposure Ages for the Lion Rock Boulders Site

Sample	Lab No.	Rock	Type	Cosmogenic ^{10}Be (ka)
HK12349	LR-01	Granite	Boulder	3.7 ± 0.4
HK12350	LR-02	Granite	Boulder	3.8 ± 0.5
HK12351	LR-03	Granite	Boulder	2.3 ± 0.4

Table 17 - Cosmogenic Exposure Ages for the Fei Ngo Shan Boulders Site

Sample	Lab No.	Rock	Type	Cosmogenic ^{10}Be (ka)
HK12352	FNS-01	Volcanic	Boulder	58.8 \pm 5.3
HK12353	FNS-02	Volcanic	Boulder	60.4 \pm 5.5
HK12354	FNS-03	Volcanic	Boulder	54.7 \pm 4.8

Table 18 - Cosmogenic Exposure Ages for the Seymour Cliffs Site

Sample	Lab No.	Rock	Type	Cosmogenic ¹⁰ Be (ka)
HK12346	SC-01	Granite	Scar	31.5±3.3
HK12347	SC-02	Granite	Scar	17.1±2.4
HK12348	SC-03	Granite	Scar	21.4±2.0

Table 19 - Age Comparisons Among the Different Dating Techniques

Table 19a - Comparison Between 'Leading Edge' SAR Luminescence Ages and Radiocarbon Determinations

Depth (m)	Sample	WLL	Trial Pit	Leading Edge SAR (ka)	¹⁴ C Cal yr BP	Location
*0.3	HK12376	221	TPA3	0.51±0.05	280 - 170	Tsing Shan
0.7	HK12398	232	TPC3	1.03±0.08	1390 - 1220	Tsing Shan
0.1	HK12473	250	TP4	1.6±0.16	1520 - 1290	Sham Wat
0.4	HK12423		TP4		1300 - 1120	Sham Wat
0.5	HK12452	251	TP8	0.77±0.06	510 - 300	Wong Lung Hang
0.3	HK12453	252	TP8	0.51±0.07	510 - 300	Wong Lung Hang
0.1	HK12479	254	TP6	0.36±0.03	690 - 540	Sai Tso Wan

Table 19b - Comparison Between 'Log Normal' SAR Luminescence Ages and Finegrain Luminescence Ages

Depth (m)	Sample	WLL	Trial Pit	Log Normal SAR (ka)	Finegrain (ka)	Location
1.0	HK12480	257	TP7	2.66±0.3	3.57±0.32	Sai Tso Wan
0.7	HK12398	232	TPC3	1.73±0.14	2.15±0.19	Tsing Shan
1.7	HK12397	231	TPC3	14.1±1.5	18.3±2.5	Tsing Shan
1.0	HK12396	230	TPC3	16.4±1.9	16.8±1.2	Tsing Shan
0.5	HK12449	247	TP7	5.74±0.35	5.18±0.61	Wong Lung Hang
1.7	HK12445	242	TP5	15.9±1.6	18.0±2.4	Wong Lung Hang
1.0	HK12361	197	TP1	18.5±2.3	21.8±3.2	Lo Lau Uk
0.9	HK12362	198	TP2	11.0±1.3	11.2±2.9	Lo Lau Uk
<0.2	HK12360	196	SPT	2.03±0.18	1.92±0.14	Lei Pui St

Table 19c - Comparison Between Finegrain Luminescence Ages and Radiocarbon Determinations

Depth (m)	Sample	WLL	Trial Pit	Log Normal SAR (ka)	Finegrain (ka)	¹⁴ C Cal yr BP	Location
1.3	HK12404	236	TP14		2.85±0.24	2780 - 2700	Pat Heung
1.1	HK12458	271	TP2	1.02±0.07	1.11±0.16	1170 - 930	Tai O (Dep. B)
1.1	HK12419		TP2			1260 - 970	Tai O (Dep. B)
1.0	HK12480	257	TP7	2.66±0.3	3.57±0.32	2550 - 2340	Sai Tso Wan
2.4	HK12490	267	BH4		10.5±1.2	13000 - 12300	Sai Tso Wan

Table 19d - Comparison Between Luminescence Ages and Cosmogenic ¹⁰Be Exposure Ages

Depth (m)	Sample	WLL	Trial Pit	Log Normal SAR (ka)	Finegrain (ka)	Cosmogenic ¹⁰ Be (ka)	Location
0.6	HK12363	199	TP1		3.48±0.32	² 6.3±1.0	Lai Cho Road
1.1	HK12366	202	TP4		12.2±1.4	³ 11.0±0.2	Ap Lei Chau
0.8	HK12365	201	TP4		13.3±2.2	³ 11.0±0.2	Ap Lei Chau
7.6	HK17956	152	BH1	32.9±2.4	28.6±3.1	¹ 32.4±5.4	Sham Wat DL
17.3	HK17957	153	BH1	32.5±2.1	32.0±2.1	¹ 32.4±5.4	Sham Wat DL
4.3	HK17958	154	BH3		34.2±3.8	¹ 32.4±5.4	Sham Wat DL
6.0	HK17959	155	BH9A		27.9±4.6	¹ 32.4±5.4	Sham Wat DL
6.6	HK17961	157	BH11A		35.2±3.8	¹ 32.4±5.4	Sham Wat DL
6.5	HK12359	155	BH7	27.5±3.4	23.9±3.6	¹ 32.4±5.4	Sham Wat DL
1.1	HK12442	253	BH1		7.04±0.53	^{**} 8.1±0.9	Sunset Peak West No.5
1.5	HK12437	276	TP2		5.57±0.4	^{**} 8.1±0.9	Sunset Peak West No.5

Depth (m)	Sample	WLL	Trial Pit	Log Normal SAR (ka)	Leading Edge SAR (ka)	Finegrain (ka)	Location
*0.3	HK12376	221	TPA3	0.63±0.05	0.51±0.05	0.908±0.097	Tsing Shan
*1.0	HK12461	273	TP3	1.54±0.2	0.6±0.08	4.26±0.37	Tai O
*0.3	HK12483	275	TP8	3.93±1.08	11.5±0.9	1.65±0.18	Sai Tso Wan

Samples in bold occur in more than one table

*Shallow disturbed material

**Average of three scar ages

¹Average of four scar and one boulder age

²Average of four scar ages

³Average of one scar and one boulder age

LIST OF FIGURES

Figure No.		Page No.
1	Location Map of Landslide Sites Selected for the Dating Study	83
2	Diagram Illustrating the Concept of Maximum and Minimum Ages for the Three Dating Techniques	84
3	API Interpretation, Sample Locations and Dating Results for the Lai Cho Road Landslide Site	85
4	Error Bar Chart Summarizing the Numerical (Absolute) Age Data for the Lai Cho Road Landslide Site	86
5	API Interpretation, Sample Locations and Dating Results for the Lo Lau Uk Landslide Site. Legend as for Figure 3	87
6	Error Bar Chart Summarizing the Numerical (Absolute) Age Data for the Lo Lau Uk Landslide Site. Symbols as for Figure 4	88
7	API Interpretation, Sample Locations and Dating Results for the Pat Heung Landslide Site. Legend as for Figure 3	89
8	Error Bar Chart Summarizing the Numerical (Absolute) Age Data for the Pat Heung Landslide Site. Symbols as for Figure 4	90
9	API Interpretation, Sample Locations and Dating Results for the Lei Pui Street Landslide Site	91
10	Error Bar Chart Summarizing the Numerical (Absolute) Age Data for the Lei Pui Street Landslide Site. Symbols as for Figure 4	92
11	API Interpretation, Sample Locations and Dating Results for the Ap Lei Chau Landslide Site. Legend as for Figure 3	93
12	Error Bar Chart Summarizing the Numerical (Absolute) Age Data for the Ap Lei Chau Landslide Site. Symbols as for Figure 4	94

Figure No.		Page No.
13	API Interpretation, Sample Locations and Dating Results for the Tsing Shan A Landslide Site. Legend as For Figure 3	95
14	Error Bar Chart Summarizing the Numerical (Absolute) Age Data for the Tsing Shan A Landslide Site. Symbols as for Figure 4	96
15	API Interpretation, Sample Locations and Dating Results for the Tsing Shan B Landslide Site. Legend as for Figure 3	97
16	Error Bar Chart Summarizing the Numerical (Absolute) Age Data for the Tsing Shan B Landslide Site. Symbols as for Figure 4	98
17	API Interpretation, Sample Locations and Dating Results for the Tsing Shan C Landslide Site. Legend as for Figure 3	99
18	Error Bar Chart Summarizing the Numerical (Absolute) Age Data for the Tsing Shan C Landslide Site. Symbols as for Figure 4	100
19	API Interpretation, Sample Locations and Dating Results for the Sham Wat Debris Lobe. Legend as for Figure 3	101
20	Error Bar Chart Summarizing the Numerical (Absolute) Age Data for the Sham Wat Debris Lobe. Symbols as for Figure 4	102
21	API Interpretation, Sample Locations and Dating Results for the Mid-Levels Landslide Site. Legend as for Figure 3	103
22	Error Bar Chart Summarizing the Numerical (Absolute) Age Data for the Mid-Levels Landslide Site. Symbols as for Figure 4	104
23	API Interpretation, Sample Locations and Dating Results for the Tung Chung East Landslide Site. Legend as for Figure 3	105
24	Error Bar Chart Summarizing the Numerical (Absolute) Age Data for the Tung Chung East Landslide Site. Symbols as for Figure 4	106

Figure No.		Page No.
25	API Interpretation, Sample Locations and Dating Results for the Sunset Peak West Landslide Site. Legend as for Figure 3	107
26	Error Bar Chart Summarizing the Numerical (Absolute) Age Data for the Sunset Peak West Landslide Site. Symbols as for Figure 4	108
27	API Interpretation, Sample Locations and Dating Results for the Tai O Landslide Site. Legend as for Figure 3	109
28	Error Bar Chart Summarizing the Numerical (Absolute) Age Data for the Tai O Landslide Site. Symbols as for Figure 4	110
29	API Interpretation, Sample Locations and Dating Results for the Sai Tso Wan Landslide Site. Legend as for Figure 3	111
30	Error Bar Chart Summarizing the Numerical (Absolute) Age Data for the Sai Tso Wan Landslide Site. Symbols as for Figure 4	112
31	API Interpretation, Sample Locations and Dating Results for the Wong Lung Hang Landslide Site. Legend as for Figure 3	113
32	Error Bar Chart Summarizing the Numerical (Absolute) Age Data for the Wong Lung Hang Landslide Site. Symbols as for Figure 4	114
33	API Interpretation, Sample Locations and Dating Results for the Southeast Tsing Yi Landslide Site. Legend as for Figure 3	115
34	Error Bar Chart Summarizing the Numerical (Absolute) Age Data for the Southeast Tsing Yi Landslide Site. Symbols as for Figure 4	116
35	API Interpretation, Sample Locations and Dating Results for the Lion Rock Boulder Site. Legend as for Figure 3	117
36	Error Bar Chart Summarizing the Numerical (Absolute) Age Data for the Lion Rock Boulder Site. Symbols as for Figure 4	118

Figure No.		Page No.
37	API Interpretation, Sample Locations and Dating Results for the Fei Ngo Shan Boulder Site. Legend as for Figure 3	119
38	Error Bar Chart Summarizing the Numerical (Absolute) Age Data for the Fei Ngo Shan Boulder Site. Symbols as for Figure 4	120
39	API Interpretation, Sample Locations and Dating Results for the Seymour Cliffs Site. Legend as for Figure 3	121
40	Error Bar Chart Summarizing the Numerical (Absolute) Age Data for the Seymour Cliffs Site. Symbols as for Figure 4	122

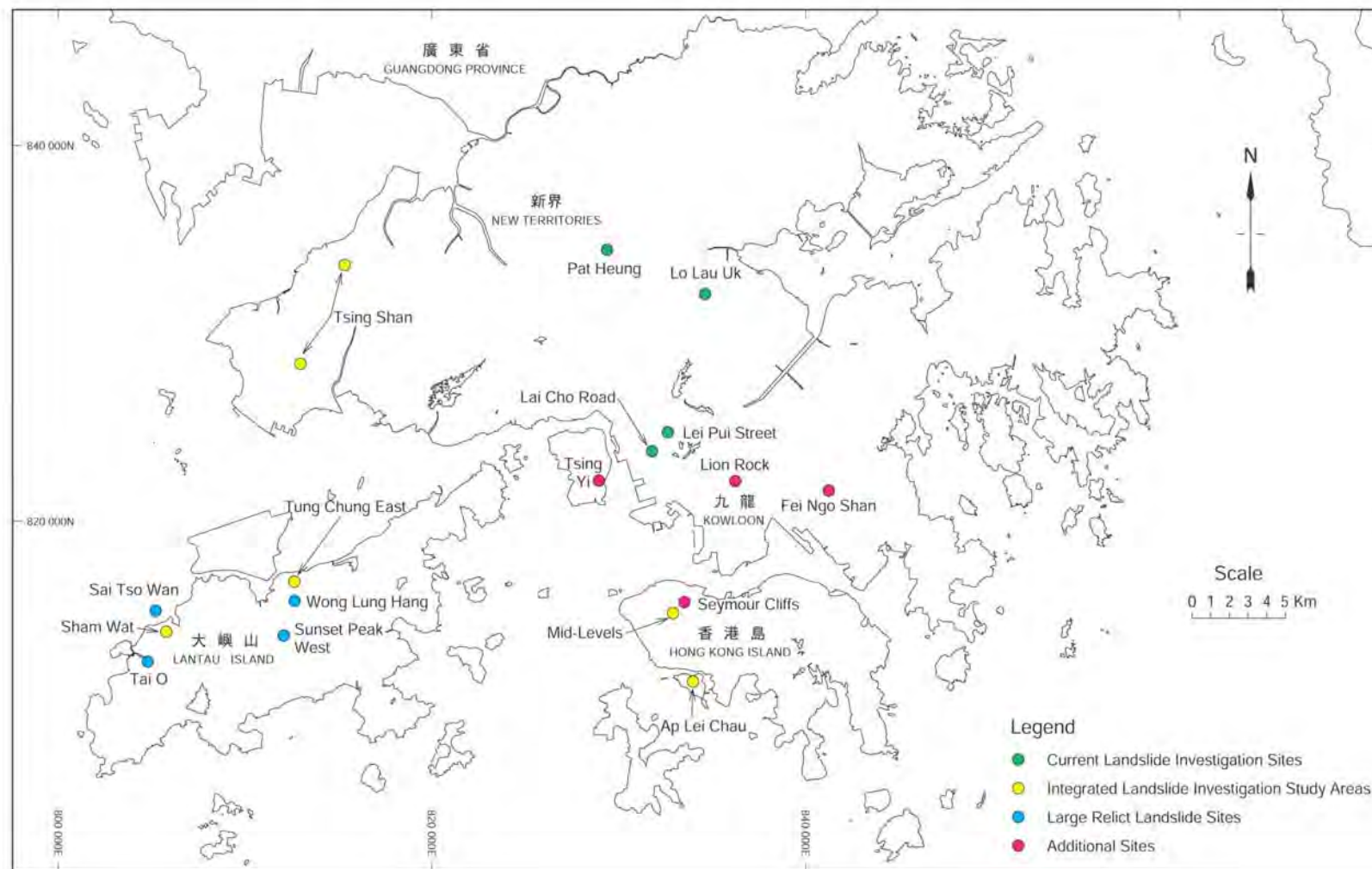


Figure 1 - Location Map of Landslide Sites Selected for the Dating Study

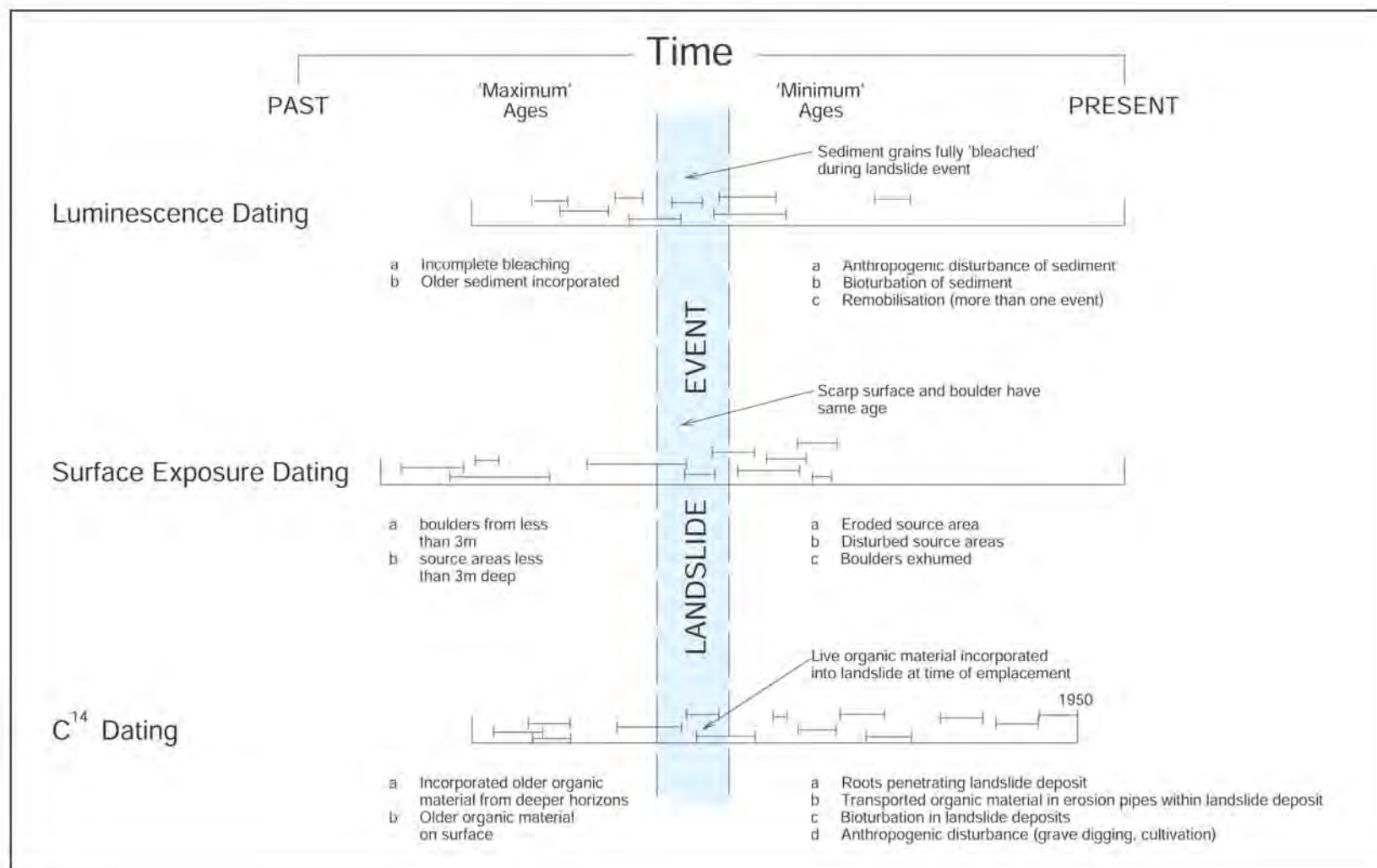


Figure 2 - Diagram Illustrating the Concept of Maximum and Minimum Ages for the Three Dating Techniques

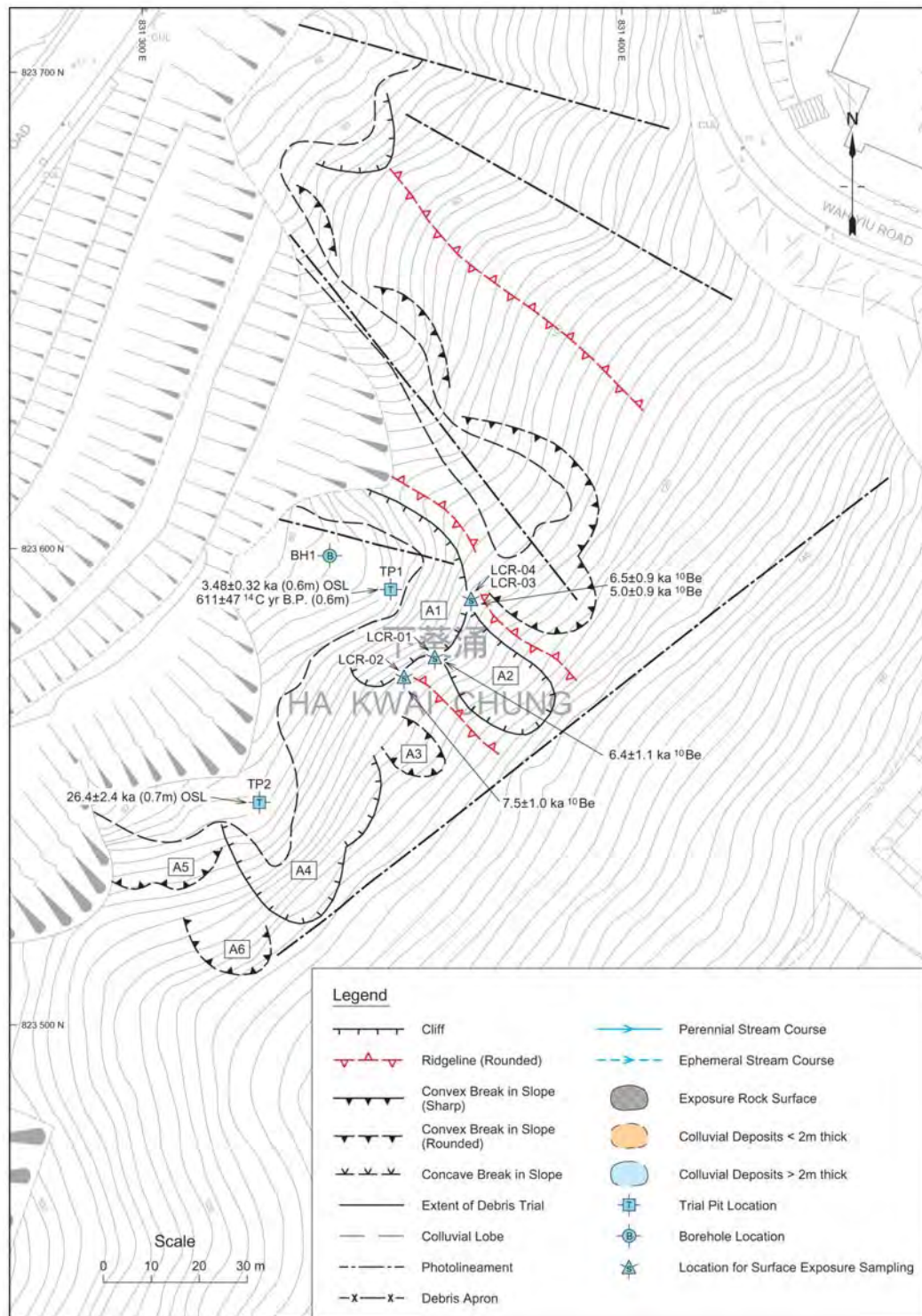


Figure 3 - API Interpretation, Sample Locations and Dating Results for the Lai Cho Road Landslide Site

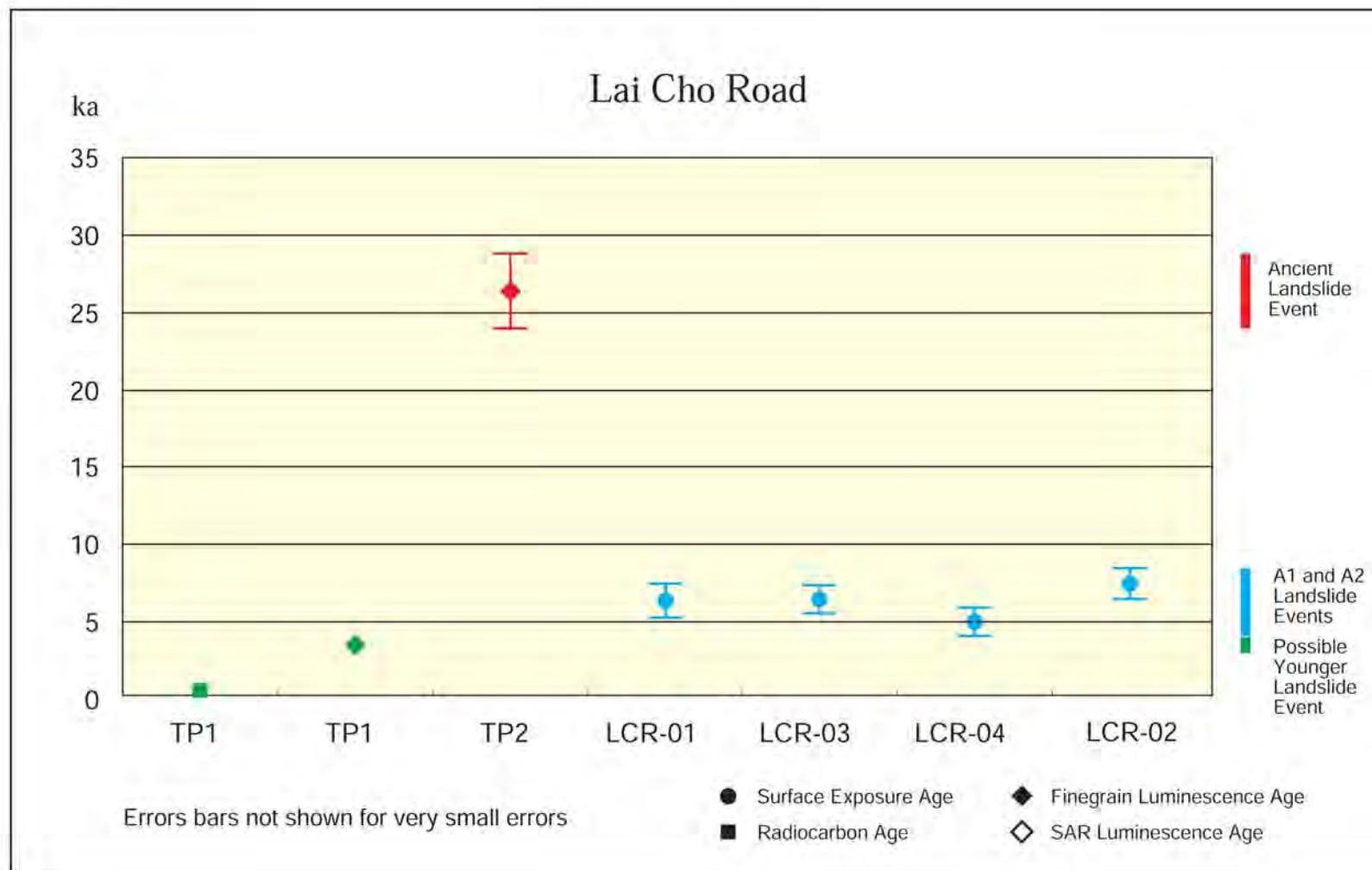


Figure 4 - Error Bar Chart Summarizing the Numerical (Absolute) Age Data for the Lai Cho Road Landslide Site

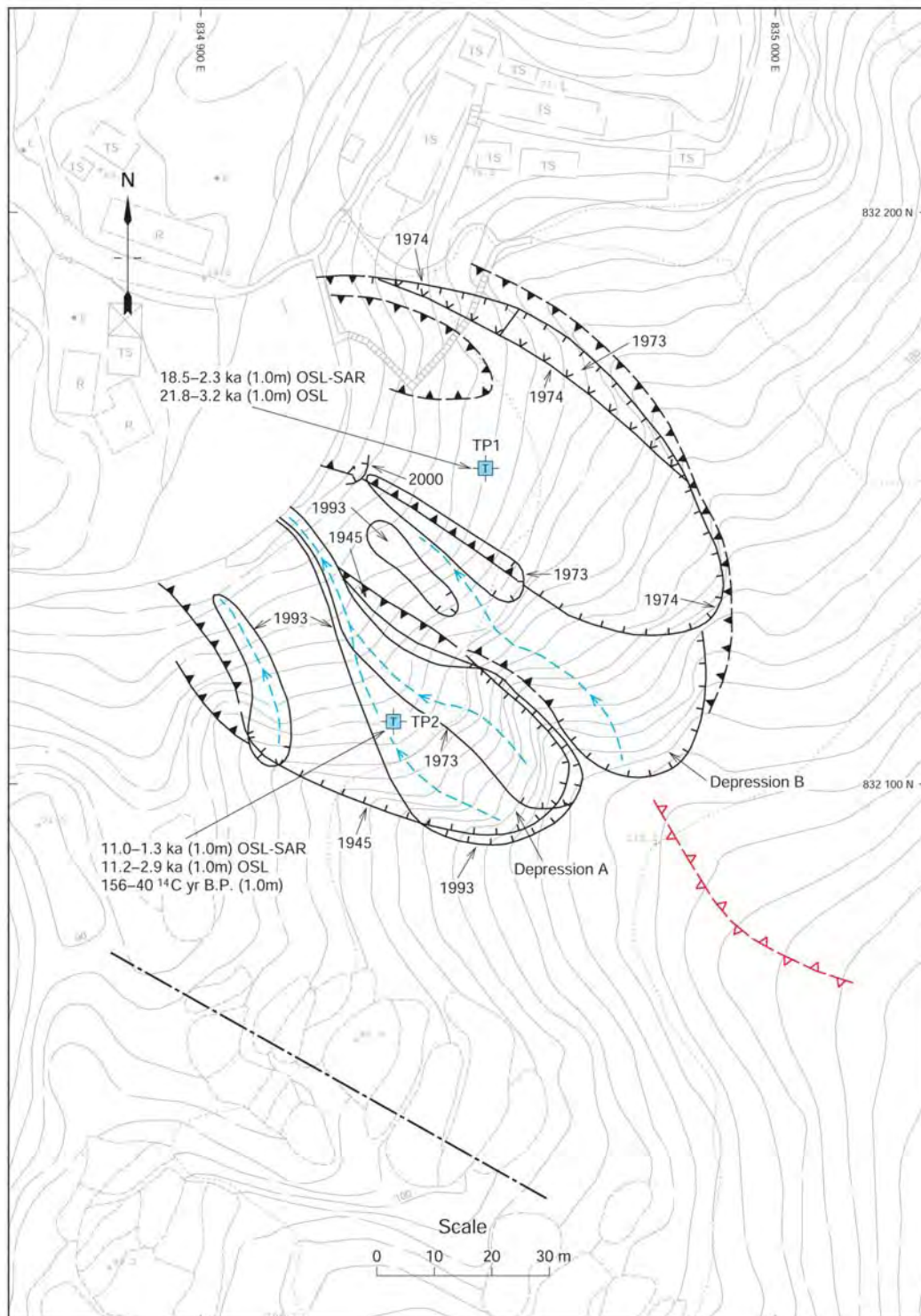


Figure 5 - API Interpretation, Sample Locations and Dating Results for the Lo Lau Uk Landslide Site. Legend as for Figure 3

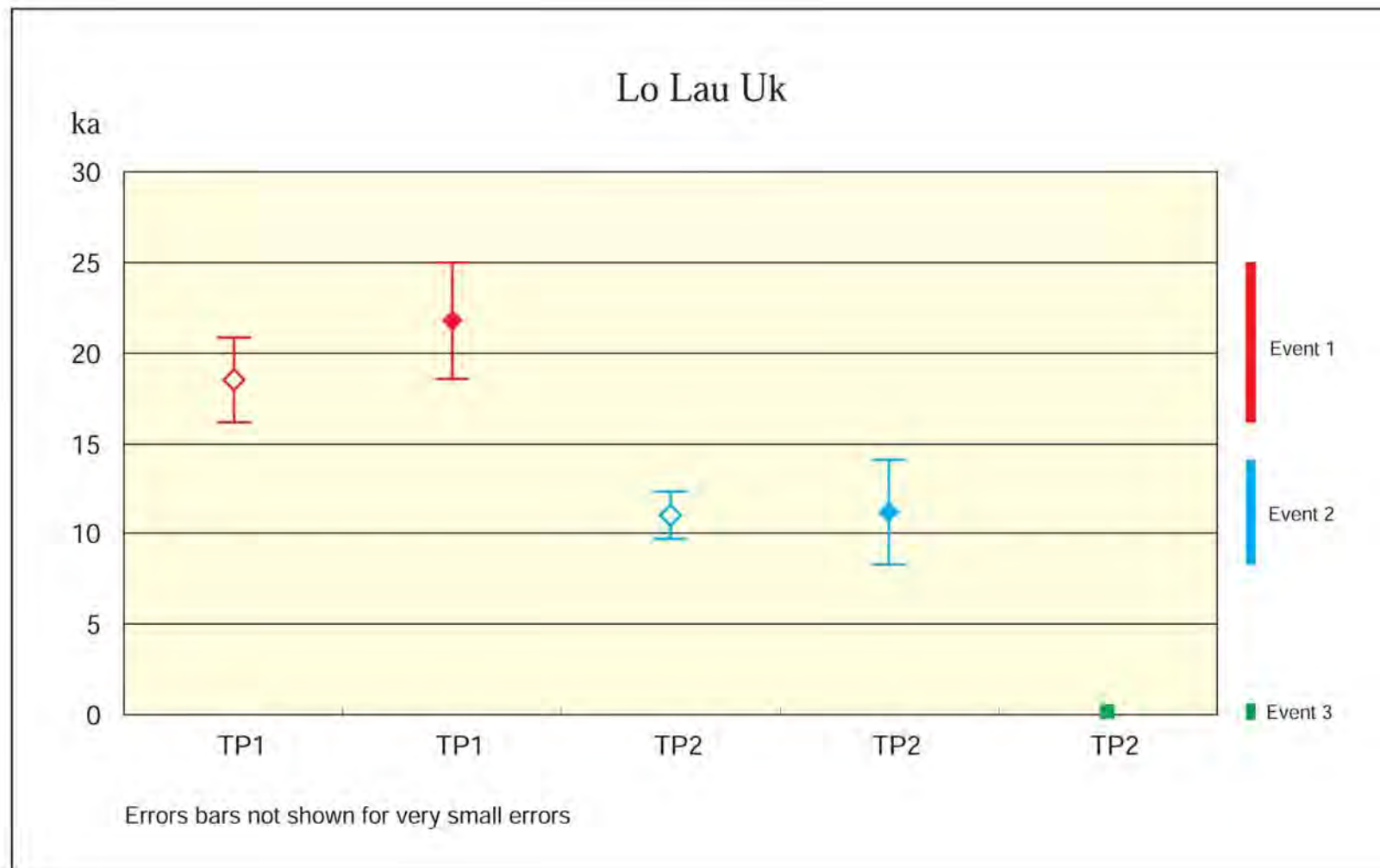


Figure 6 - Error Bar Chart Summarizing the Numerical (Absolute) Age Data for the Lo Lau Uk Landslide Site. Symbols as for Figure 4



Figure 7 - API Interpretation, Sample Locations and Dating Results for the Pat Heung Landslide Site. Legend as for Figure 3

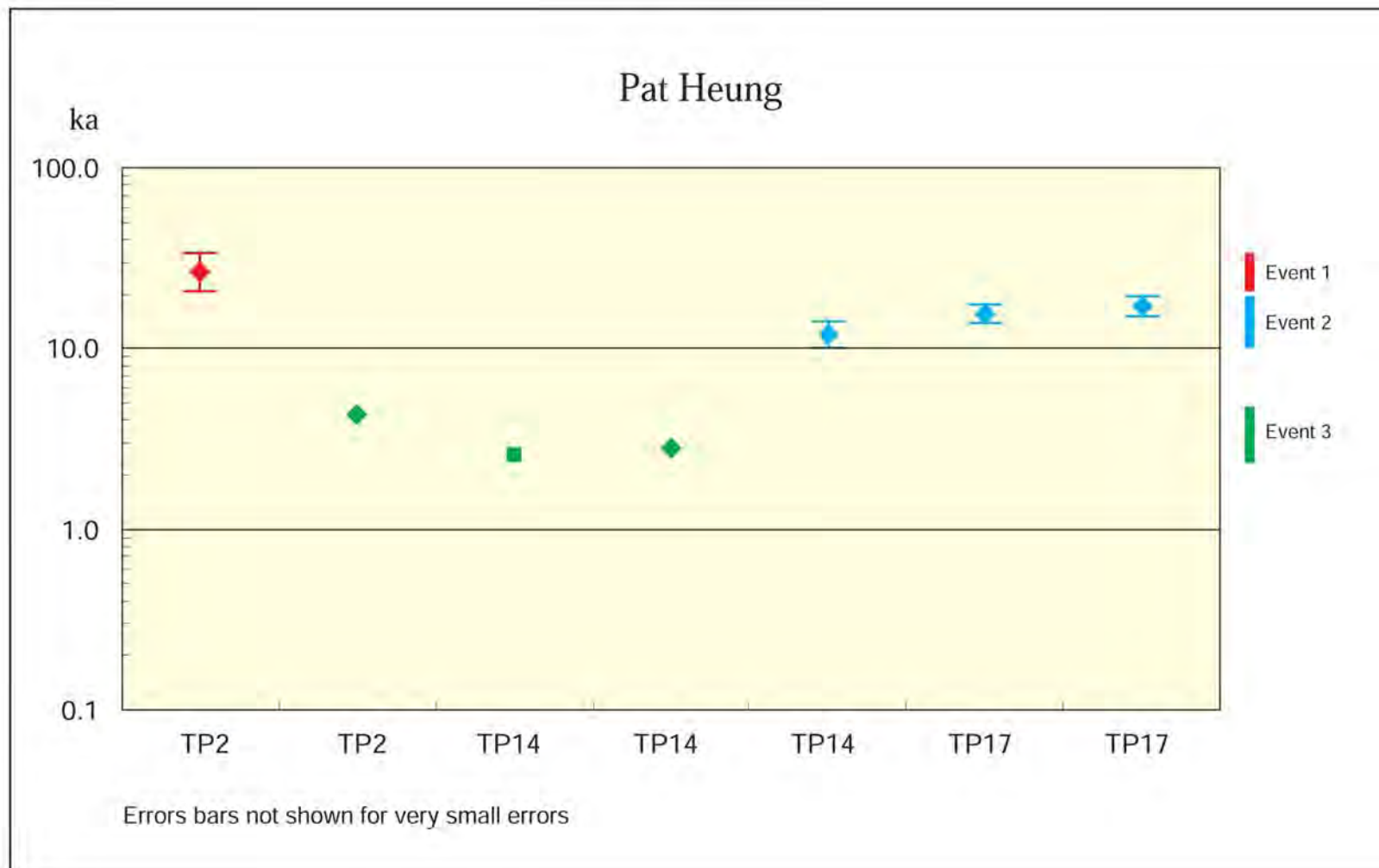


Figure 8 - Error Bar Chart Summarizing the Numerical (Absolute) Age Data for the Pat Heung Landslide Site. Symbols as for Figure 4

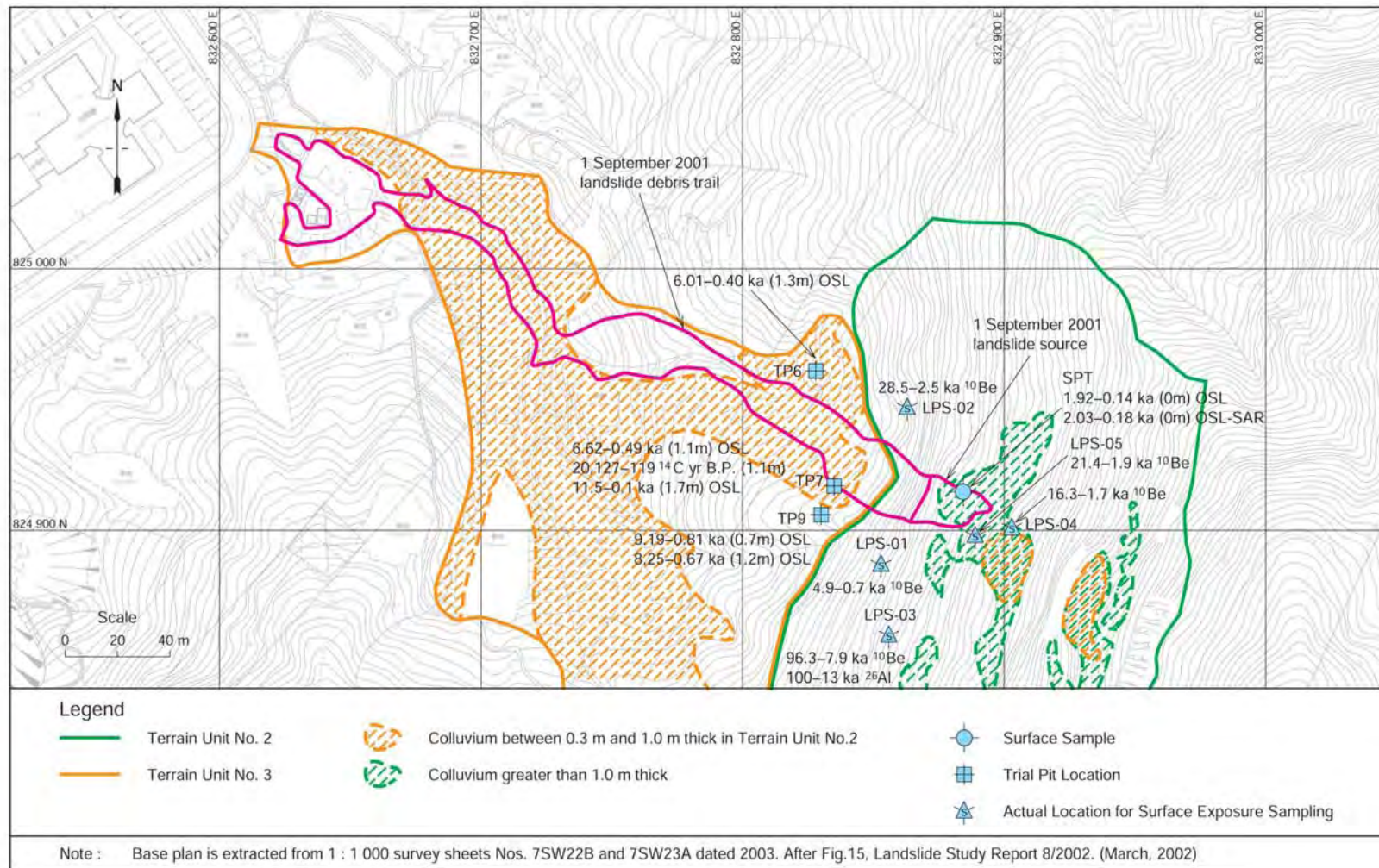


Figure 9 - API Interpretation, Sample Locations and Dating Results for the Lei Pui Street Landslide Site



Figure 10 - Error Bar Chart Summarizing the Numerical (Absolute) Age Data for the Lei Pui Street Landslide Site. Symbols as for Figure 4

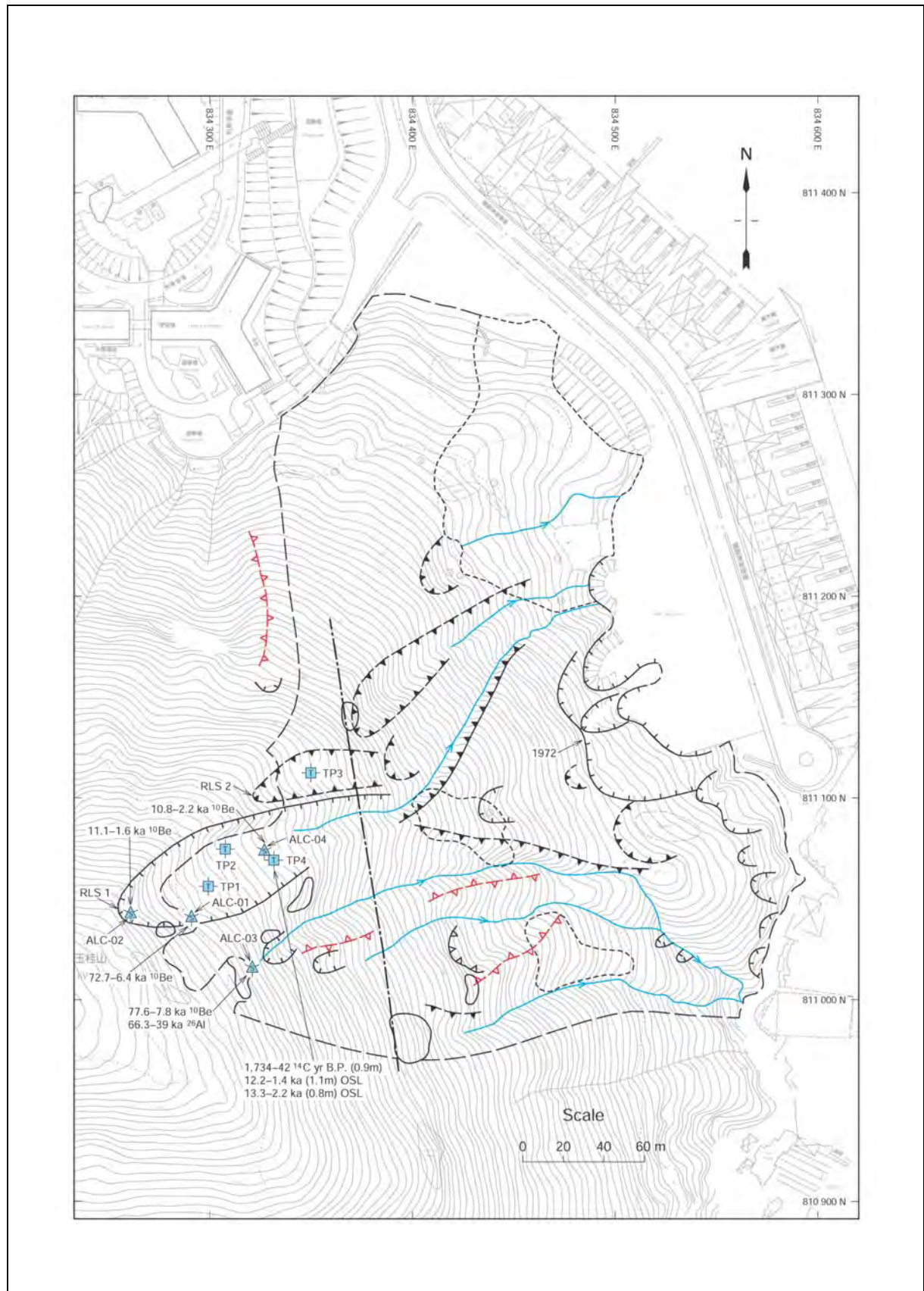


Figure 11 - API Interpretation, Sample Locations and Dating Results for the Ap Lei Chau Landslide Site. Legend as for Figure 3

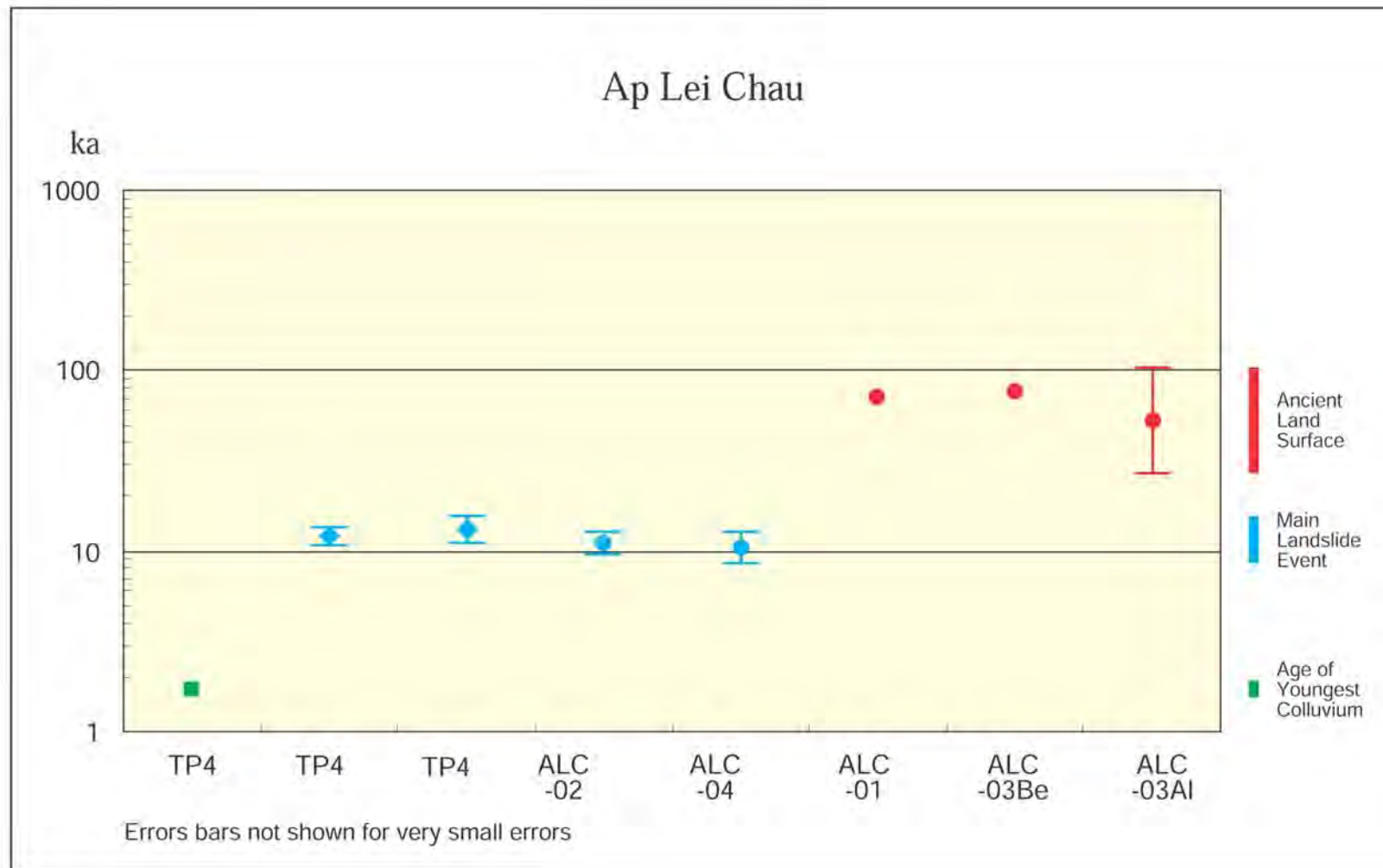


Figure 12 - Error Bar Chart Summarizing the Numerical (Absolute) Age Data for the Ap Lei Chau Landslide Site. Symbols as for Figure 4

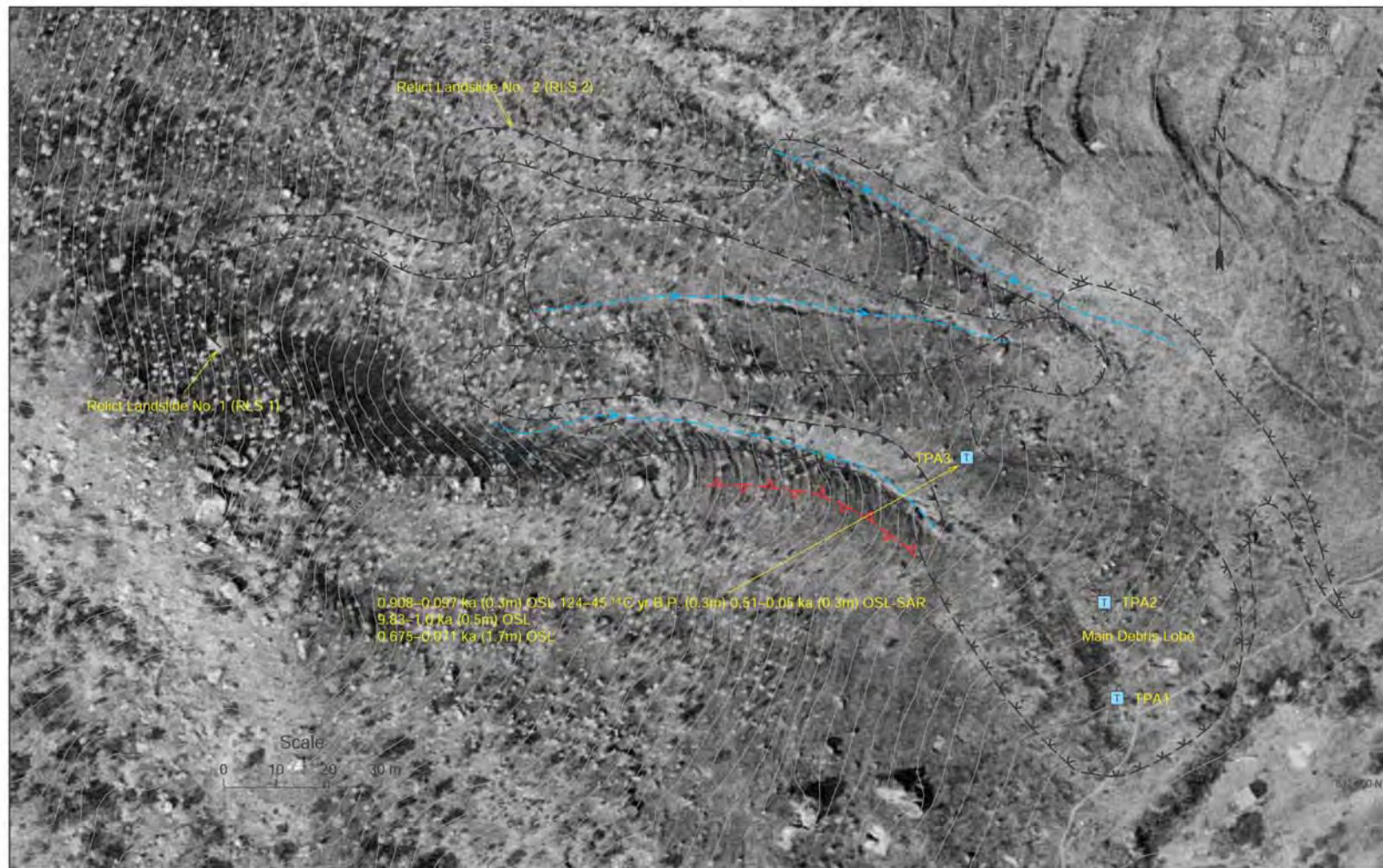


Figure 13 - API Interpretation, Sample Locations and Dating Results for the Tsing Shan A Landslide Site. Legend as For Figure 3

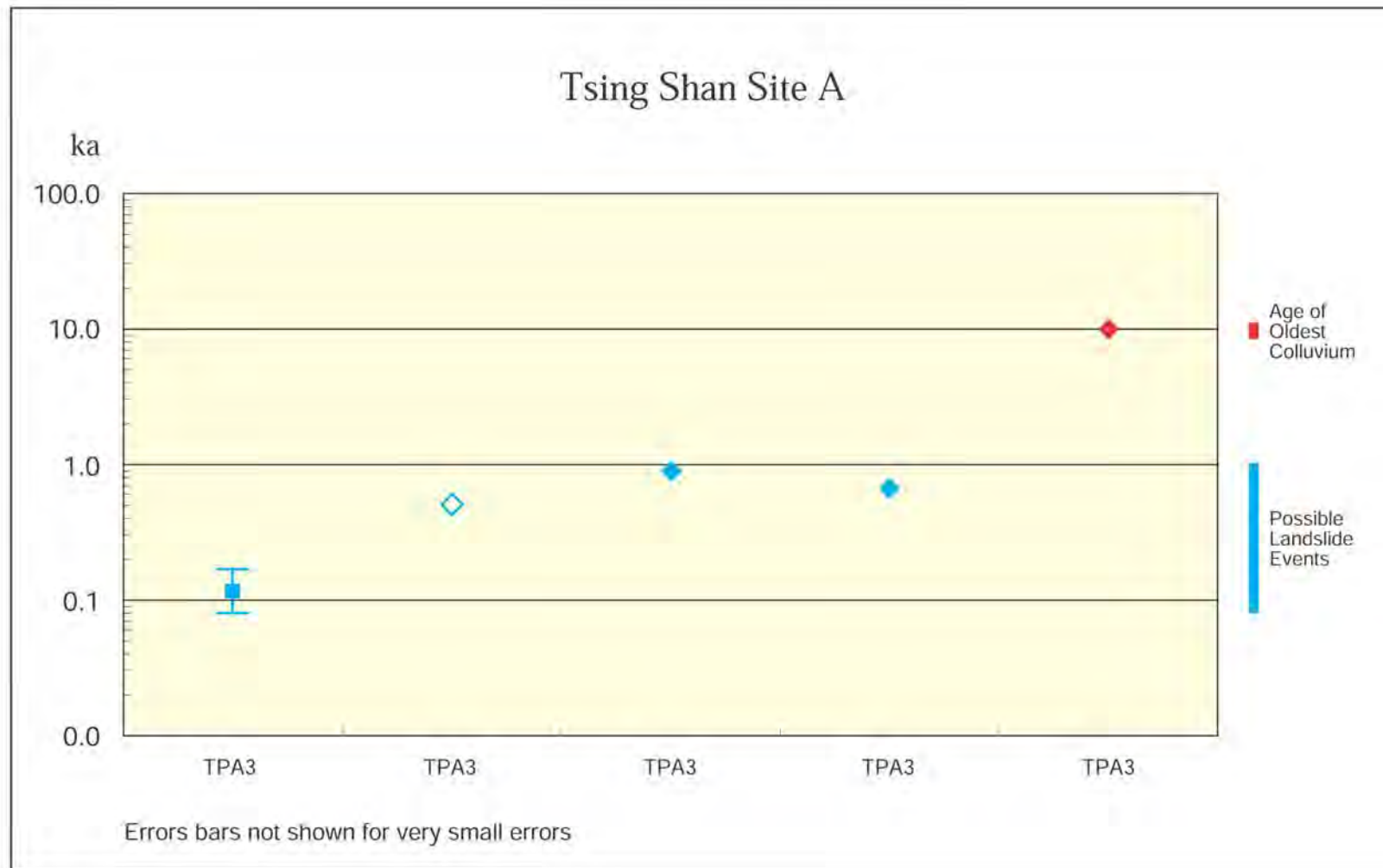


Figure 14 - Error Bar Chart Summarizing the Numerical (Absolute) Age Data for the Tsing Shan A Landslide Site. Symbols as for Figure 4

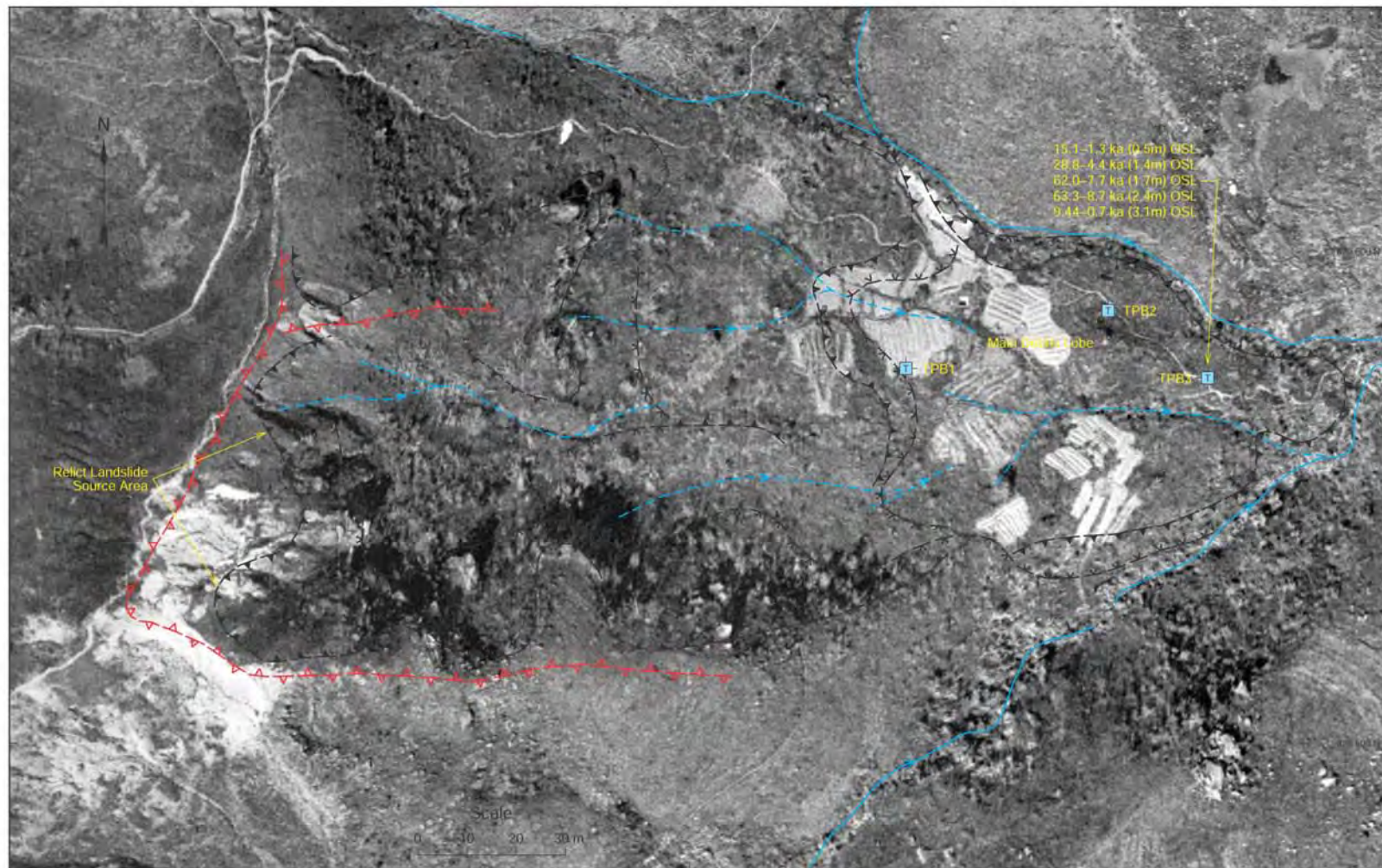


Figure 15 - API Interpretation, Sample Locations and Dating Results for the Tsing Shan B Landslide Site. Legend as for Figure 3



Figure 16 - Error Bar Chart Summarizing the Numerical (Absolute) Age Data for the Tsing Shan B Landslide Site. Symbols as for Figure 4

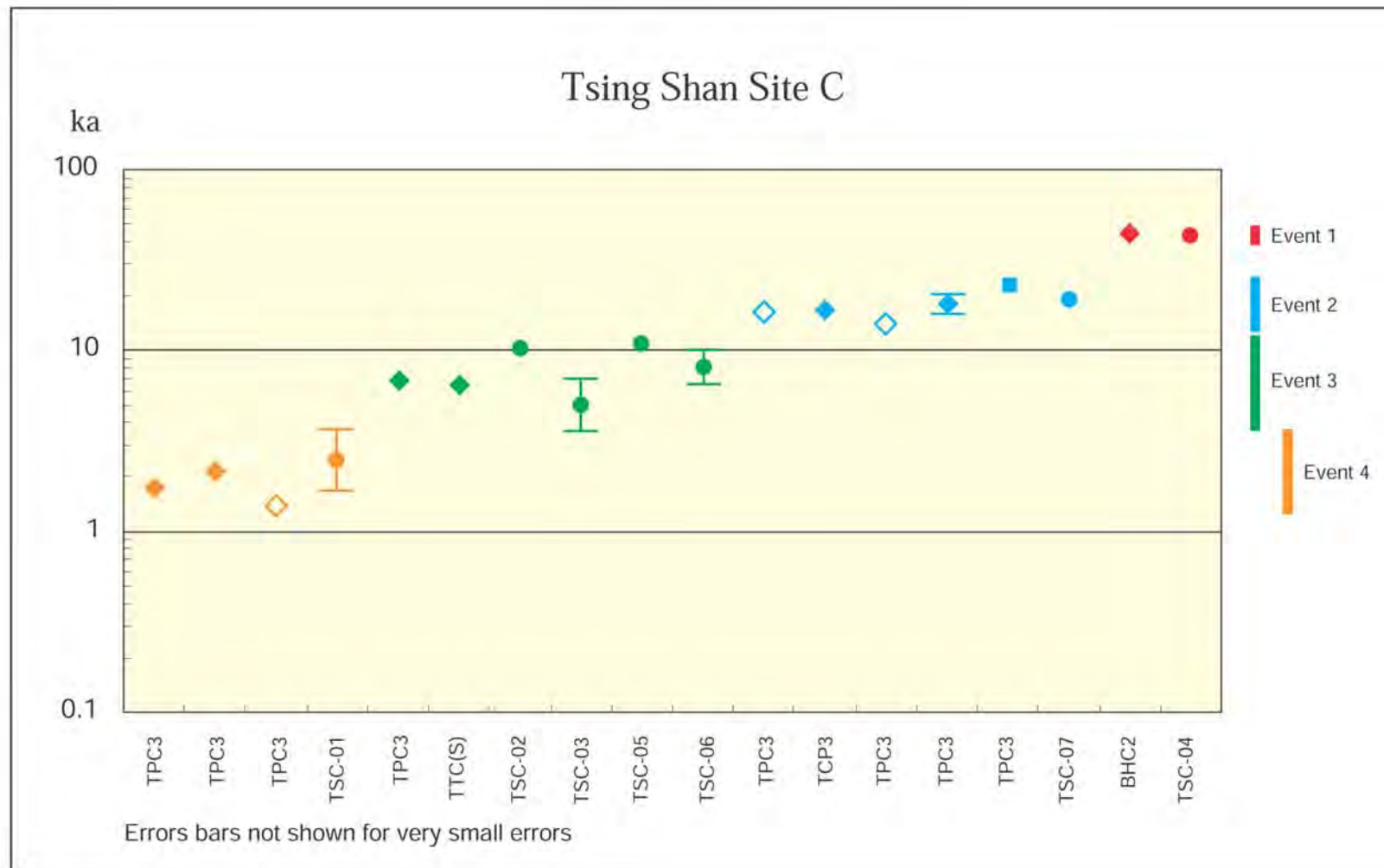


Figure 18 - Error Bar Chart Summarizing the Numerical (Absolute) Age Data for the Tsing Shan C Landslide Site. Symbols as for Figure 4

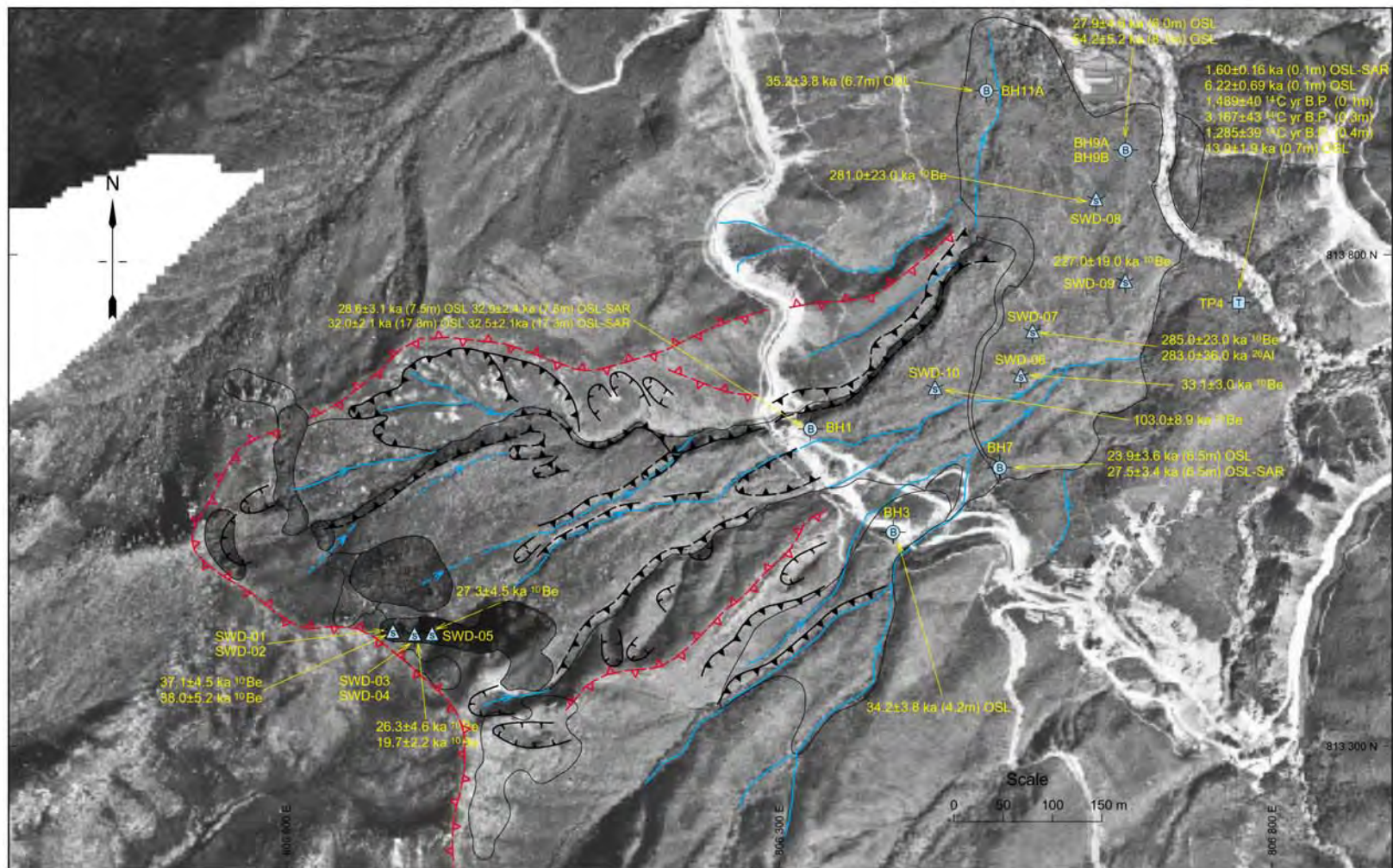


Figure 19 - API Interpretation, Sample Locations and Dating Results for the Sham Wat Debris Lobe. Legend as for Figure 3

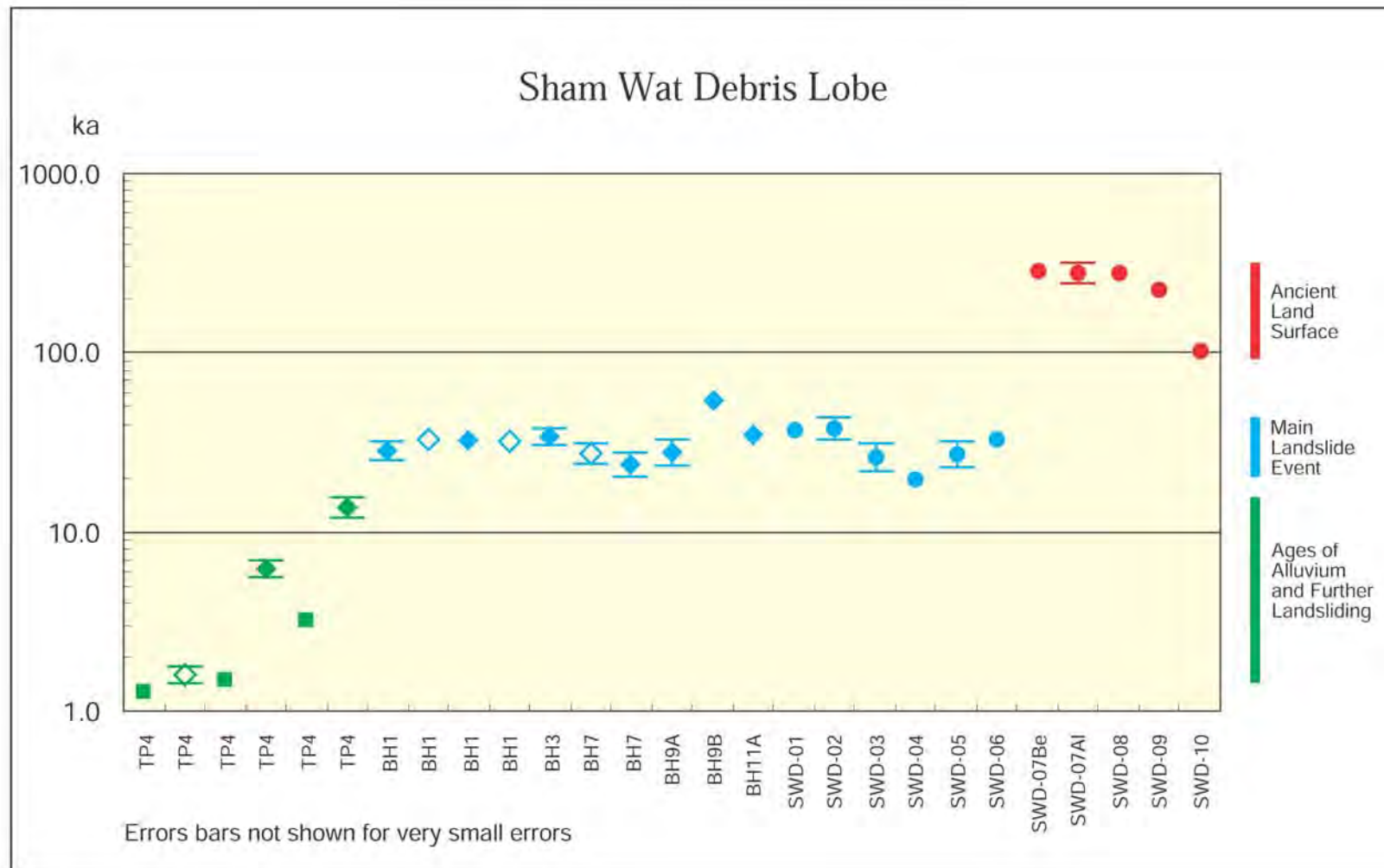


Figure 20 - Error Bar Chart Summarizing the Numerical (Absolute) Age Data for the Sham Wat Debris Lobe. Symbols as for Figure 4

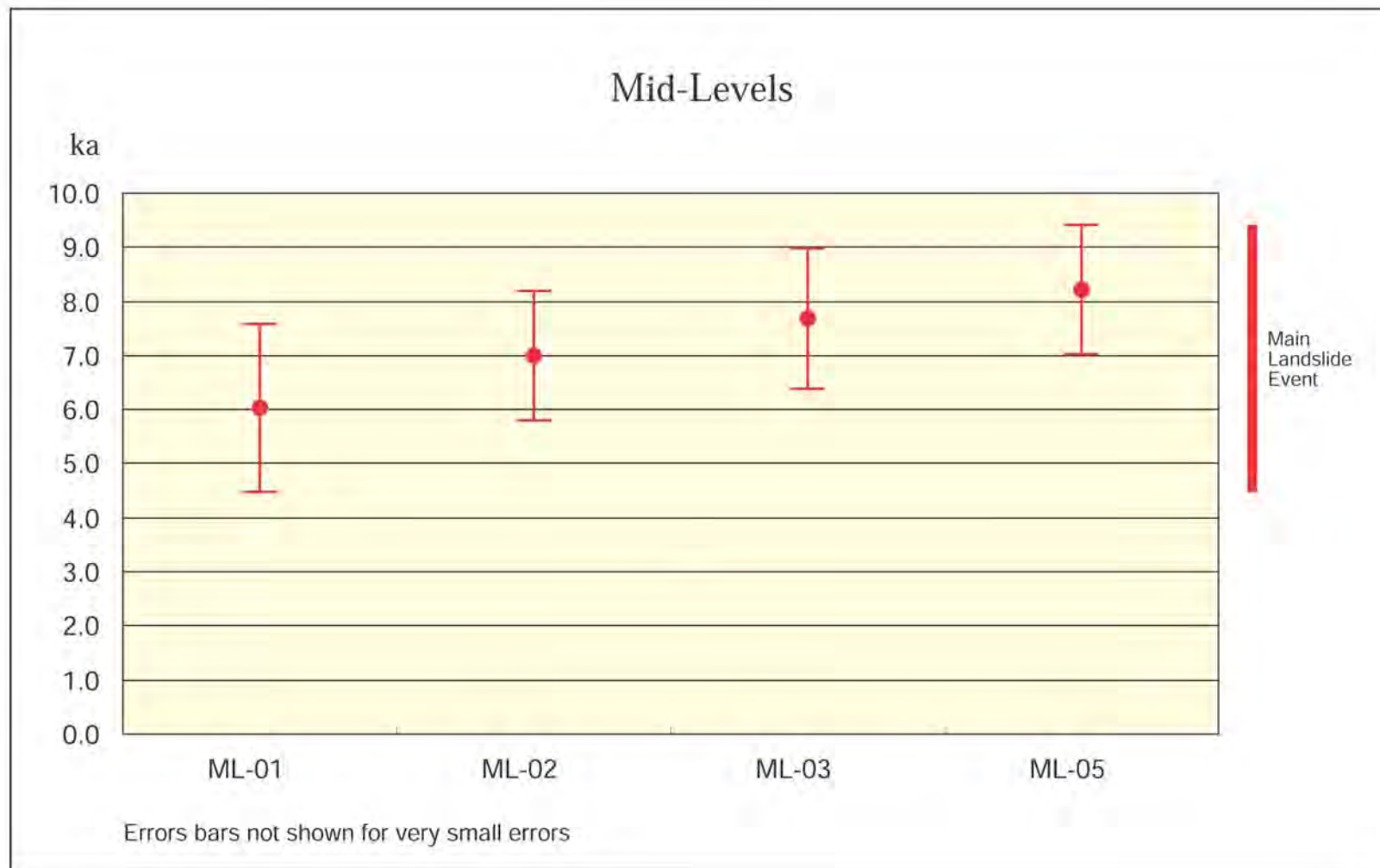


Figure 22 - Error Bar Chart Summarizing the Numerical (Absolute) Age Data for the Mid-Levels Landslide Site. Symbols as for Figure 4

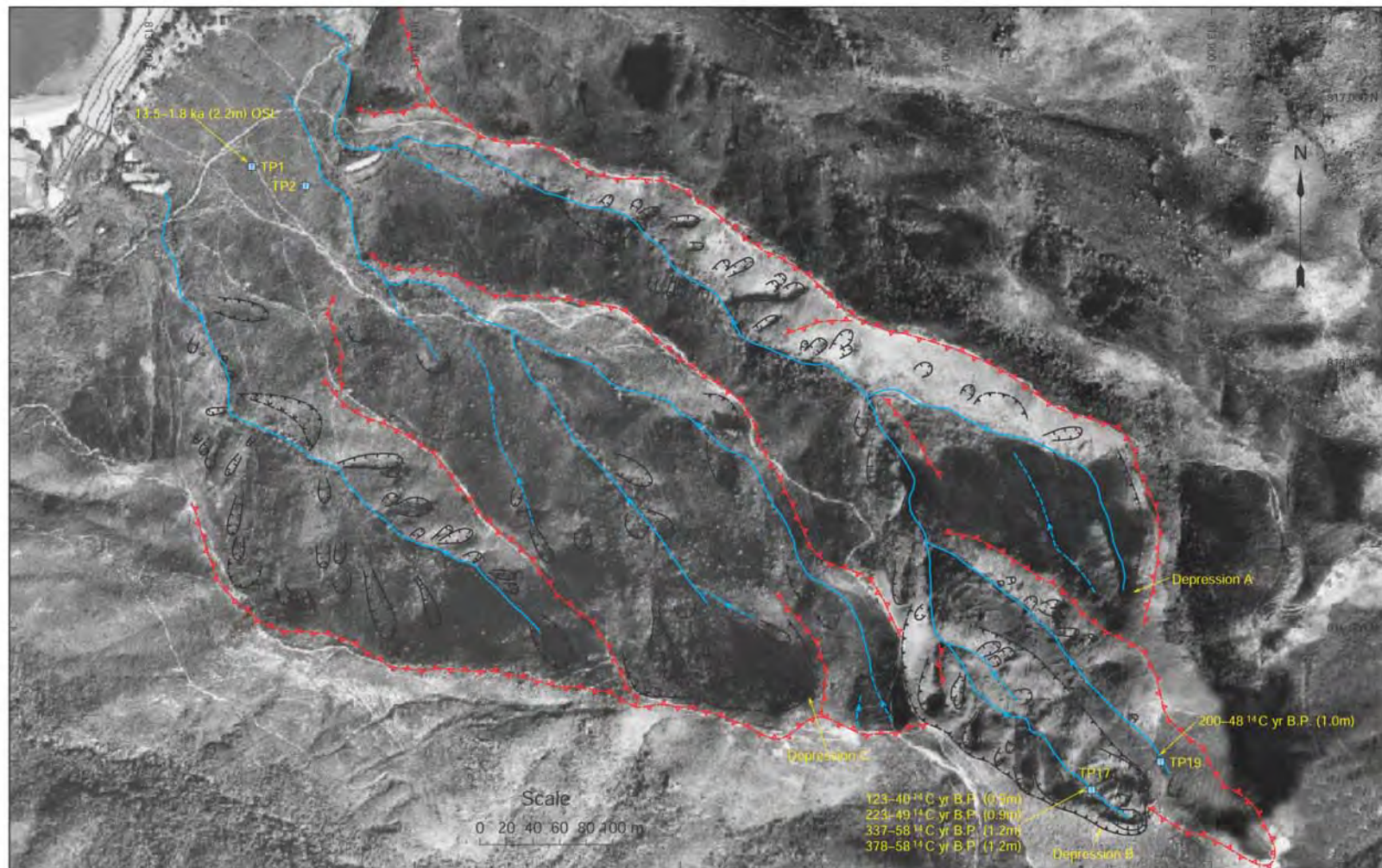


Figure 23 - API Interpretation, Sample Locations and Dating Results for the Tung Chung East Landslide Site. Legend as for Figure 3

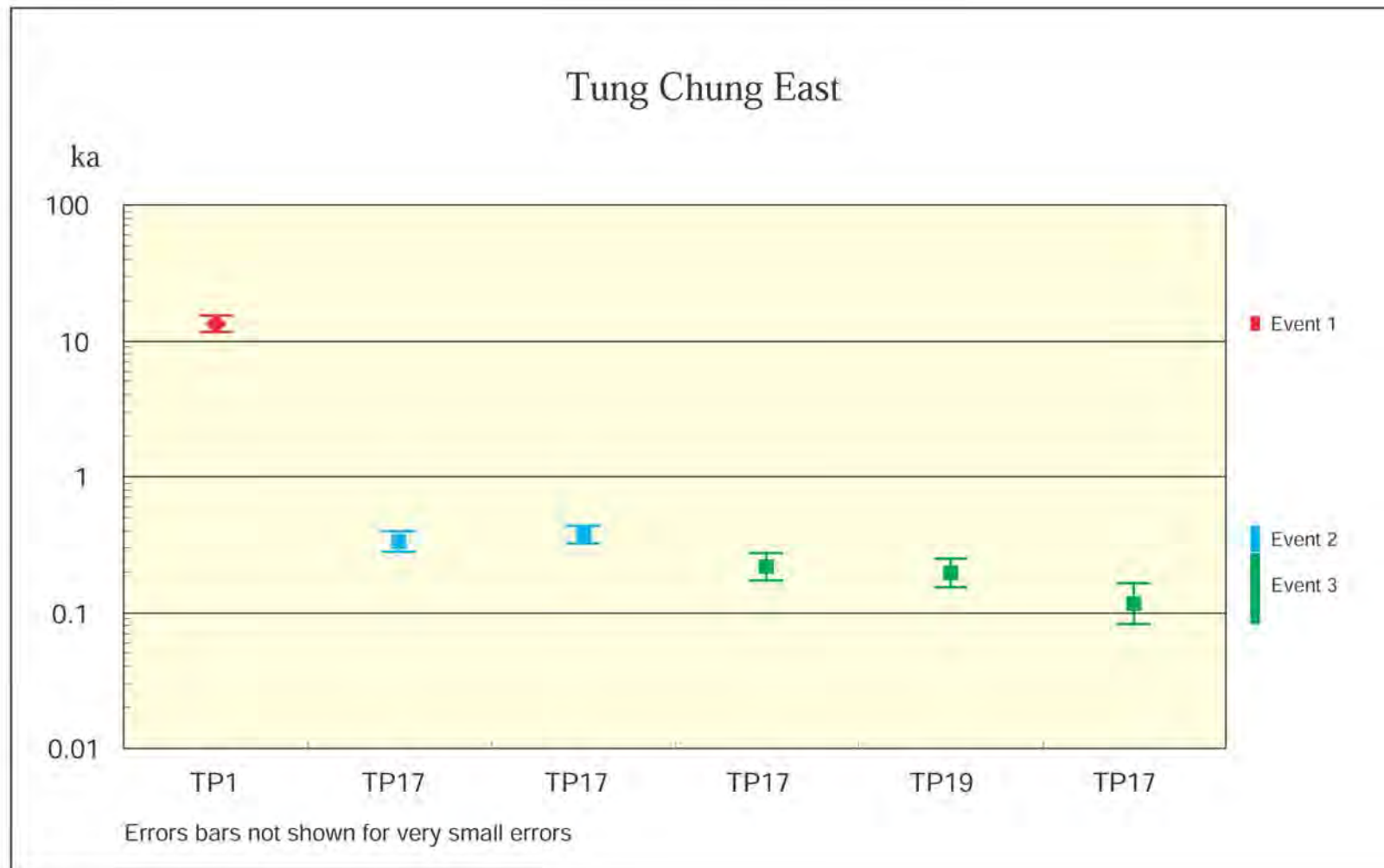


Figure 24 - Error Bar Chart Summarizing the Numerical (Absolute) Age Data for the Tung Chung East Landslide Site. Symbols as for Figure 4

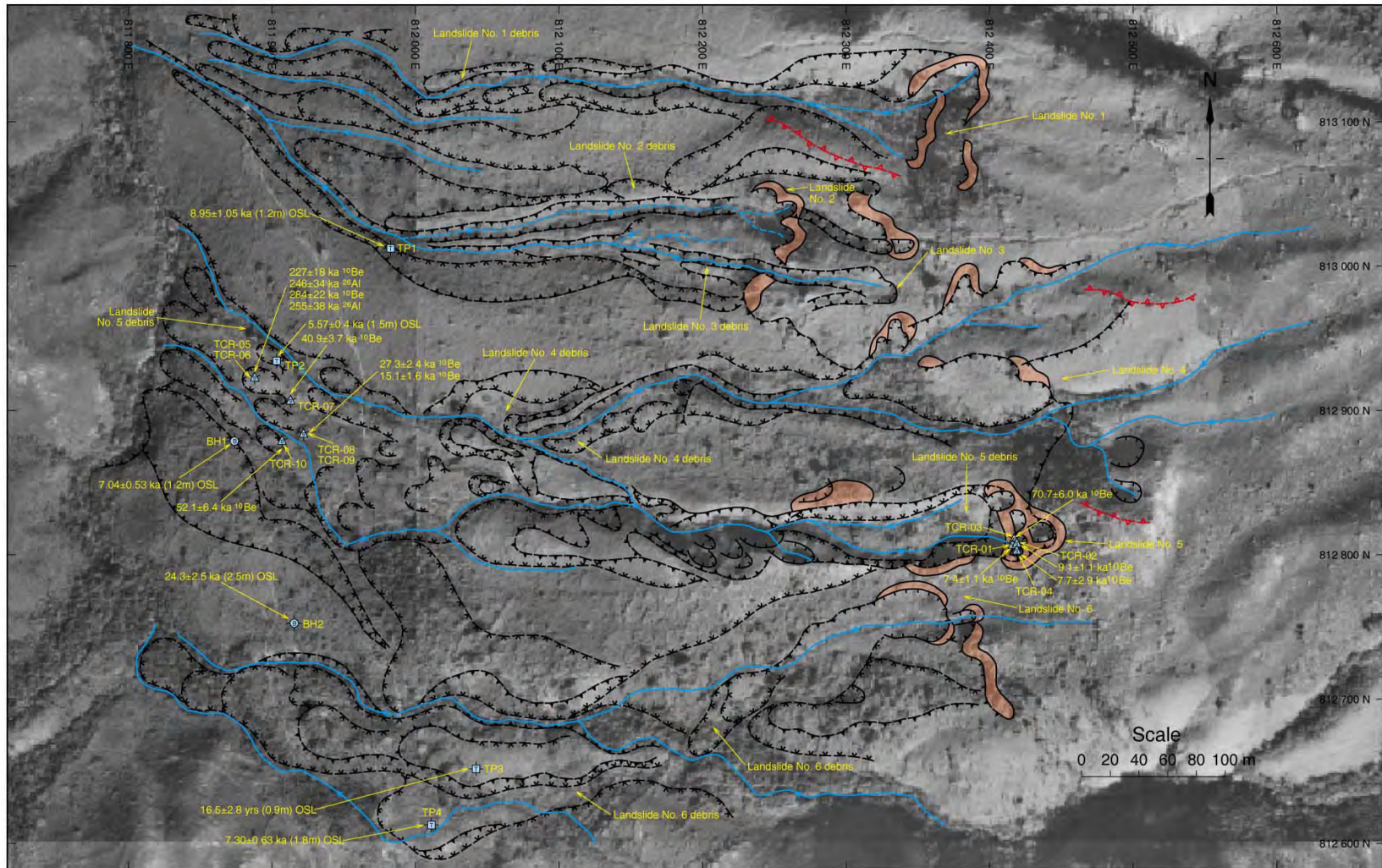


Figure 25 - API Interpretation, Sample Locations and Dating Results for the Sunset Peak West Landslide Site. Legend as for Figure 3

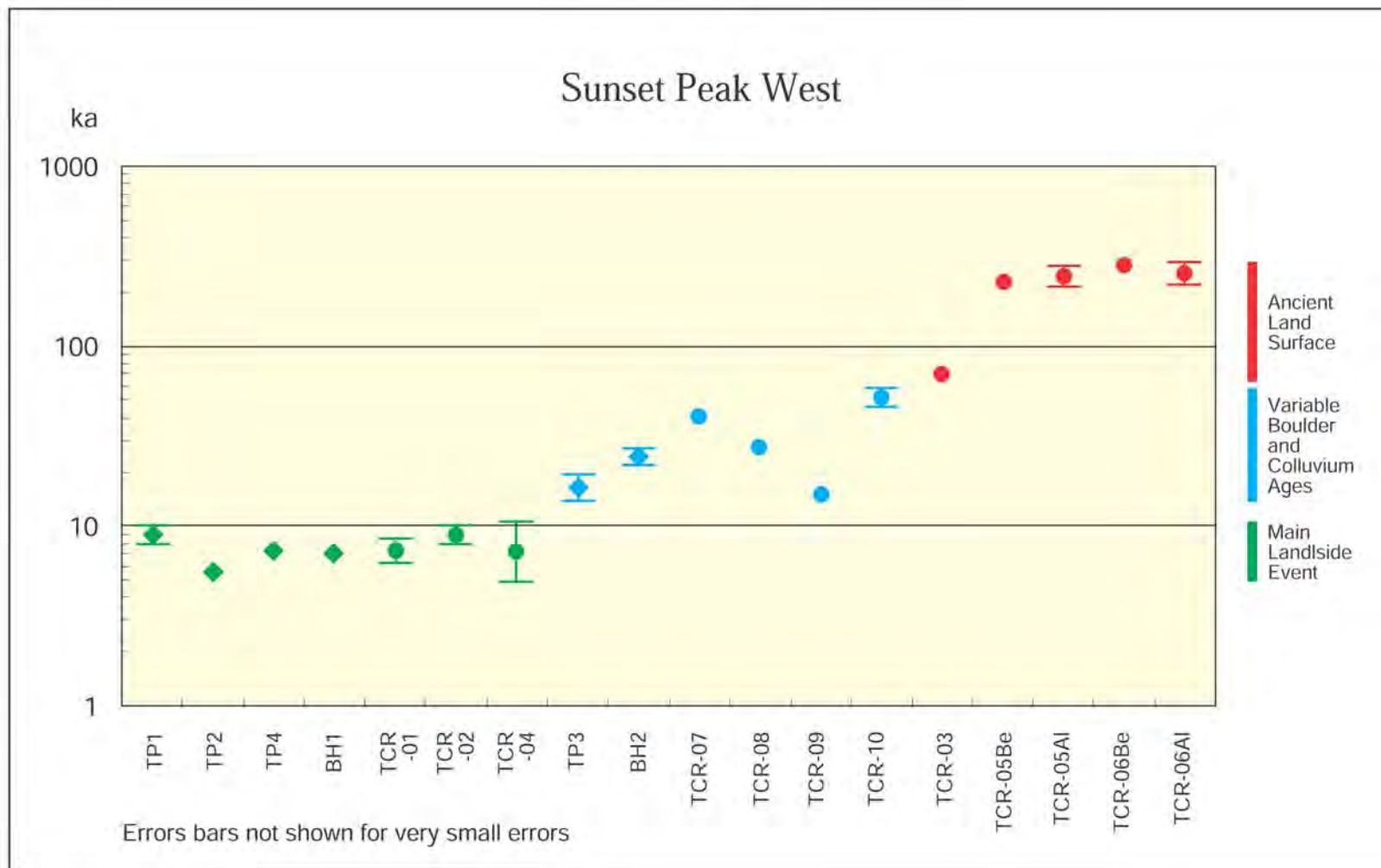


Figure 26 - Error Bar Chart Summarizing the Numerical (Absolute) Age Data for the Sunset Peak West Landslide Site. Symbols as for Figure 4

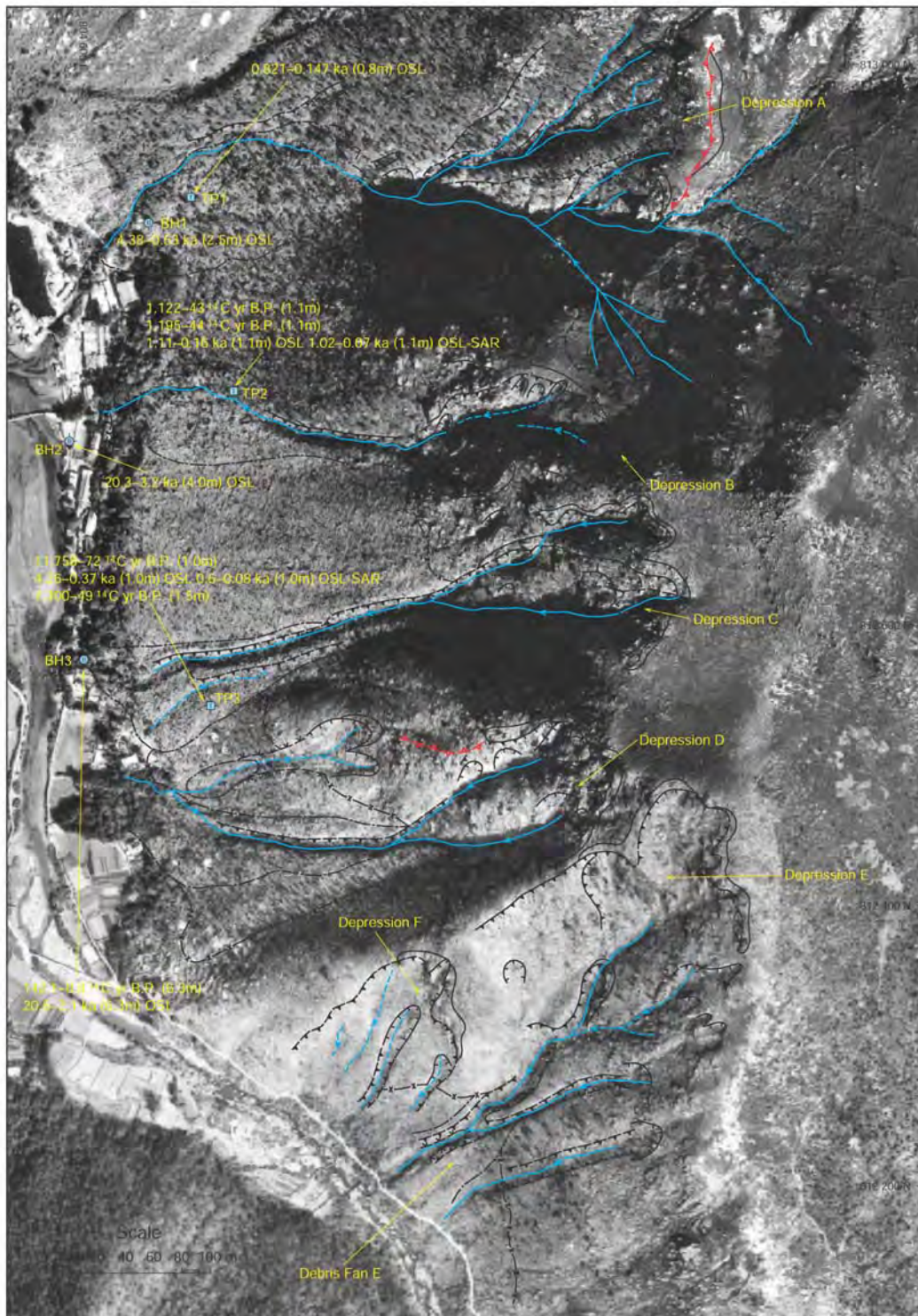


Figure 27 - API Interpretation, Sample Locations and Dating Results for the Tai O Landslide Site. Legend as for Figure 3

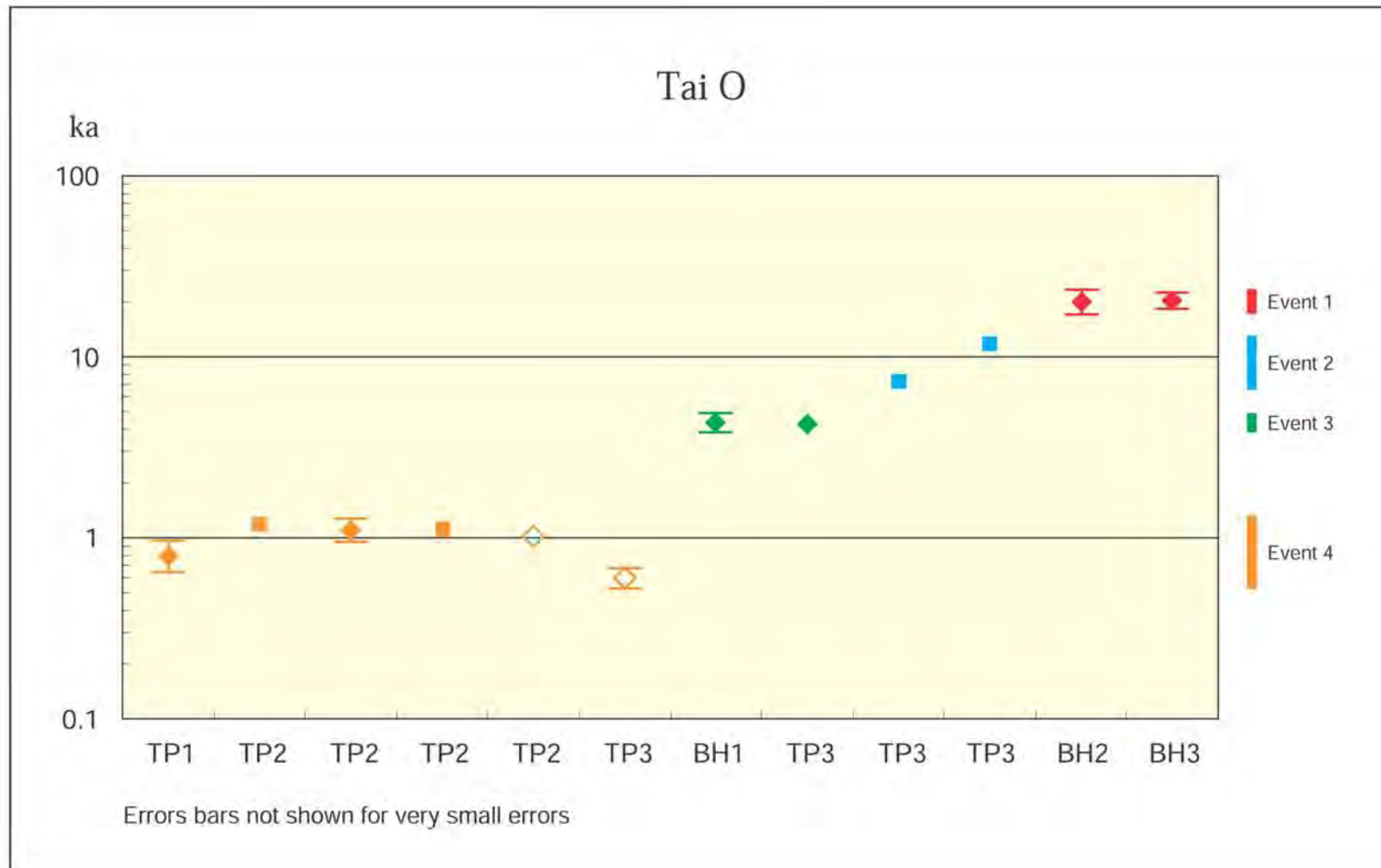


Figure 28 - Error Bar Chart Summarizing the Numerical (Absolute) Age Data for the Tai O Landslide Site. Symbols as for Figure 4

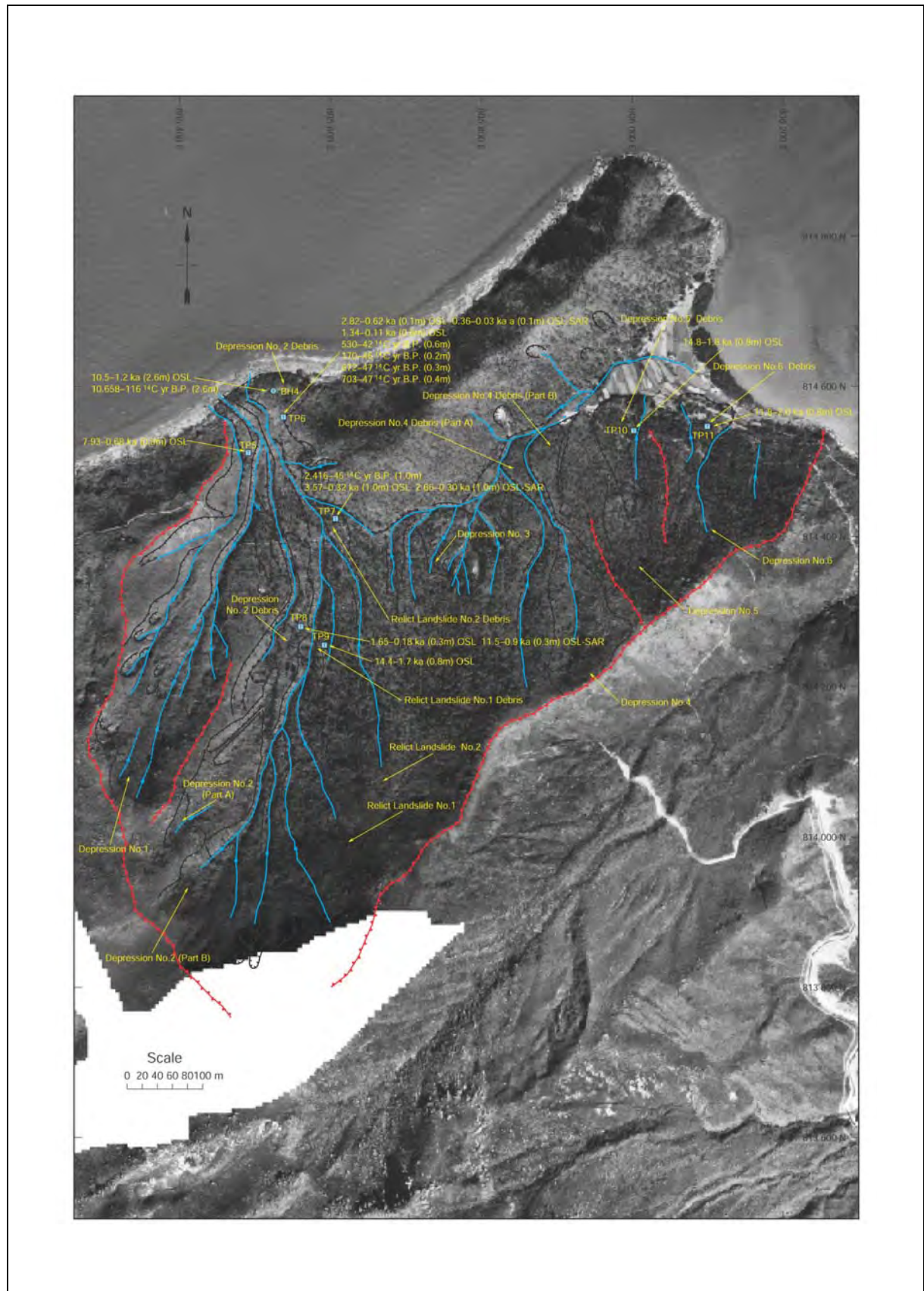


Figure 29 - API Interpretation, Sample Locations and Dating Results for the Sai Tso Wan Landslide Site. Legend as for Figure 3

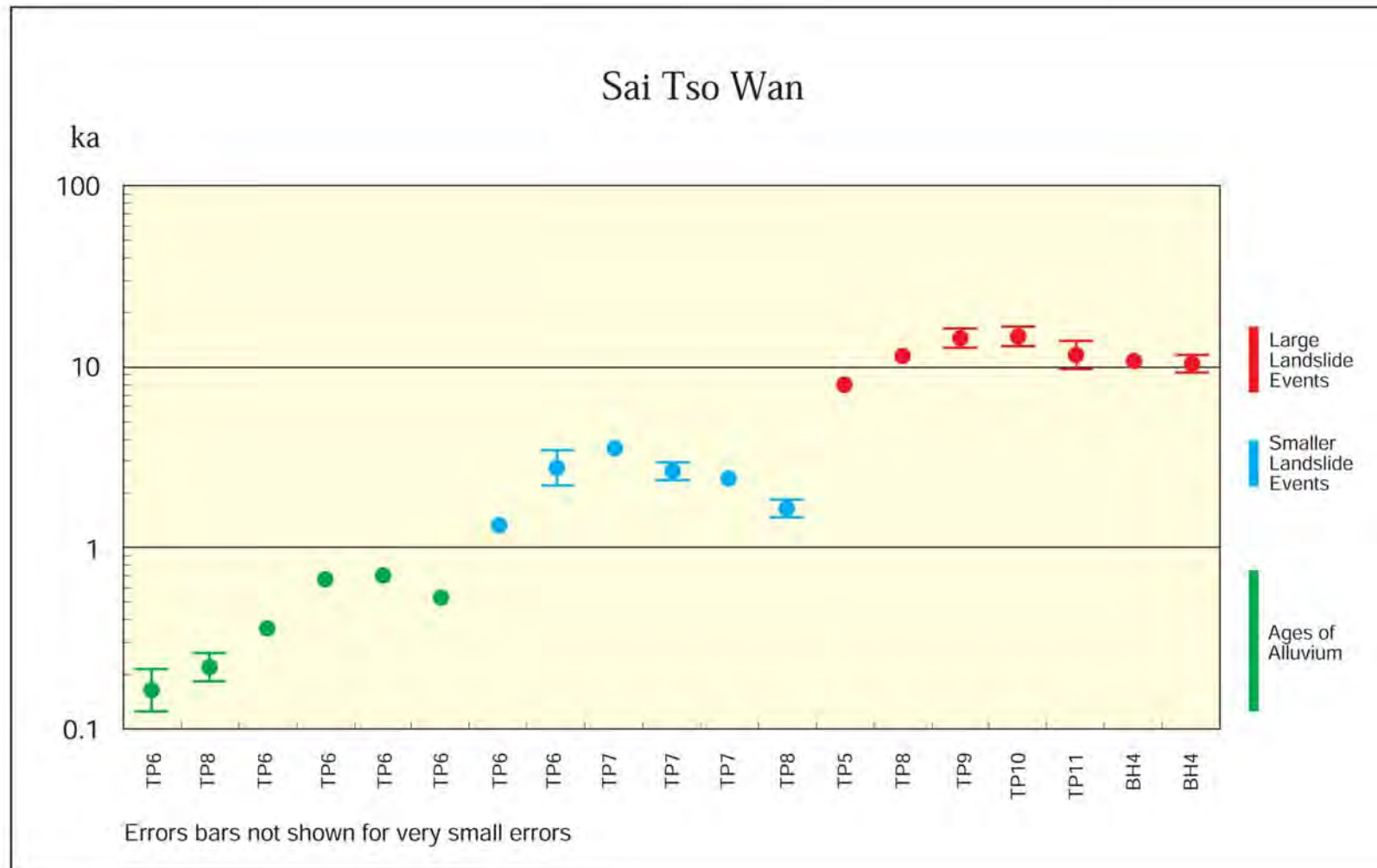


Figure 30 - Error Bar Chart Summarizing the Numerical (Absolute) Age Data for the Sai Tso Wan Landslide Site. Symbols as for Figure 4

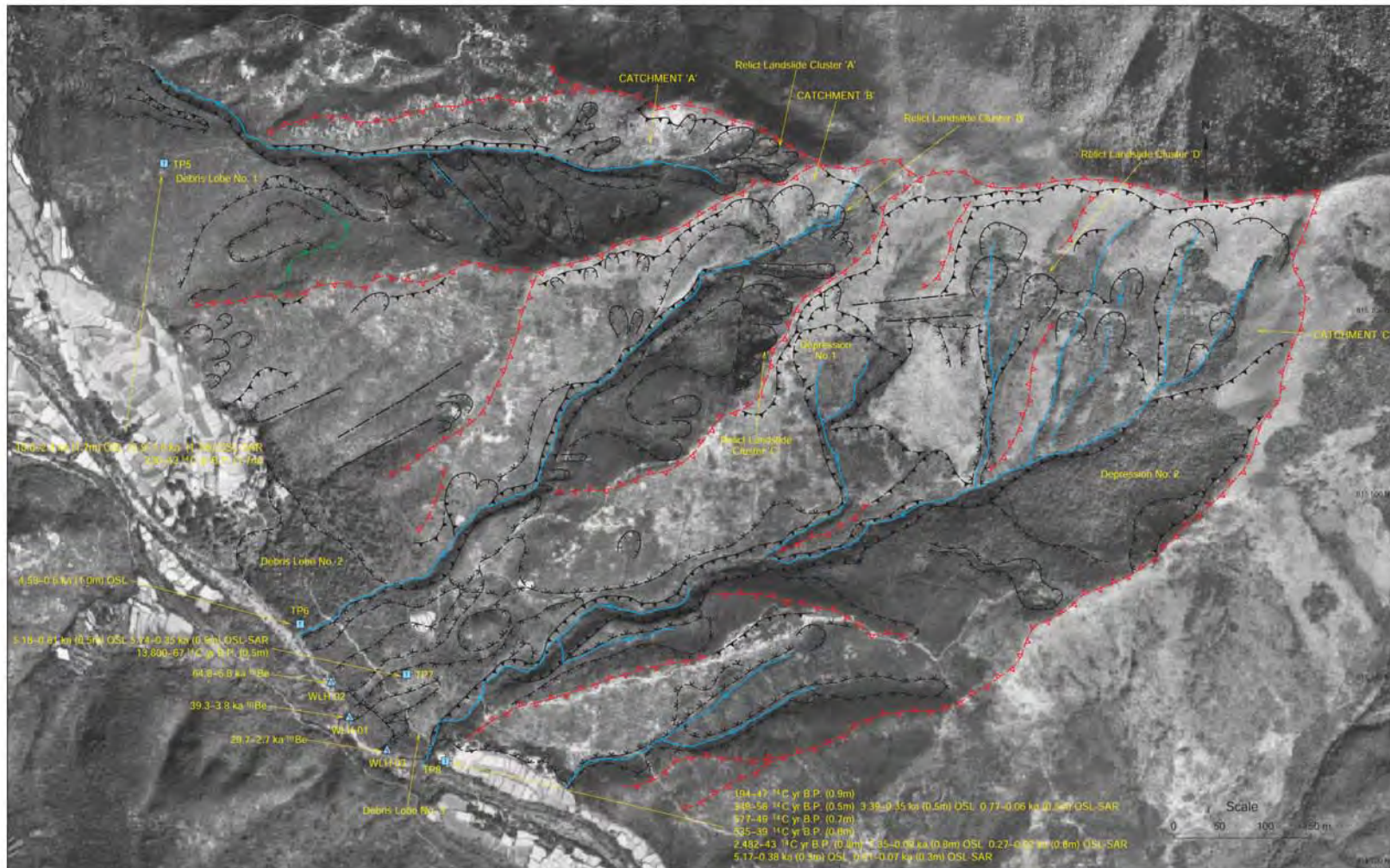


Figure 31 - API Interpretation, Sample Locations and Dating Results for the Wong Lung Hang Landslide Site. Legend as for Figure 3

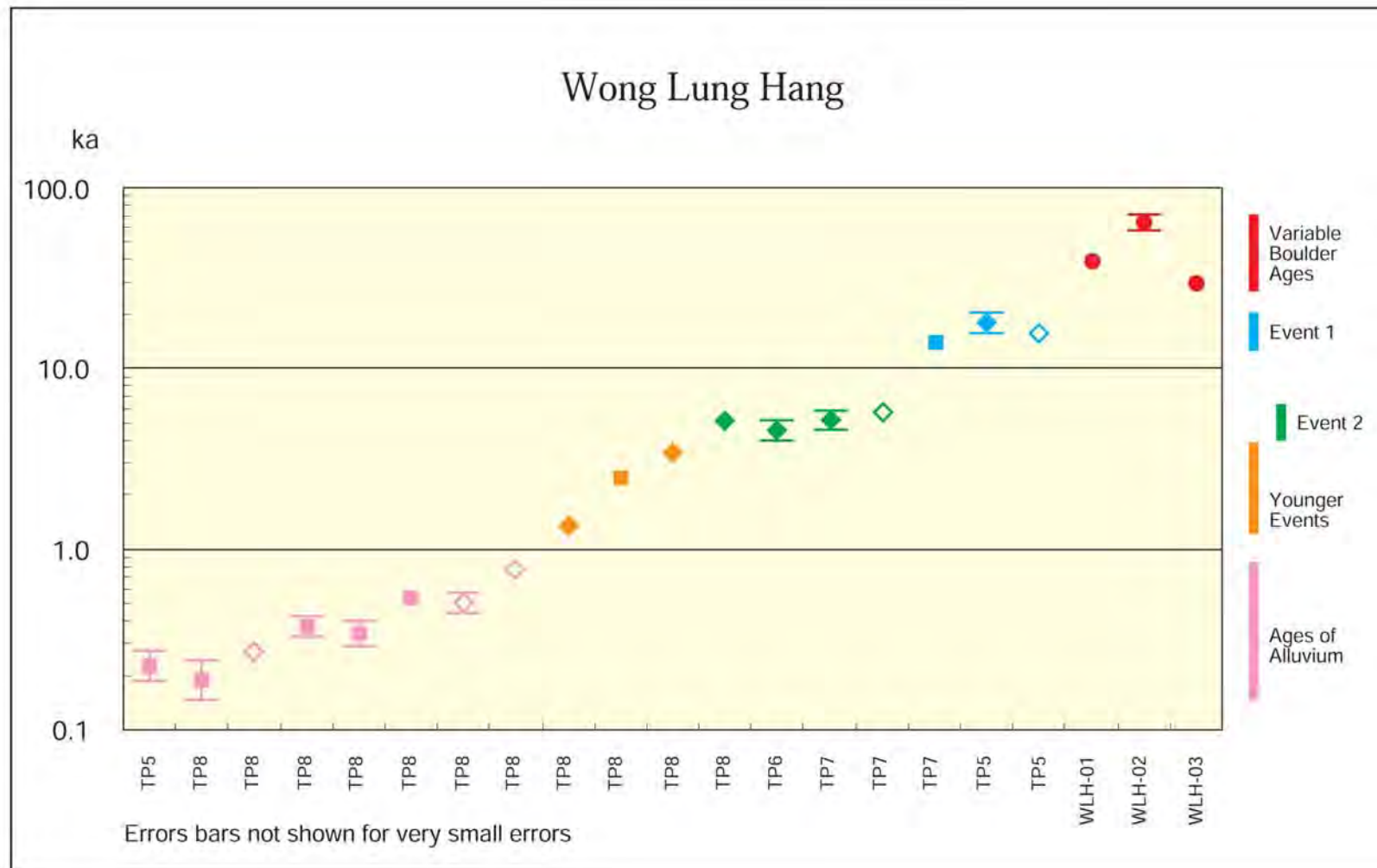


Figure 32 - Error Bar Chart Summarizing the Numerical (Absolute) Age Data for the Wong Lung Hang Landslide Site.
Symbols as for Figure 4

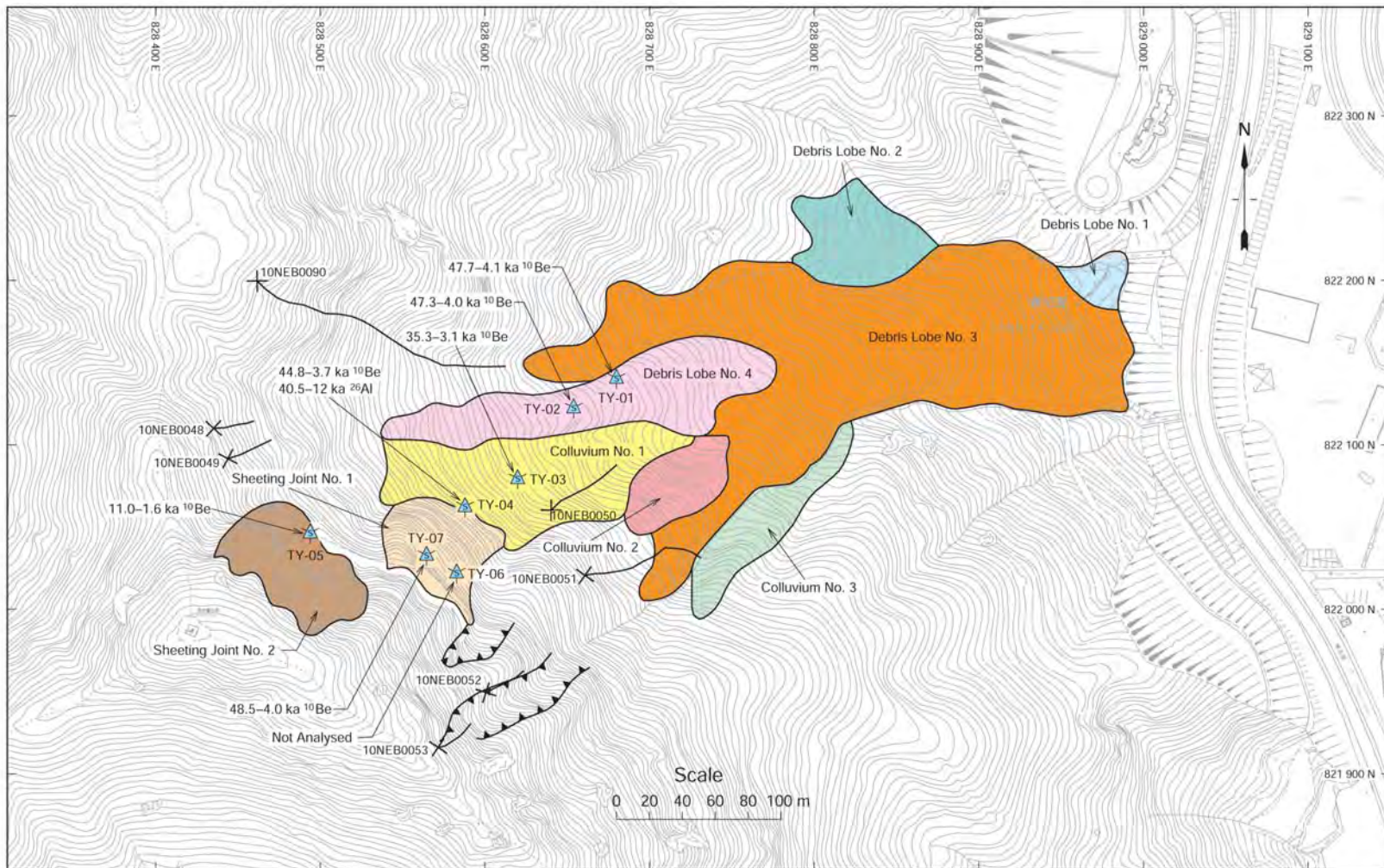


Figure 33 - API Interpretation, Sample Locations and Dating Results for the Southeast Tsing Yi Landslide Site. Legend as for Figure 3

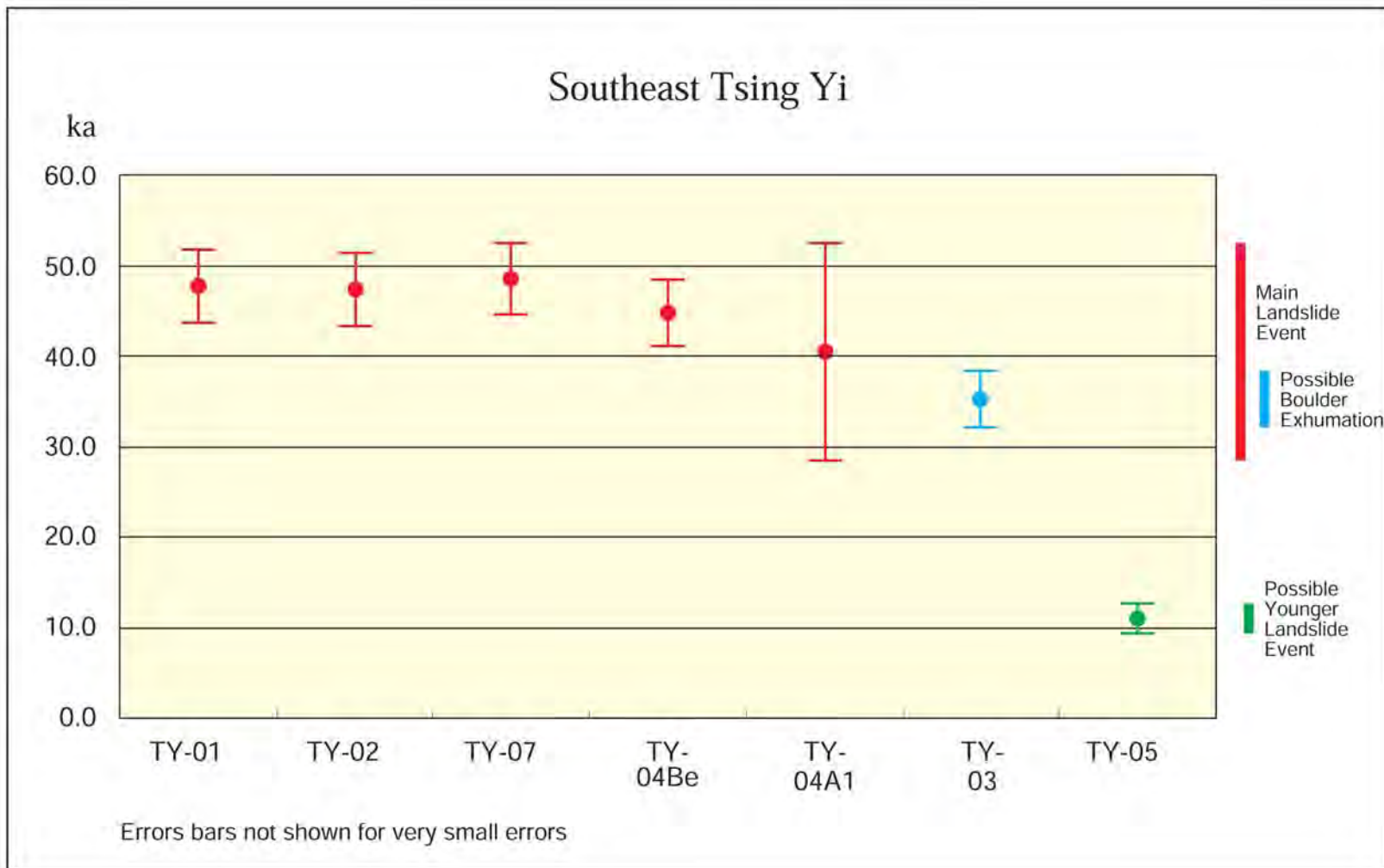


Figure 34 - Error Bar Chart Summarizing the Numerical (Absolute) Age Data for the Southeast Tsing Yi Landslide Site. Symbols as for Figure 4

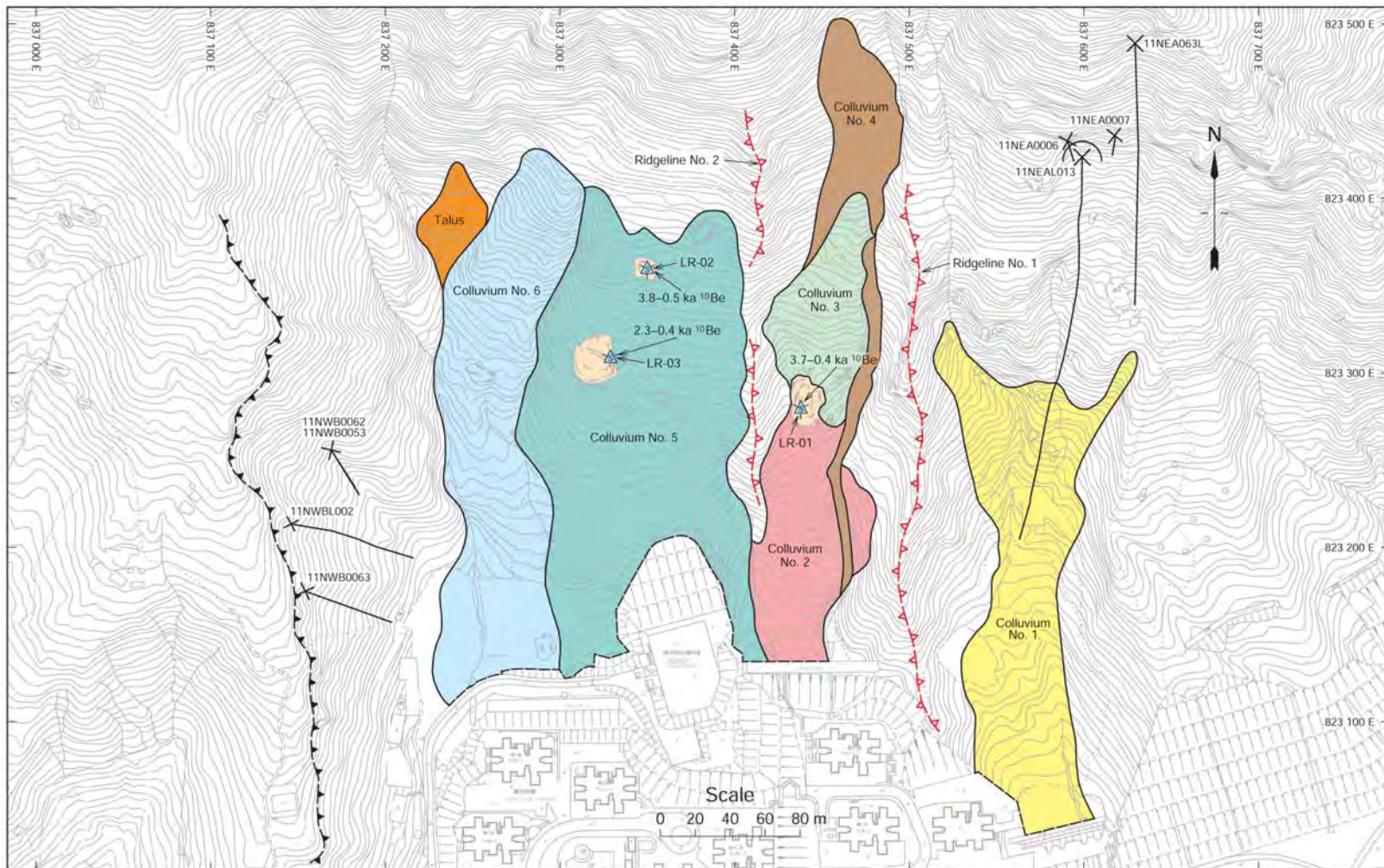


Figure 35 - API Interpretation, Sample Locations and Dating Results for the Lion Rock Boulder Site. Legend as for Figure 3

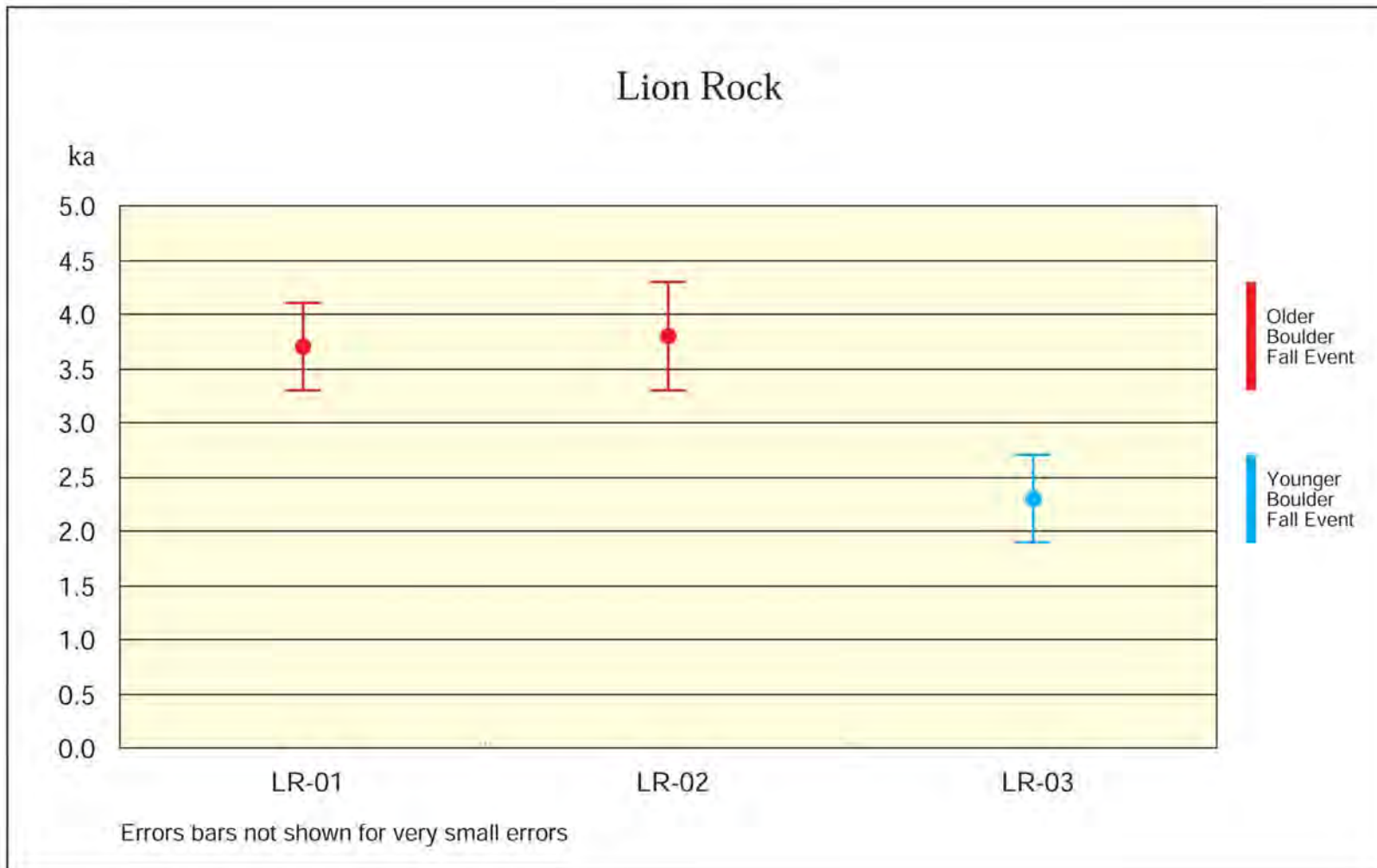


Figure 36 - Error Bar Chart Summarizing the Numerical (Absolute) Age Data for the Lion Rock Boulder Site. Symbols as for Figure 4

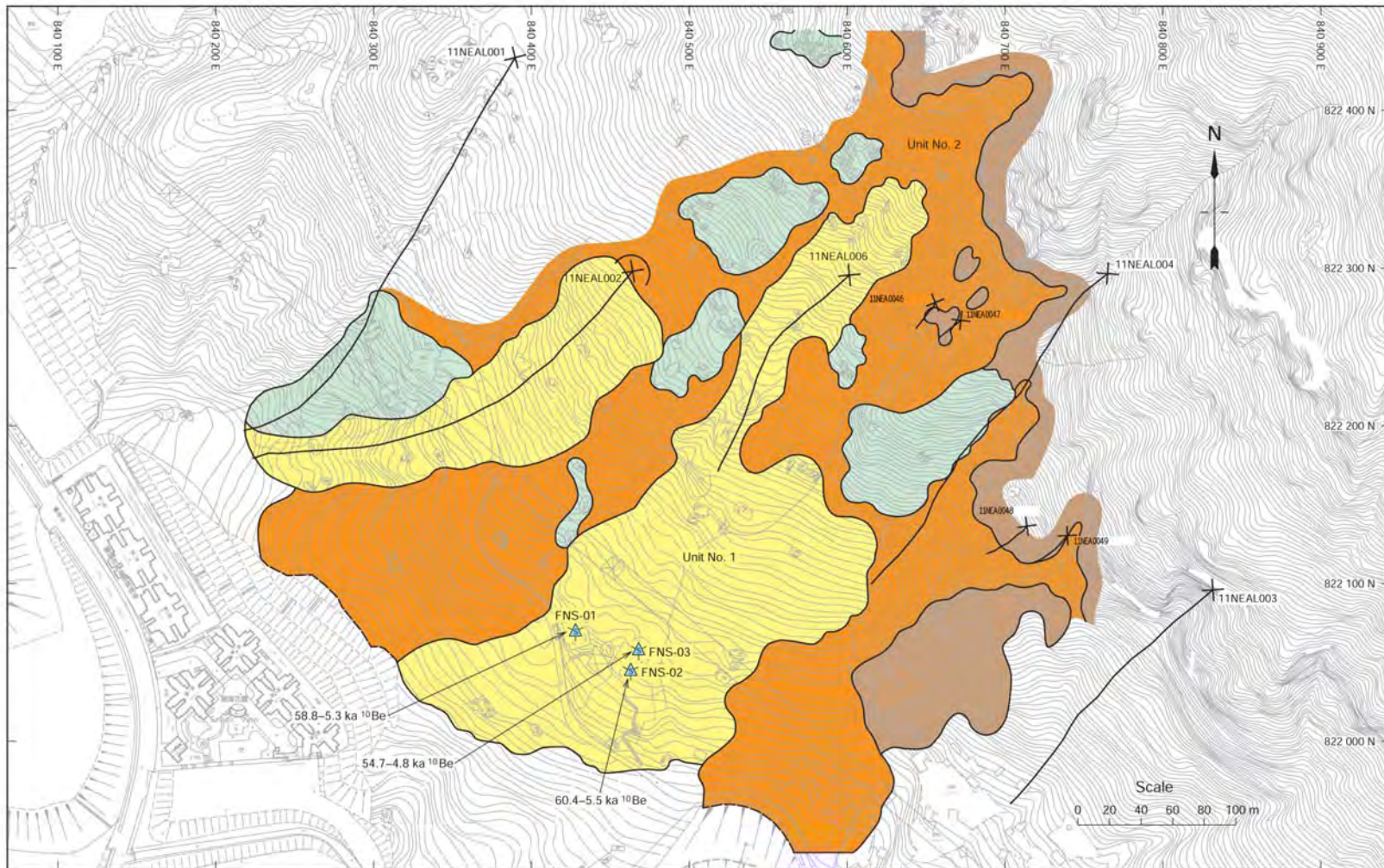


Figure 37 - API Interpretation, Sample Locations and Dating Results for the Fei Ngo Shan Boulder Site. Legend as for Figure 3

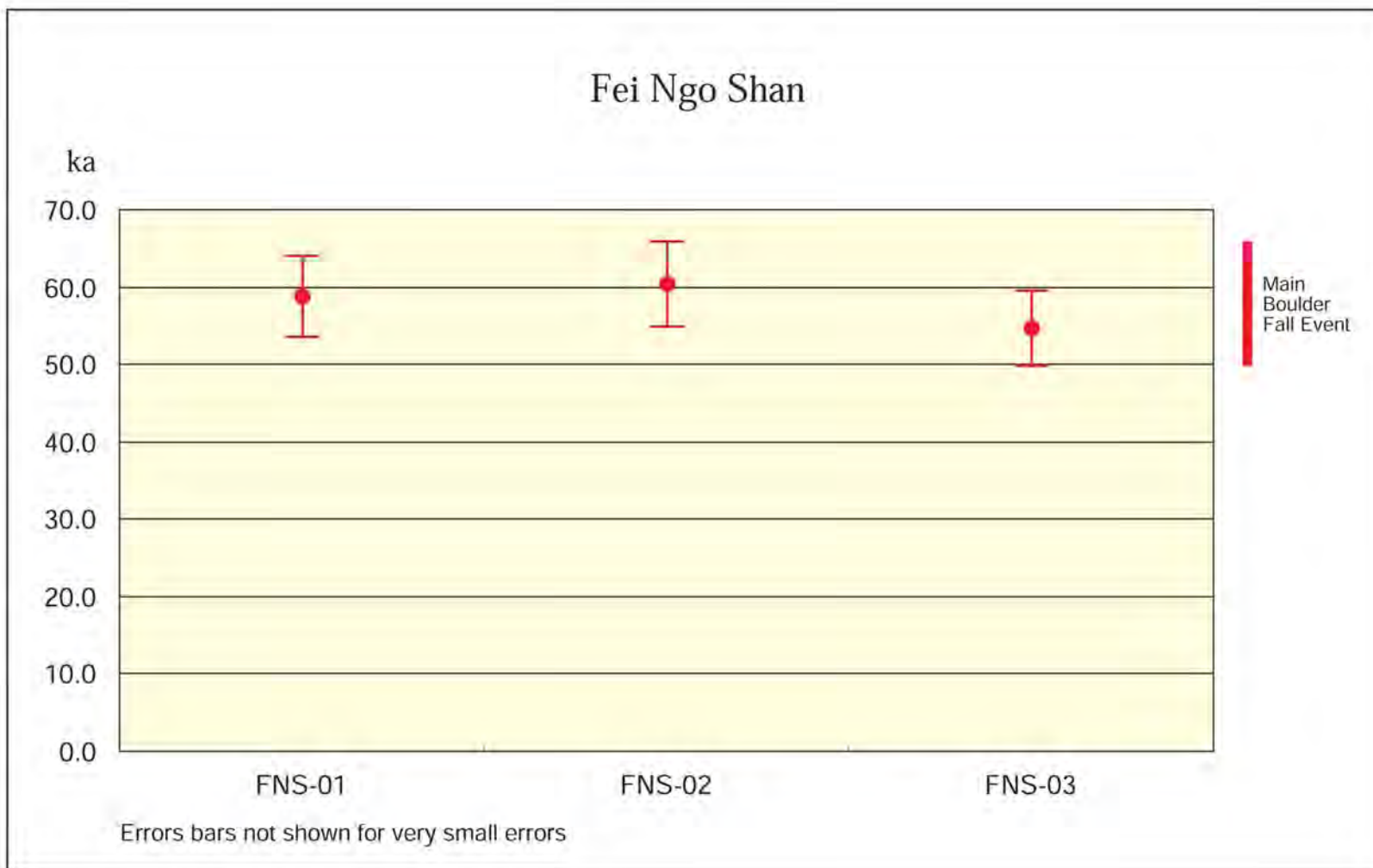


Figure 38 - Error Bar Chart Summarizing the Numerical (Absolute) Age Data for the Fei Ngo Shan Boulder Site. Symbols as for Figure 4

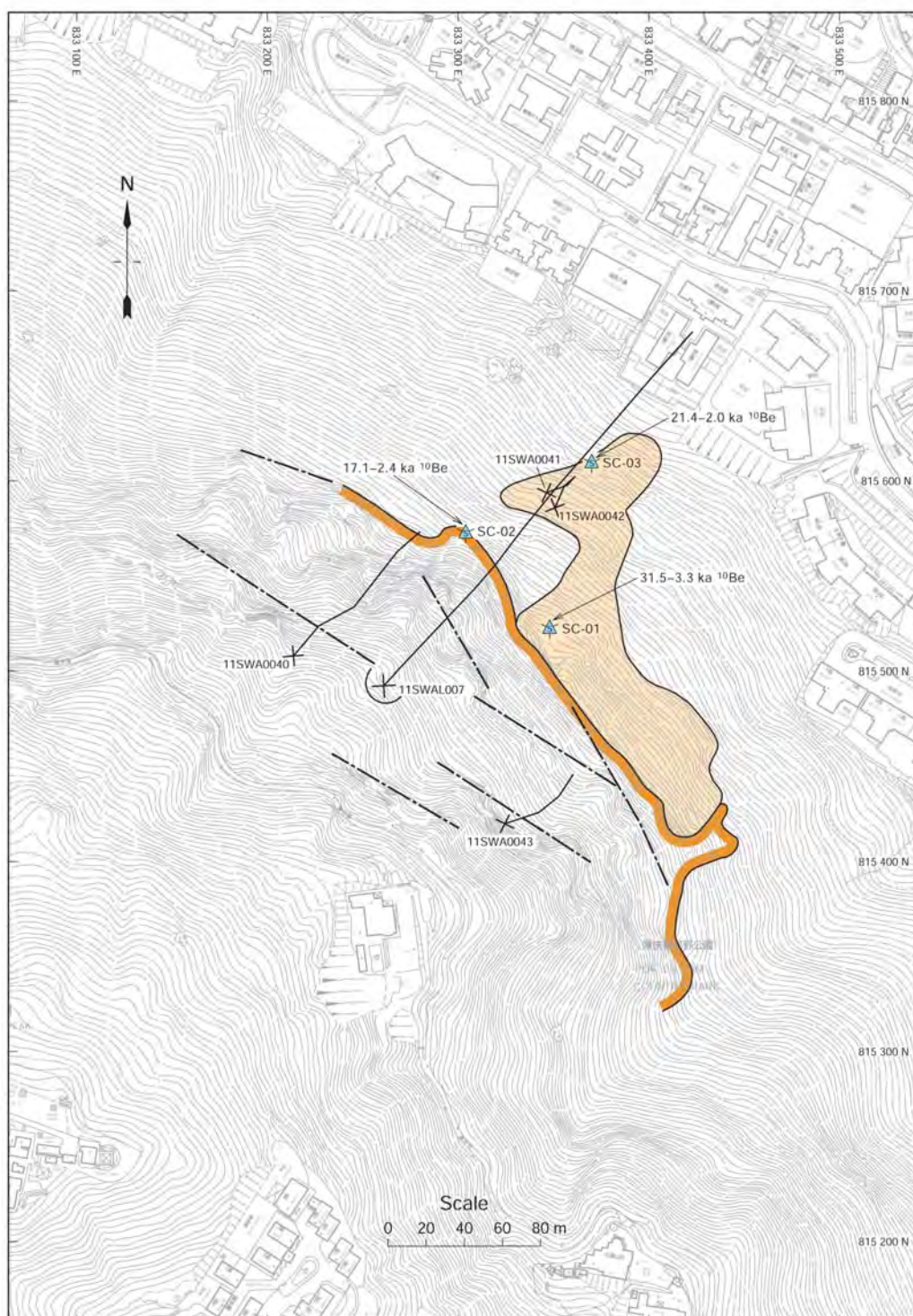


Figure 39 - API Interpretation, Sample Locations and Dating Results for the Seymour Cliffs Site. Legend as for Figure 3

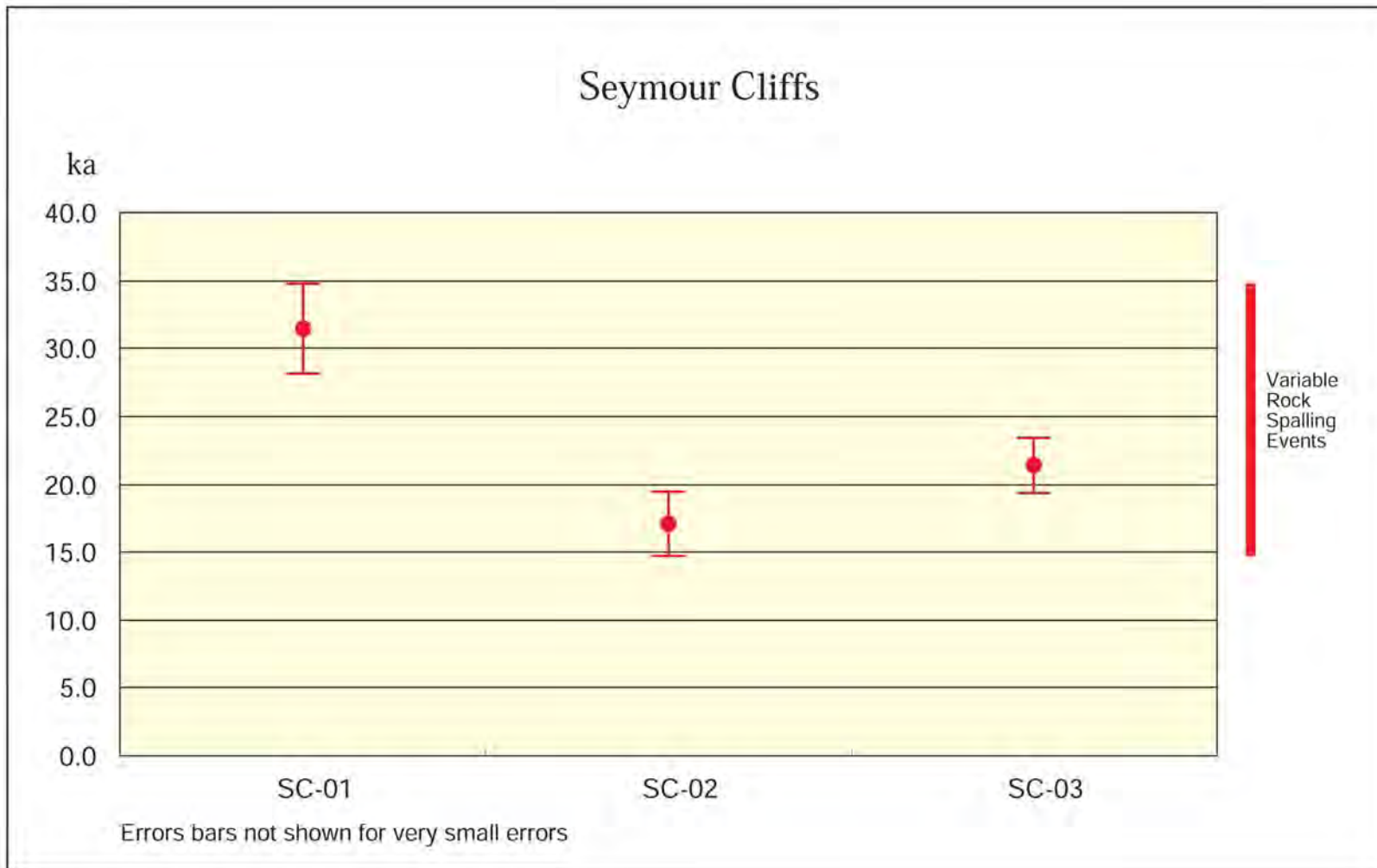


Figure 40 - Error Bar Chart Summarizing the Numerical (Absolute) Age Data for the Seymour Cliffs Site. Symbols as for Figure 4

LIST OF PLATES

Plate No.		Page No.
1	Aerial Photograph of Lai Cho Road Landslide Site, Kwai Chung, Taken on 27.1.63 Prior to Construction of Slope 11NW-A/C9	124
2	Aerial Photograph of Ap Lei Chau Landslide Site, on Mount Johnston North, Ap Lei Chau, Taken on 1.2.63	124
3	View of Two Mega-Boulders (One in Foreground and One in Background) Sampled Beneath Lion Rock for Surface Exposure Dating (Taken on 13.1.00, GS00/006C/17)	125
4	Sampling a 50 mm Thick Slab of Rock From a Boulder at the Sunset Peak West Landslide Site for Surface Exposure Dating (Taken on 13.1.00, GS00/006C/22)	125
5	Small Fragments of Charcoal Found Disseminated Within Colluvium as Viewed Under a Binocular Microscope (Taken on 13.1.00, GS00/006C/18)	126
6	Buried Soil Horizon Exposed in TP2 at the Lo Lau Uk Landslide Site. Samples of Charcoal From the Soil Horizon Yielded a Radiocarbon Date of 156 ± 49 ¹⁴ C yr B.P. (Taken on 13.1.00, GS00/0063/0-4 and GS00/005C/17-24)	126



Plate 1 - Aerial Photograph of Lai Cho Road Landslide Site, Kwai Chung, Taken on 27.1.63 Prior to Construction of Slope 11NW-A/C9

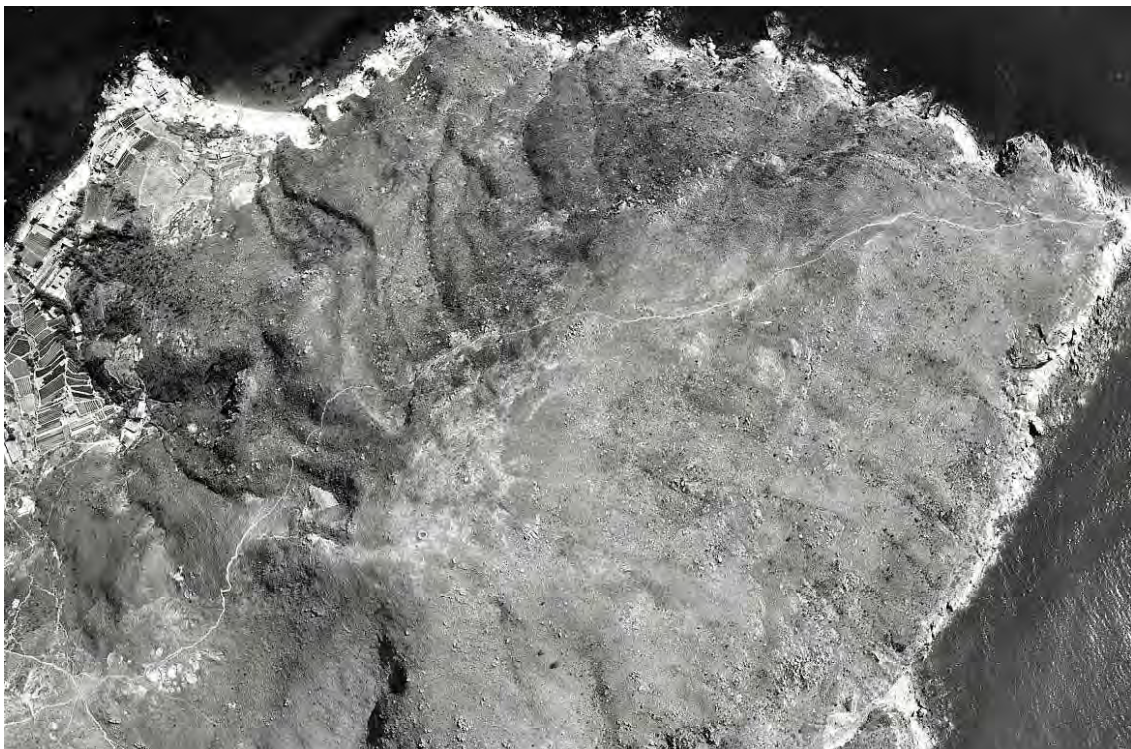


Plate 2 - Aerial Photograph of Ap Lei Chau Landslide Site, on Mount Johnston North, Ap Lei Chau, Taken on 1.2.63.



Plate 3 - View of Two Mega-Boulders (One in Foreground and One in Background)
Sampled Beneath Lion Rock for Surface Exposure Dating (Taken on 7.6.02)



Plate 4 - Sampling a 50 mm Thick Slab of Rock From a Boulder at the Sunset Peak West
Landslide Site for Surface Exposure Dating (Taken on 28.3.02)



Plate 5 - Small Fragments of Charcoal Found Disseminated Within Colluvium as Viewed Under a Binocular Microscope (Taken on 13.1.00, GS00/006C/18)



Plate 6 - Buried Soil Horizon Exposed in TP2 at the Lo Lau Uk Landslide Site
Samples of Charcoal From the Soil Horizon Yielded a Radiocarbon Date of 156 ± 49 ^{14}C yr B.P. (Taken on 13.1.00, GS00/0063/0-4 and GS00/005C/17-24)

APPENDIX
PRINCIPLES, ANALYTICAL PROCEDURES, CALIBRATIONS
AND CALCULATIONS OF THE DATING METHODS

APPENDIX A1 - Part Report to Geotechnical Engineering Office, Civil Engineering Department, on Radiocarbon Dating of Relict Natural Terrain Landslides in Hong Kong Page 128

APPENDIX A2 - Part Report to Geotechnical Engineering Office, Civil Engineering Department, on Determination of Sediment Deposition Ages by Luminescence Dating (Silt Fraction) Page 134

APPENDIX A3 - Part Report to Geotechnical Engineering Office, Civil Engineering Department on Radiocarbon Dating of Relict Natural Terrain Landslides in Hong Kong (Sand Fraction) Page 138

APPENDIX A4 - Report to Geotechnical Engineering Office on In Situ Cosmogenic Nuclide Exposure Dating (^{10}Be , ^{26}Al) of Relict Natural Terrain Landslides in Hong Kong Page 142

APPENDIX A1

Part Report to
Geotechnical Engineering Office
Civil Engineering Department
On
Radiocarbon Dating of Relict Natural Terrain Landslides
in Hong Kong

Performed by the
Radiocarbon Dating Laboratory
University of Waikato
Hillcrest Road
Hamilton
New Zealand

1. SAMPLE PRETREATMENT METHODS

1.1 Charcoal and Soil

Samples were initially physically inspected and visible contaminants removed. They were then washed in hot 10% HCl, rinsed and treated with hot 1% NaOH. The NaOH insoluble fraction was treated with hot 10% HCl, filtered, rinsed and dried.

1.2 Shell and Coral

Samples were physically cleaned in an ultra-sonic bath, then the outer shell surfaces removed by etching in 2 M dil. HCl for 60 seconds, then rinsed and dried.

2. C14 ANALYSIS BY AMS

2.1 Preparation of Carbon Dioxide

Charcoal and soil samples were combusted at 800° C in sealed quartz tubes containing CuO and Ag wool.

2.2 Preparation of Graphite

Carbon dioxide was converted to graphite by the staff from the Institute of Geological & Nuclear Sciences in Wellington, New Zealand. In the graphitization laboratory, the sample CO₂ is mixed with a stoichiometric amount of hydrogen gas inside a glass reaction vessel. The reaction vessel contains a small amount of iron powder which will act as a catalyst for the reaction. The reaction vessel is placed in a 700° C furnace and in about 5 hours the CO₂ converts to graphite. Water is trapped out as a by-product of the reaction.

2.3 Measurement of C14 Activity By AMS Spectroscopy

The following description comes from the Institute of Geological & Nuclear Sciences web site (R Sparks, pers comm). Accelerator Mass Spectrometry (AMS) is a technique for measuring the concentrations of rare isotopes that cannot be detected with conventional mass spectrometers. The original, and best known, application of AMS is radiocarbon dating, where the technical problem to be solved is the detection of the rare isotope ¹⁴C in the presence of the much more abundant isotopes ¹²C and ¹³C. The natural abundance of ¹⁴C is about one ¹⁴C atom per trillion (10¹²) atoms of ¹²C. Attempts to build a mass spectrometer to detect ¹⁴C were all unsuccessful for the reason that it was not possible to construct an instrument that could distinguish between ¹⁴C and the common nitrogen isotope ¹⁴N, which comprises 75% of the earth's atmosphere. AMS works by injecting negatively charged carbon ions from the material being analysed into a nuclear particle accelerator based on the electrostatic tandem accelerator principle. This device consists essentially of two linear accelerators joined end-to-end, with the join section (called the terminal) charged to a very high positive potential (3 million volts or higher). The negative ions are accelerated towards the positive potential. At the terminal they pass through either a very thin carbon film or a tube filled with gas at low pressure (the stripper), depending on the particular

accelerator. Collisions with carbon or gas atoms in the stripper removes several electrons from the carbon ions, changing their polarity from negative to positive. The positive ions are then accelerated through the second stage of the accelerator, reaching kinetic energies of the order of 10 to 30 million electron volts. The significance of this process for ^{14}C measurements is that nitrogen negative ions are very unstable and do not survive long enough to reach the accelerator terminal. This has the effect of eliminating the ^{14}N ions which would otherwise swamp the ^{14}C ions. However, ^{14}N is not the only problem. The instrument that produces the negative ions, the ion source, also inevitably produces negatively charged molecules that can mimic ^{14}C , viz. $^{13}\text{CH}^-$ and $^{12}\text{CH}_2^-$. These ions are stable, and while of relatively low abundance, are still intense enough to overwhelm the ^{14}C ions. This problem is solved in the tandem accelerator at the stripper. Provided three or more electrons are removed from the molecular ions the molecules dissociate into their component atoms at the stripping stage. The kinetic energy they had accumulated up to now is distributed among the separate atoms, none of which has the same energy as a single ^{14}C ion. It is thus easy to distinguish the ^{14}C from the more intense "background" caused by the dissociated molecules on the basis of their kinetic energy. Accelerating the ions to high energy has one more advantage. At the kinetic energies typically used in an AMS system it is possible to use well-established nuclear physics techniques to detect the individual ^{14}C ions as they arrive at a suitable particle detector. This may be a solid-state detector or a device based on the gridded ionisation chamber. The latter type of detector can measure both the total energy of the incoming ion, and also the rate at which it slows down as it passes through the gas-filled detector. These two pieces of information are sufficient to completely identify the ion as ^{14}C .

3. RADIOCARBON AGE CALCULATION

The following description comes from the University of Waikato Web Info (T Higham, pers comm). The radiocarbon age of a sample is calculated through careful measurement of the ^{14}C remaining in a sample whose age is Unknown, compared with the activity present in Modern and Background samples.

3.1 Modern Standard

The principal modern radiocarbon standard is N.I.S.T (National Institute of Standards and Technology; Gaithersburg, Maryland, USA) Oxalic Acid I. Oxalic acid I is N.I.S.T designation SRM 4990 B and is termed HOx1 . This is the International Radiocarbon Dating Standard. Ninety-five percent of the activity of Oxalic Acid from the year 1950 is equal to the measured activity of the absolute radiocarbon standard which is 1890 wood. 1890 wood was chosen as the radiocarbon standard because it was growing prior to the fossil fuel effects of the industrial revolution. The activity of 1890 wood is corrected for radioactive decay to 1950. Thus 1950, is year 0 BP by convention in radiocarbon dating and is deemed to be the 'present'.

3.2 Background

It is vital for a radiocarbon laboratory to know the contribution to routine sample activity of non-sample radioactivity. Obviously, this activity is additional and must be

removed from calculations. In order to make allowances for background activity and to evaluate the limits of detection, materials which radiocarbon specialists can be sure contain no activity are measured under identical measurement conditions as normal samples. Background samples usually consist of geological samples of infinite age such as coal, lignite, limestone, ancient carbonate, anthracite, marble or swamp wood. By measuring the activity of a background sample, the normal radioactivity present while a sample of unknown age is being measured can be accounted for and deducted.

3.3 Conventional Radiocarbon Ages (BP)

A radiocarbon measurement, termed a conventional radiocarbon age (or CRA) is obtained using a set of parameters outlined by Stuiver and Polach (1977), in the journal Radiocarbon. A time-independent level of C14 activity for the past is assumed in the measurement of a CRA.

A CRA embraces the following recommended conventions:

- * a half-life of 5568 years;
- * the use of Oxalic acid I or II, or appropriate secondary radiocarbon standards (e.g. ANU sucrose) as the modern radiocarbon standard;
- * correction for sample isotopic fractionation ($\delta^{13}\text{C}$) to a normalized or base value of -25.0 per mille relative to the ratio of C12/C13 in the carbonate standard VPDB (more on fractionation and $\delta^{13}\text{C}$);
- * the use of 1950 AD as 0 BP, ie all C14 ages head back in time from 1950;
- * the assumption that all C14 reservoirs have remained constant through time.

Three further terms are sometimes given with reported radiocarbon dates. $\delta^{14}\text{C}$, D^{14}C and $\delta^{13}\text{C}$. All are expressed in per mille notation rather than per cent notation (%).

3.4 Age Reporting

If the reservoir corrected conventional radiocarbon age calculated is within the past 200 years, it should by convention be termed 'Modern' (Stuiver and Polach, 1977:362). If a sample age falls after 1950, it is termed greater than Modern, or >Modern.

If the sample approaches $\text{D}^{14}\text{C} = -1000$ per mille within 2 standard deviations, it is considered to be indistinguishable from the laboratory background, ie, not able to be separated with confidence from the laboratory measurement which result from a sample which contains no radionuclide. In this instance, a minimum age is calculated. An example of a minimum age is >40,000 yr.

Should the activity of the sample be indistinguishable from the background activity at 1 standard deviation, it is released as 'Background'.

Samples whose age falls between modern and background and are given finite ages.

3.5 Standard Error

Each radiocarbon date is released as a conventional radiocarbon age with a 'standard error'. This is the ' \pm ' value and by convention is ± 1 sigma. The standard error is based upon repeated measurement of the sample.

4. CALIBRATION

Radiocarbon measurements are always reported in terms of years 'before present' (BP). This number is directly based on the proportion of radiocarbon found in the sample. It is calculated on the assumption that the atmospheric radiocarbon concentration has always been the same as it was in 1950 and that the half-life of radiocarbon is 5568 years. For this purpose 'present' refers to 1950.

In order to see what a radiocarbon determination means in terms of a true age we need to know how the atmospheric concentration has changed with time.

4.1 How Tree Rings Are Used As a Radiocarbon Record

Many types of tree reliably lay down one tree ring every year. The wood in these rings once laid down remains unchanged during the life of the tree. This is very useful as a record of the radiocarbon concentration in the past. If we have a tree that is 500 years old we can measure the radiocarbon in the 500 rings and see what radiocarbon concentration corresponds to each calendar year. Using very old trees (such as the Bristlecone Pines in the western U.S.A.), it is possible to make measurements back to a few thousand years ago. To extend this method further we must use the fact that tree ring widths vary from year to year with changing weather patterns. By using these widths, it is possible to compare the tree rings in a dead tree to those in a tree that is still growing in the same region. By using dead trees of different but overlapping ages, you can build up a library of tree rings of different calendar ages. This has now been done for Bristlecone Pines in the U.S.A and waterlogged Oaks in Ireland and Germany to provide records extending back over the last 11,000 years.

4.2 How Radiocarbon Calibration Works

Calibration of radiocarbon determinations is in principle very simple. If you have a radiocarbon measurement on a sample, you can try to find a tree ring with the same proportion of ^{14}C . Since the calendar age of the tree rings is known, this then tells you the age of your sample.

In practice this is complicated by two factors:

- * the measurements on both the tree rings and the samples have a limited precision and so there will be a range of possible calendar years.
- * given the way the atmospheric radiocarbon concentration has varied, there might be several possible ranges.

4.3 The Calibrated Time Scales

Once calibrated a radiocarbon date should be expressed in terms of CalBP. The Cal prefix indicates that the dates are the result of radiocarbon calibration using tree ring data. The term CalBP means the number of years before 1950 and can be directly compared to calendar years.

4.4 Method of Calculating Ranges

We have used the 'probability method' for calibrating the radiocarbon ages. This requires a computer since the calculations are more complicated. It gives the time range from which you can be 95% sure the sample came. The calibration programme 'Oxcal' has been used to compute the calibrations. For the terrestrial material, we have used the InCal98 calibration curve.

5. REFERENCES

Stuiver, Minze and Polach, H.A. (1977). Discussion: reporting of ^{14}C data. Radiocarbon, Vol. 19, No. 3, pp. 355-363.

APPENDIX A2

**Part Report to
Geotechnical Engineering Office
Civil Engineering Department
on
Determination of
sediment deposition ages
by Luminescence Dating**

by
Dr. Uwe Rieser

Luminescence Dating Laboratory
School of Earth Sciences
Victoria University of Wellington
e-mail: uwe.rieser@vuw.ac.nz
ph: 0064-4-463-6125
fax: 0064-4-463-5186

Technical Report

EXPERIMENTAL TECHNIQUES FOR DEPOSITION AGES DETERMINED FOR SAMPLES USING THE SILT FRACTION

1. INTRODUCTION

The palaeodose, i.e. the radiation dose accumulated in the sample after the last light exposure (assumed at deposition), was determined by measuring the blue luminescence output during infrared optical stimulation (which selectively stimulates the feldspar fraction). The doserate was estimated on the basis of a low level gammaspectrometry measurement.

Sample preparation and luminescence measurements were done in the Luminescence Dating Laboratory, School of Earth Sciences, Victoria University of Wellington, and gamma spectrometry by the National Radiation Laboratory (NRL), Christchurch.

2. LUMINESCENCE MEASUREMENTS

The samples, which were described as being of colluvial origin by the submitter, consisted mainly of silt. It was decided to use this dominant fraction for dating, using the finegrain technique after Aitken and Xie (1992) and a protocol as described by Lang and Wagner (1997).

Sample preparation was done under extremely subdued safe orange light in a darkroom. Outer surfaces, which may have seen light during sampling, were removed and discarded.

The actual water content and the saturation content were measured using 'fresh' inside material.

The samples were treated with 10% HCl to remove carbonates until the reaction stopped, then carefully rinsed with distilled water. Thereafter, all organic matter was destroyed with 10% H₂O₂ until the reaction stopped, then carefully rinsed with distilled water. By treatment with a solution of sodium citrate, sodium bicarbonate and sodium dithionate, iron oxide coatings were removed from the mineral grains and then the sample was carefully rinsed again.

The grain size 4-11 µm was extracted from the samples in a water-filled (with added dispersing agent to deflocculate clay) measuring cylinder using Stokes' Law. The other fractions were discarded. The samples then were brought into suspension in pure acetone and deposited evenly in a thin layer on 70 aluminum discs (1cm diameter).

Luminescence measurements were done using a standard Riso TL-DA15 measurement system, equipped with Kopp 5-58 and Schott BG39 optical filters to select the luminescence blue band. Stimulation was done at about 30 mW/cm² with infrared diodes at 880±80 nm. β-irradiations were done on a Daybreak 801E ⁹⁰Sr, ⁹⁰Y β-irradiator and the Riso TL-DA15 ⁹⁰Sr, ⁹⁰Y β-irradiator, both calibrated against SFU, Vancouver, Canada to about 3% accuracy. β-irradiations were done on a ²⁴¹Am irradiator supplied and calibrated by ELSEC, Littlemore, UK. The paleodoses were estimated by use of the multiple aliquot additive-dose method (with late-light subtraction). After an initial test-measurement, 30 aliquots were β-irradiated

in six groups up to five times of the dose result taken from the test. Nine aliquots were α -irradiated in three groups up to three times of the dose result taken from the test. These 39 disks were stored in the dark for four weeks to relax the crystal lattice after irradiation.

After storage, these 39 disks and nine unirradiated disks were preheated for 5min at 220°C to remove unstable signal components, and then measured for 100sec each, resulting in 39 shinedown curves. These curves were then normalized for their luminescence response, using 0.1s shortshine measurements taken before irradiation from all aliquots.

The luminescence growth curve (β -induced luminescence intensity vs added dose) is then constructed by using the initial 10 seconds of the shine down curves and subtracting the average of the last 20 sec, the so called late light which is thought to be a mixture of background and hardly bleachable components. The shine plateau was checked to be flat after this manipulation. Extrapolation of this growth curve to the dose-axis gives the equivalent dose D_e , which is used as an estimate of the paleodose.

A similar plot for the alpha-irradiated discs allows an estimate of the β -efficiency, the a-value (Luminescence/dose generated by the β -source divided by the luminescence/dose generated by the β -source).

3. FADING TEST

Samples containing feldspars in rare cases show an effect called anomalous fading. This effect inhibits accurate dating of the sample, as the electron traps in the crystal lattice of these feldspars are unable to store the age information over longer periods of time.

None of the analyzed samples has given an indication of this problem so far, but a routine test must be carried out after six months storage of an irradiated subsample to be sure. Thus, all ages reported below must be seen as preliminary until the fading test has been carried out. The result will be notified as soon as it is available.

4. GAMMA SPECTROMETRY

The dry, ground and homogenized soil samples were embedded in a two-part epoxy resin to retain ^{222}Rn within the sample and allowed to set. This casting procedure reduces the radon loss from the sample to less than 0.5% and the ^{226}Ra concentration in these samples can be determined from the emissions of the short lived ^{222}Rn daughters, ^{214}Pb and ^{214}Bi . A waiting period of 30 days is necessary to reach equilibrium between ^{226}Ra and its daughter nuclides before the gamma count.

The samples were counted using high resolution gamma spectrometry with a broad energy Ge detector for a minimum time of 24 hours. The spectra were analysed using GENIE2000 software.

The doserate calculation is based on the activity concentration of the nuclides ^{40}K , ^{208}Tl , ^{212}Pb , ^{228}Ac , ^{210}Pb , ^{214}Bi , ^{214}Pb , ^{226}Ra and ^{234}Th , as reported by NRL. The latter five of these isotopes allow, if applicable, an estimate of the degree of radioactive disequilibrium in the Uranium decay chain.

5. REFERENCES

- Adamiec G. and Aitken M. (1998). Dose-rate conversion factors: update. Ancient TL, Vol. 16, pp. 37-50.
- Aitken M. and Xie J. (1992). Optical dating using infra-red diodes: young samples. Quaternary Science Reviews, Vol. 11, pp. 147-152.
- Lang A. and Wagner G.A. (1997) Infrared stimulated luminescence dating of Holocene colluvial sediments using the 410nm emission. Quaternary Geochronology (Quaternary Science Reviews) Vol. 16, pp. 393-396.
- Prescott & Hutton (1994), Radiation Measurements, Vol. 23.

APPENDIX A3

**Part Report to
Geotechnical Engineering Office
Civil Engineering Department
on
Determination of
sediment deposition ages
by Luminescence Dating**

by
Dr. Uwe Rieser

Luminescence Dating Laboratory
School of Earth Sciences
Victoria University of Wellington
e-mail: uwe.rieser@vuw.ac.nz
ph: 0064-4-463-6125
fax: 0064-4-463-5186

Technical Report

EXPERIMENTAL TECHNIQUES FOR DEPOSITION AGES DETERMINED FOR SAMPLES USING THE SAND FRACTION (90-200 μ M)

1. INTRODUCTION

The palaeodose, i.e. the radiation dose accumulated in the sample after the last light exposure (assumed at deposition), was determined by measuring the ultraviolet luminescence output during greenlight optical stimulation of the quartz fraction. The doserate was estimated on the basis of a low level gammaspectrometry measurement.

Sample preparation and luminescence measurements were done in the Luminescence Dating Laboratory, School of Earth Sciences, Victoria University of Wellington, and gamma spectrometry by the National Radiation Laboratory (NRL), Christchurch.

2. LUMINESCENCE MEASUREMENTS

The samples, which were described as being of colluvial origin by the submitter, consisted mainly of silt. It was requested by the submitter that the quartz coarse fraction was used for a Single Aliquot Regenerative (SAR) dating attempt in order to determine if there was a partial bleaching event, caused by recent sediment movement. The relatively new SAR technique is described by Murray and Wintle (2000).

Sample preparation was done under extremely subdued safe orange light in a darkroom. Outer surfaces, which may have seen light during sampling, were removed and discarded. The actual water content and the saturation content were measured using 'fresh' inside material.

The samples were treated with 10% HCl to remove carbonates until the reaction stopped, then carefully rinsed with distilled water. Thereafter, all organic matter was destroyed with 10% H₂O₂ until the reaction stopped, then carefully rinsed with distilled water.

The grain size 90-200 μ m was extracted from the samples by sieving, in some cases by wet sieving. The other fractions were discarded, except the 4-11 μ m fraction which was used for finegrain dating (see report phase IIA). Then heavy liquid separation was carried out in Lithium-polytungstate to obtain a quartz enriched fraction (2.58-2.65g/cm³). Though relatively pure, this density fraction still may contain minor amounts of plagioclase feldspars. These were destroyed by subsequent HF (40%) etching and washing. The HF etching also removed the outer 10 μ m of the quartz grains, which may have stored a dose from alpha-radiation. Then the grain size fraction 90-125 μ m was obtained by a final sieving, and the quartz grains were fixed on 1cm aluminum discs with silicon oil.

Luminescence measurements were done using a standard Riso TL-DA15 measurement system, equipped with 3 Hoya U340 optical filters (stack thickness ~9mm) to select the ultraviolet luminescence band centered around 340nm. Stimulation was done by a green halogen light source (420-575nm), β -irradiations were done on the Riso TL-DA15 ⁹⁰Sr, ⁹⁰Y β -irradiator, calibrated against the Risø National Laboratory, Denmark, to about 3% accuracy.

The palaeodoses were estimated by use of the Single Aliquot Regenerative method (SAR). In the SAR method a number of aliquots are subjected to a repetitive cycle of

irradiation, preheat and measurement. In the first cycle the natural luminescence output is measured, in all following cycles an artificial dose is applied. Usually four or five of these dose points are used to build the luminescence growth curve (β -induced luminescence intensity vs added dose) and bracket the natural luminescence output. This allows interpolation of the equivalent dose (the β -dose equivalent to the palaeodose). In order to correct for potential sensitivity changes from cycle to cycle, a test dose is applied between the cycles, preheated ('cut heat') and measured.

For the samples reported here 30 aliquots were measured, preheat temperature was 260°C for 10s, cut heat was 220°C for 10s, and measurement time 150s (which resets the luminescence signal to a negligible residual).

The measurement of 30 aliquots resulted in 30 equivalent doses, spread over the so called dose distribution. The extreme scatter within this distribution is usually attributed to partial bleaching of the mineral grains (see e.g. Olley *et al*, 1998), i.e. those aliquots with high equivalent doses contain quartz grains which have not seen light during sediment deposition. The interpretation of these dose distributions is a major cause of uncertainty in the SAR technique, and much research effort is put into a better understanding.

3.2 GAMMA SPECTROMETRY

The dry, ground and homogenized soil samples were embedded in a two-part epoxy resin to retain ^{222}Rn within the sample and allowed to set. This casting procedure reduces the radon loss from the sample to less than 0.5% and the ^{226}Ra concentration in these samples can be determined from the emissions of the short lived ^{222}Rn daughters, ^{214}Pb and ^{214}Bi . A waiting period of 30 days is necessary to reach equilibrium between ^{226}Ra and its daughter nuclides before the gamma count.

The samples were counted using high resolution gamma spectrometry with a broad energy Ge detector for a minimum time of 24 hours. The spectra were analysed using GENIE2000 software.

The doserate calculation is based on the activity concentration of the nuclides ^{40}K , ^{208}Tl , ^{212}Pb , ^{228}Ac , ^{210}Pb , ^{214}Bi , ^{214}Pb , ^{226}Ra and ^{234}Th , as reported by NRL. The latter five of these isotopes allow, if applicable, an estimate of the degree of radioactive disequilibrium in the Uranium decay chain.

3.3 INTERPRETATION

The interpretation of the SAR dose distributions is rather complex. The samples showed, as it is very common, extreme scatter between aliquots. Usually two ages are reported:

- (a) The 'mean age', calculated using the arithmetic mean and standard deviation of the distribution. This is thought to give the best age estimate if the scatter is not caused by incomplete bleaching during deposition. The error is usually given as the error of the mean, assuming that the

mean will follow a normal distribution even if the data does not.

- (b) The 'leading edge age', calculated using only the lowest 5% of the dose distribution (see Olley et al, 1998). This is thought to give the best age estimate only if incomplete bleaching is causing the scatter.

3.4 REFERENCES

- Adamiec G. and Aitken M. (1998). Dose-rate conversion factors: update. Ancient TL, Vol. 16, pp. 37-50.
- Murray A.S. and Wintle A.G. (2000). Luminescence dating of quartz using an improved single-aliquot regenerative-dose protocol. Radiation Measurements Vol. 32, pp. 57-73.
- Olley J., Caitcheon G. & Murray A.S. (1998). The distribution of apparent dose as determined by optically stimulated luminescence in small aliquots of fluvial quartz: Implications for dating young sediments. Quaternary Geochronology Vol. 17, pp. 1033-1040.
- Prescott & Hutton (1994). Radiation Measurements, Vol. 23.

APPENDIX A4

Report to
Geotechnical Engineering Office
On
***In Situ* Cosmogenic Nuclide Exposure Dating (^{10}Be , ^{26}Al) of**
Relict Natural Terrain Landslides in Hong Kong

Performed by the
Department of Nuclear Physics
Research School of Physical Sciences and Engineering
Institute of Advanced Studies
The Australian National University
Canberra ACT 0200
Australia

1. BASIC PRINCIPLES OF THE DATING METHOD

Long-lived radioactive isotopes are produced in surface rocks by cosmic rays. At the earth's surface, these are principally highly-energetic neutrons and muons that are secondary products of collisions between the primary cosmic rays (protons and helium nuclei) and atmospheric atoms. The isotopes of interest for exposure dating are beryllium-10 (half-life, $t_{1/2} = 1.5$ million years), aluminium-26 ($t_{1/2} = 705,000$ years) and chlorine-36 ($t_{1/2} = 301,000$ years). These are produced principally from oxygen, silicon, and calcium/potassium atoms in the rock respectively. Because attenuation lengths of the fast neutrons and muons are typically 60 cm and 5m respectively, almost all of the isotope production takes place within the top few metres of the rock surface.

The concentration N [atoms g^{-1}] of a particular isotope increases with the duration t of exposure (Fig.1) according to

$$N = P/\lambda (1 - e^{-\lambda t}) \dots \dots \dots (1)$$

where λ is the decay constant of the isotope ($\lambda = \ln 2/t_{1/2}$), and P is its local production rate by cosmic rays.

Hence the exposure age of a sample is

$$t = -\ln(1 - \lambda N/P) / \lambda \dots \dots \dots (2)$$

For exposure dating applications of beryllium-10 and aluminium-26, quartz is almost exclusively selected as the target mineral. There are several reasons for this (Nishiizumi *et al.*, 1986):

- Quartz is a geochemically closed system. Hence, any isotopes created by cosmic rays are retained in the crystal structure.
- Quartz is very resistant to chemical attack. This allows a rigorous cleaning procedure to be applied to produce a very pure quartz mineral separate. The rigorous cleaning has the added advantage of completely removing any ^{10}Be adsorbed on to surfaces. This is extremely important because ^{10}Be is also produced in the atmosphere, falls out in rainfall, and attaches readily to rock surfaces. It is orders of magnitude more abundant than the ^{10}Be produced *in situ* and must be removed for exposure dating to be possible.
- Production rates for ^{10}Be and ^{26}Al have been calibrated specifically for quartz using surfaces of known age.
- Both ^{10}Be and ^{26}Al can be measured in the same quartz sample with minimal additional chemistry.

2. ANALYTICAL PROCEDURES

The analytical procedure breaks into three distinct stages:

- Quartz extraction and purification.
- Be and Al separation from the pure quartz samples for AMS analysis.
- Isotopic ratio determination.

2.1 QUARTZ EXTRACTION AND PURIFICATION

The first stage includes both physical and chemical separations.

After initial clean up and removal of foreign objects (rootlets, lichens, etc.), rock samples are dried and weighed, and then crushed to ensure that individual grains are separated. The material is then sieved and separated into >600 μm , 600-420 μm , 420-250 μm , 250-125 μm and <125 μm fractions. After visual and microscopic examination, the 420-250 μm and 600-420 μm fractions were selected for further processing as they contained the most quartz. After washing, de-silting (removing of fine dust) and drying, samples went through a magnetic separation stage. The fraction with the lowest magnetic susceptibility was selected, thus effectively cleaning the samples of mica, magnetite, etc. A density separation with heavy liquid (lithium polytungstate) followed in order to separate the samples into three fractions with densities of <2.64, 2.65, and > 2.66 g cm^{-3} respectively. The quartz is in the middle fraction. Microscopic examination has shown that for granites the yield is often more than 90% pure quartz. For samples of volcanic origin (e.g. rhyolite), the purification is generally worse due to an abundance of composite grains and lower quartz content, and often does not exceed 40%.

Chemical purification commences with soaking samples in hot concentrated Aqua Regia for a few hours (typically overnight) in order to remove possible carbonates present as well as various trace metals, mainly to reduce the iron load of the samples. After washing and drying, samples go to the final cleaning stage - extensive days-to-weeks long etching in dilute HF acid (1-2%) at about 70° C in an ultrasonic bath. This removes the remaining feldspar grains, causes the composite grains to disintegrate, and cleans the surfaces of the quartz grains of any possible external contamination. High Density Polypropylene ware is used throughout this procedure. The result is better than 99.9% pure quartz samples ready for Al and Be isolation. The purity was determined by analysing small subsamples for residual Al and Ti by ICP-OES. Generally, only samples with residual Al contents of <200 ppm were allowed to the next stage, although a few samples could not be cleaned to better than 500 ppm.

2.2 Be AND Al SEPARATION FROM THE PURE QUARTZ FOR AMS ANALYSIS

In the next stage Be, and Al if required, are extracted from pure quartz samples and separated from the remaining metals (typically Fe, Ti, alkalis, Mg and Ca). All procedures are carried out in Teflon[®] lab ware. Quartz samples are weighed and up to 50 g of material

selected. A precisely known amount of Be carrier (prepared from deep-mined beryl which has a negligible ^{10}Be concentration) is added to each sample. This is typically 0.25 mg of Be. The quartz is then dissolved in concentrated HF acid. The resulting solution is sub-sampled for determination of total Al content, then dried to remove Si as volatile SiF_4 . Ion exchange methods are then employed to extract the Be and Al as follows:

- The dried sample is re-dissolved in 10M HCl and passed through an anion exchange resin (AG-1 X8, 200-400 mesh) contained in a Biorad[®] 10 ml column. Fe, as well as some Ti, are retained on the resin and thereby eliminated.
- The collected solutions are converted to sulphate form by multiple drying with 0.5M H_2SO_4 and redissolving in the presence of H_2O_2 to convert any remaining Ti to the $(\text{TiO}[\text{H}_2\text{O}_2])^{2+}$ complex.
- Separation of Al, Be and the remaining Ti is performed on DOWEX-50 X8, 200-400 mesh cation exchange resin in a Biorad[®] 10 ml column. Samples are introduced as a ~0.2 M H_2SO_4 solution. Ti is eluted with 0.5M H_2SO_4 . Beryllium is then eluted with 1.2M HCl, and finally the Al is eluted with 4M HCl.
- Samples are then converted to nitrate form by multiple drying down and taking up in 8M HNO_3 solution.

Once pure solutions of Be and Al have been obtained, the Be and Al are precipitated as the hydroxides by making the solutions alkaline. This has the additional advantage of eliminating any residual sodium or potassium because these do not precipitate. In order to make the final material electrically and thermally conductive, these precipitations are carried out after the addition of about 1 mg of Ag in the form of AgNO_3 . In this case, Ag_2O co-precipitates with the beryllium or aluminium hydroxide. After rinsing to remove any residual sodium salts, the precipitates are dried and baked at 850°C in quartz crucibles to convert the hydroxides to oxides and the Ag_2O to silver metal.

Finally, the beryllium samples are mixed with Nb powder and pressed into a 1 mm recess in copper holders for AMS measurements. The aluminium samples are usually not mixed with Nb.

Each batch of samples (6 to 9) was accompanied by a blank sample of carrier only, processed in the same manner, in order to quantify any contamination introduced in the course of sample preparation.

2.3 ACCELERATOR MASS SPECTROMETRY (AMS)

AMS measurements were performed on the 14UD tandem accelerator in the Department of Nuclear Physics at the ANU. A detailed discussion of the methodology and its applications can be found in the review article by Fifield (1999). The methodology is somewhat different for ^{10}Be and ^{26}Al , so a brief description of each is given below.

2.3.1 Beryllium-10

Figure 1 illustrates the essential features of AMS for ^{10}Be . Negative BeO^- ions are produced by sputtering the beryllium oxide sample with Cs^+ ions in the presence of Cs vapour. A magnetic mass analysis selects mass 26 ($^{10}\text{Be}^{16}\text{O}^-$), and these ions are injected into the accelerator operating at 8 MV. In the high voltage terminal of the accelerator, the ions pass through an 8 mm diameter canal containing oxygen gas at a pressure of about 10^{-5} atmospheres. Collisions with the gas cause the molecular ions to dissociate, and also strip electrons off the constituent Be and O atoms, converting them to positively-charged ions. These positive ions are then further accelerated back to ground potential. A second mass analysis selects ^{10}Be ions in the 3^+ charge state (i.e. with 3 of its 4 electrons removed). This is followed by a velocity analysis to remove any background ions with different velocities before the 27 MeV ^{10}Be ions are identified and counted in a gas-filled ionisation chamber.

Boron has a stable isotope of mass 10 which has a natural abundance of 20%. Because it is not possible to remove boron completely in the chemistry or ion source, $^{10}\text{B}^{3+}$ ions will traverse the entire beam transport system in the same way as $^{10}\text{Be}^{3+}$ ions and hence arrive at the detector. The rate of these unwanted ions can be very high, greater than a million per second, which is much higher than the ionisation counter can handle. Fortunately, the range of ^{10}B ions in gas is much shorter than ^{10}Be ions of the same energy, and it is possible to stop the ^{10}B ions in an absorbing region at the front of the detector.

The measured quantity in AMS is invariably a ratio of atomic abundances, in this case, of ^{10}Be to ^9Be . The ^{10}Be intensity is determined from the counting rate in the ionisation chamber. It is possible to monitor the ^9Be intensity continuously by using a method first proposed by Middleton and Klein (1987). This exploits the fact that the $^9\text{Be}^{17}\text{O}$ molecule also has mass 26 (^{17}O is a stable isotope with an abundance of 0.04% of natural oxygen) and hence is injected into the accelerator. After dissociation of the molecule in the gas stripper, a significant fraction of the ^{17}O atoms are stripped to the 5^+ charge state. Coincidentally, the radius of curvature of these $^{17}\text{O}^{5+}$ ions in the final analysing magnet differs by only 1% from $^{10}\text{Be}^{3+}$. Hence a slightly off-axis Faraday cup is employed to monitor continuously the electric current of the ^{17}O ions as a proxy for ^9Be . Periodically, the ^{10}Be to ^{17}O ratio is measured for a standard (see below) and this is used for normalisation.

2.3.2 Aluminium-26

The methodology differs in two main essentials from that for ^{10}Be .

- i) Atomic $^{26}\text{Al}^-$ ions are selected for injection into the accelerator. Because magnesium does not have a stable negative ion, this eliminates ^{26}Mg , which is the stable isotope of the same mass. This greatly simplifies the detection problem. Essentially only ^{26}Al ions arrive at the detector.
- ii) In order to determine the $^{26}\text{Al}/^{27}\text{Al}$ ratio, it is necessary to pass ^{27}Al through the accelerator periodically. This is accomplished by changing the field in the injection magnet to pass $^{27}\text{Al}^-$ ions, and changing the field in the final

analysing magnet to pass $^{27}\text{Al}^{7+}$ ions. The intensity of these is measured as an electric current in a Faraday cup.

For AMS of ^{26}Al , the accelerator is operated at 14 MV, and the 7^+ charge state is selected following acceleration. The energy of the ^{26}Al ions is 112 MeV.

3. DATA ANALYSIS

The $^{10}\text{Be}/^9\text{Be}$ ratios for individual samples were derived by normalisation to an NIST standard with a $^{10}\text{Be}/^9\text{Be}$ ratio of 3.00×10^{-11} . Concentrations of ^{10}Be in atoms/g of quartz were then derived from the known masses of quartz dissolved and the amount of ^9Be carrier added. Corrections for the blank were applied.

Similarly, $^{26}\text{Al}/\text{Al}$ ratios were obtained by normalisation to a standard with a ratio of 4.11×10^{-11} . This standard was prepared by Dr Stephan Vogt of PRIME Lab at Purdue University. Aluminium carrier was not added to the samples because they contained sufficient intrinsic aluminium. Aluminium concentrations were determined by ICP-OES. Concentrations of ^{26}Al in atoms/g of quartz were then determined from the measured $^{26}\text{Al}/\text{Al}$ ratio and the aluminium concentrations.

The cosmogenic isotope production rate of ^{10}Be in quartz at sea level and high latitude (5.02 ± 0.35 at/a/g quartz) was taken from Barrows *et al.*, 2002. The ^{26}Al production rate was obtained from that for ^{10}Be using the known $^{26}\text{Al}/^{10}\text{Be}$ production rate ratio of 6.1 (Nishiizumi *et al.*, 1989). Cosmic ray fluxes increase with altitude by approximately a factor of two for each 1000m. They are also higher at the poles than at the equator due to the shielding effect of the earth's magnetic field. In this regard, production rates in Hong Kong, where the sites are at low altitude and near the equator, are lower than at most sites where exposure dating has been attempted. The altitude and latitude scaling factors applicable to each individual site were derived using the prescription of Lal (1991) and assuming that the muon contribution at sea-level is 3% of the fast neutron contribution. Horizon corrections to account for shielding of cosmic rays by the surrounding landscape were introduced at this stage. Exposure ages were determined by applying Formula (2) to the data. Errors were propagated according to standard statistical methods.

^{10}Be was measured first for all of the samples. Samples were then selected for ^{26}Al analysis based on predicted $^{26}\text{Al}/\text{Al}$ ratios, using the fact that the $^{26}\text{Al}/^{10}\text{Be}$ concentration ratio should be close to 6 for a simple exposure history. In order to achieve reasonable counting statistics, and hence sensible results, samples with the highest values of predicted $^{26}\text{Al}/\text{Al}$ ratios were selected. This favoured samples with higher ^{26}Al atoms/g, which are necessarily the older samples, and low aluminium concentrations. Predicted ratios were generally low, however, and fell between 0.4 and 1.7×10^{-12} for the selected samples.

4. DISCUSSION

The AMS ^{10}Be measurements for this project went well, and the results are considered to be reliable within the stated uncertainties. The uncertainties are dominated by counting statistics and by the 7% uncertainty on the production rate calibration. Some of the rock types involved in the project presented particular challenges. Although these were

surmounted, they resulted in larger uncertainties for a few samples, and in the project taking somewhat longer than anticipated. For example, unexpectedly low quartz contents were encountered for some samples, and the amount of quartz extracted was rather less than optimal. The total number of ^{10}Be atoms in these samples was correspondingly reduced resulting in a lower measured $^{10}\text{Be}/\text{Be}$ ratio and hence poorer counting statistics. In addition, it proved impossible to reduce the aluminium concentrations below 500 ppm for some samples. As a result, some aluminium oxide was present in those particular beryllium oxide samples. This reduces the output from those samples, again resulting in fewer ^{10}Be counts and hence in larger uncertainties.

Aluminium-26 was also measured in six selected samples as a quality control measure. The independent ^{26}Al ages agree well with the ^{10}Be ages in all cases. Indeed, these data are as good as are to be found anywhere in the exposure-dating literature.

5. CONCLUSIONS

Cosmogenic nuclide analysis using ^{10}Be and ^{26}Al was successful in determining exposure ages of surfaces associated with landslides in the Hong Kong area. The sensitivity of the AMS technique is sufficiently high to measure ages of a few thousand years at some sites, despite the unfavourable circumstances of low latitude and low altitude.

6. REFERENCES

- Barrows, T. T., Stone, J. O., Fifield, L. K., Cresswell, R. G. (2001). Late Pleistocene glaciation of the Kosciuszko Massif, Snowy Mountains, Australia. Quaternary Research, Vol. 55, pp. 179-189.
- Fifield, L.K. (1999). Accelerator Mass Spectrometry and its Applications. Reports on Progress in Physics, Vol. 62, pp. 1223-1274.
- Middleton, R. and Klein, J. (1987), A novel method for ^{10}Be AMS. Philosophical Transactions of the Royal Society, Vol. A323, p.121.
- Lal, D. (1991). Cosmic ray labeling of erosion surfaces: *in situ* nuclide production rates and erosion models. Earth and Planetary Science Letters. Vol. 104, pp. 424-439.
- Nishiizumi, K., Lal, D., Klein, J., Middleton, R., Arnold, J.R. (1986) Production of ^{10}Be and ^{26}Al By cosmic rays in terrestrial quartz *in situ* and implication for erosion rates. Nature, Vol. 319, pp. 134-136.
- Nishiizumi, K., Winterer, E.L., Kohl, C.P., Klein, J., Middleton, R. (1989). Cosmic ray produced rates of ^{10}Be and ^{26}Al in quartz From glacially polished rocks. Journal of Geophysical Research, Vol. 97, pp. 17907-17915.

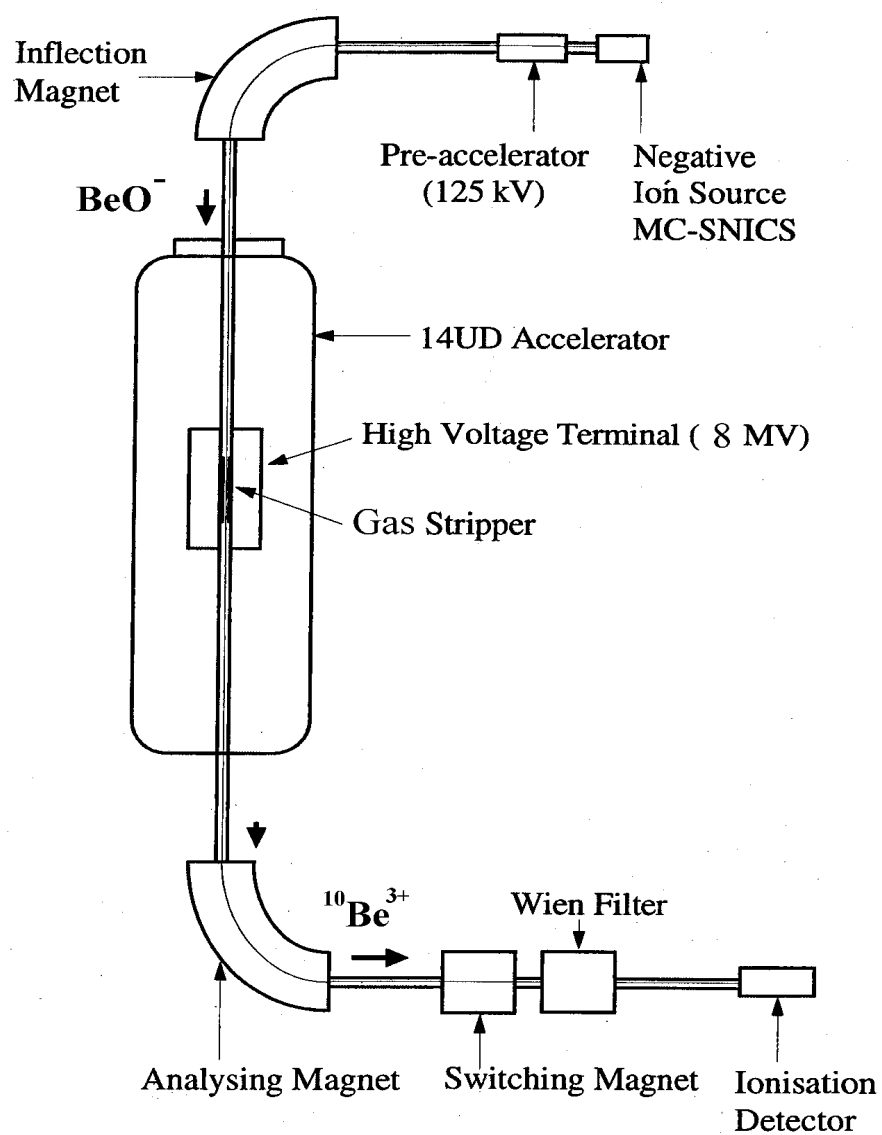


Figure 1 - Schematic representation of the principle of accelerator mass spectrometry for ^{10}Be .

APPENDIX A CONSIDERATIONS FOR SAMPLING OF LANDSLIDES FOR EXPOSURE DATING

Procedures used by Dr Timothy T. Barrows
Department of Nuclear Physics
Australian National University

A1. LOCATION SELECTION

The first step to deciding whether a landslide is suitable for exposure dating is to reconstruct the boundaries of the scarp, the extent of the resultant debris, and then to estimate the average depth of the landslide. Do not attempt to exposure date shallow landslides (< 3 m depth). Where possible, both the scarp and the debris should be equally focused upon for sampling. This is because each feature has its own potential geological uncertainties. Scarps are likely to be biased towards minimum ages if rock fall has continued after the landslide. Blocks on the debris are likely to be biased towards maximum ages if pre-existing talus or regolith was incorporated into the flow. Additionally, scarps are heavily shielded from cosmic radiation whereas the debris usually has a clearer horizon. This means that the concentration of cosmogenic nuclides will be higher in the latter, making AMS measurements easier. Where the ages of both the scarp and the debris can be directly linked, the age of the landslide is best constrained.

At least 3 and preferably 5-6 samples should be taken from both the scarp and the debris to provide a population of exposure ages. This number of samples from a range of sites allows outliers to be identified. Samples should be geographically spread across the scarp and the debris to encompass as much of the feature as possible.

A2. SITE SELECTION

On a scarp, faces should be chosen that would have been at least 3 m below the former land surface. Select faces where there is the least shielding of the horizon. Where possible, keep the maximum amount of shielding on the horizon less than 45°, often this is the slope of the face. Remember that a 90° cliff receives only half the cosmic radiation as a sample with a clear horizon, meaning the concentration of cosmogenic nuclides is reduced by the same amount. The largest blocks on the debris should be chosen, at least 3 m and preferably 6 m long.

The horizon should be recorded by measuring the bearing and angle subtended by key points, namely peaks, saddles, and flat horizon. Accuracy is not vital for angles less than ~30° but high angles should be measured to the nearest degree. The greatest care should be taken with near vertical angles. The best visual way to record the horizon is as a pie chart where the bearings divide the circle into sectors. Define sectors by roughly constant elevation angle or slope. Small variations along a ridge or down a spur can be averaged out. Note a description of key features for orientation. Avoid choosing a site where the obstruction (esp. part of the face or block) is thinner than 3 m, because this leads to complicated mass corrections and introduces errors. If unavoidable, accurately measure the 'depth' of the obstruction. Vegetation does not need to be corrected for.

Photographs should be taken so as to record the context of the sample site and the location of the sample on the site.

A3. SAMPLE SELECTION

At the scarp, samples can be taken along a face, either flat lying or sloped. Avoid surfaces that may have lost a block due to spalling and try to sample original detachment faces. On a block, select samples near the middle, as far from the top and bottom of the block as possible. Flow banding, cleavage, or joint direction can determine the orientation of the block or bedding planes. Avoid blocks lying on a slope greater than 5-10°, to ensure stability of the block and therefore orientation of the exposed surfaces through time.

Once a suitable site is chosen, sample selection is often dictated by the availability of material that can be removed from the surface. In most cases, a small sledgehammer and chisel are sufficient for sampling. For very difficult samples at a crucial site, a larger sledgehammer or a power tool can be used. Cracks, joints, flow bands and bedding planes are useful for providing planes of weakness that can be focused on to remove a sample. Where possible, sample along a face where the original surface can be determined, such as shown by the presence of silken sides along a joint.

Avoid highly weathered surfaces (thick weathering rinds, solution weathering, quartz veins or leucocratic bands protruding from the surface, rounded edges, etc). These are most likely to indicate a former exposed rock surface, and therefore will give exposure ages greater than the age of the landslide.

On a scarp, it is useful to take duplicate samples from a face at different heights (at least 2-3 m difference). This helps constrain the former depth of the samples in case the uppermost sample was unexpectedly within 3 m of the surface. It is also useful to take duplicate samples on large blocks, especially those that are very large (> 3m long) or where the upper and lower surfaces are not clear.

Keep samples to less than 5 cm thick and do not damage the surface. Mark a sample with a permanent marker where the sample is thicker than 5 cm or where a lower part of the sample was shielded. Remove the extraneous material on a rock saw. Mark the top or the outer surface of the sample and orient other faces with arrows. Try to collect at least 500 g of total rock, preferably as one piece. Multiple flakes or pieces from the same point can be combined to bulk up a sample if necessary, but try to collect from the same depth. The sample bag can be made of any material and should be clearly labeled and sealed. Make detailed notes about the sample and site (esp. dimensions and shape of face/block), focusing on anything that could affect the exposure age. Record the elevation of the sample site to within 10 m where possible. Photocopies of topographic maps are useful in the field for this purpose.

GEO PUBLICATIONS AND ORDERING INFORMATION

土力工程處刊物及訂購資料

A selected list of major GEO publications is given in the next page. An up-to-date full list of GEO publications can be found at the CEDD Website <http://www.cedd.gov.hk> on the Internet under "Publications". Abstracts for the documents can also be found at the same website. Technical Guidance Notes are published on the CEDD Website from time to time to provide updates to GEO publications prior to their next revision.

Copies of GEO publications (except maps and other publications which are free of charge) can be purchased either by:

writing to

Publications Sales Section,
Information Services Department,
Room 402, 4th Floor, Murray Building,
Garden Road, Central, Hong Kong.
Fax: (852) 2598 7482

or

- Calling the Publications Sales Section of Information Services Department (ISD) at (852) 2537 1910
- Visiting the online Government Bookstore at <http://bookstore.esdlife.com>
- Downloading the order form from the ISD website at <http://www.isd.gov.hk> and submit the order online or by fax to (852) 2523 7195
- Placing order with ISD by e-mail at puborder@isd.gov.hk

1:100 000, 1:20 000 and 1:5 000 maps can be purchased from:

Map Publications Centre/HK,
Survey & Mapping Office, Lands Department,
23th Floor, North Point Government Offices,
333 Java Road, North Point, Hong Kong.
Tel: 2231 3187
Fax: (852) 2116 0774

Requests for copies of Geological Survey Sheet Reports, publications and maps which are free of charge should be sent to:

For Geological Survey Sheet Reports and maps which are free of charge:

Chief Geotechnical Engineer/Planning,
(Attn: Hong Kong Geological Survey Section)
Geotechnical Engineering Office,
Civil Engineering and Development Department,
Civil Engineering and Development Building,
101 Princess Margaret Road,
Homantin, Kowloon, Hong Kong.
Tel: (852) 2762 5380
Fax: (852) 2714 0247
E-mail: jsewell@cedd.gov.hk

For other publications which are free of charge:

Chief Geotechnical Engineer/Standards and Testing,
Geotechnical Engineering Office,
Civil Engineering and Development Department,
Civil Engineering and Development Building,
101 Princess Margaret Road,
Homantin, Kowloon, Hong Kong.
Tel: (852) 2762 5345
Fax: (852) 2714 0275
E-mail: ykhui@cedd.gov.hk

部份土力工程處的主要刊物目錄刊載於下頁。而詳盡及最新的土力工程處刊物目錄，則登載於土木工程拓展署的互聯網網頁 <http://www.cedd.gov.hk> 的“刊物”版面之內。刊物的摘要及更新刊物內容的工程技術指引，亦可在這個網址找到。

讀者可採用以下方法購買土力工程處刊物(地質圖及免費刊物除外):

書面訂購

香港中環花園道
美利大廈4樓402室
政府新聞處
刊物銷售組
傳真: (852) 2598 7482

或

- 致電政府新聞處刊物銷售小組訂購 (電話: (852) 2537 1910)
- 進入網上「政府書店」選購，網址為 <http://bookstore.esdlife.com>
- 透過政府新聞處的網站 (<http://www.isd.gov.hk>) 於網上遞交訂購表格，或將表格傳真至刊物銷售小組 (傳真: (852) 2523 7195)
- 以電郵方式訂購 (電郵地址: puborder@isd.gov.hk)

讀者可於下列地點購買1:100 000, 1:20 000及1:5 000地質圖:

香港北角渣華道333號
北角政府合署23樓
地政總署測繪處
電話: 2231 3187
傳真: (852) 2116 0774

如欲索取地質調查報告、其他免費刊物及地質圖，請致函:

地質調查報告及地質圖:

香港九龍何文田公主道101號
土木工程拓展署大樓
土木工程拓展署
土力工程處
規劃部總土力工程師
(請交:香港地質調查組)
電話: (852) 2762 5380
傳真: (852) 2714 0247
電子郵件: jsewell@cedd.gov.hk

其他免費刊物:

香港九龍何文田公主道101號
土木工程拓展署大樓
土木工程拓展署
土力工程處
標準及測試部總土力工程師
電話: (852) 2762 5345
傳真: (852) 2714 0275
電子郵件: ykhui@cedd.gov.hk

MAJOR GEOTECHNICAL ENGINEERING OFFICE PUBLICATIONS

土力工程處之主要刊物

GEOTECHNICAL MANUALS

Geotechnical Manual for Slopes, 2nd Edition (1984), 300 p. (English Version), (Reprinted, 2000).

斜坡岩土工程手冊(1998)，308頁(1984年英文版的中文譯本)。

Highway Slope Manual (2000), 114 p.

GEOGUIDES

Geoguide 1 Guide to Retaining Wall Design, 2nd Edition (1993), 258 p. (Reprinted, 2000).

Geoguide 2 Guide to Site Investigation (1987), 359 p. (Reprinted, 2000).

Geoguide 3 Guide to Rock and Soil Descriptions (1988), 186 p. (Reprinted, 2000).

Geoguide 4 Guide to Cavern Engineering (1992), 148 p. (Reprinted, 1998).

Geoguide 5 Guide to Slope Maintenance, 3rd Edition (2003), 132 p. (English Version).

岩土指南第五冊 斜坡維修指南，第三版(2003)，120頁(中文版)。

Geoguide 6 Guide to Reinforced Fill Structure and Slope Design (2002), 236 p.

GEOSPECS

Geospec 1 Model Specification for Prestressed Ground Anchors, 2nd Edition (1989), 164 p. (Reprinted, 1997).

Geospec 2 Model Specification for Reinforced Fill Structures (1989), 135 p. (Reprinted, 1997).

Geospec 3 Model Specification for Soil Testing (2001), 340 p.

GEO PUBLICATIONS

GCO Publication No. 1/90 Review of Design Methods for Excavations (1990), 187 p. (Reprinted, 2002).

GEO Publication No. 1/93 Review of Granular and Geotextile Filters (1993), 141 p.

GEO Publication No. 1/96 Pile Design and Construction (1996), 348 p. (Reprinted, 2003).

GEO Publication No. 1/2000 Technical Guidelines on Landscape Treatment and Bio-engineering for Man-made Slopes and Retaining Walls (2000), 146 p.

GEOLOGICAL PUBLICATIONS

The Quaternary Geology of Hong Kong, by J.A. Fyfe, R. Shaw, S.D.G. Campbell, K.W. Lai & P.A. Kirk (2000), 210 p. plus 6 maps.

The Pre-Quaternary Geology of Hong Kong, by R.J. Sewell, S.D.G. Campbell, C.J.N. Fletcher, K.W. Lai & P.A. Kirk (2000), 181 p. plus 4 maps.

TECHNICAL GUIDANCE NOTES

TGN 1 Technical Guidance Documents